ADVANTAGES OF INTERMITTENT FLOW CONTROL SCHEMES ON THE PURDUE HOG COOLING PAD FOR MITIGATING HEAT STRESS IN LACTATING SOWS

by

Tyler C. Field

A Thesis

Submitted to the Faculty of Purdue University

In Partial Fulfillment of the Requirements for the degree of

Master of Science in Agricultural and Biological Engineering

School of Agricultural and Biological Engineering

West Lafayette, Indiana

December 2020

THE PURDUE UNIVERSITY GRADUATE SCHOOL
STATEMENT OF COMMITTEE APPROVAL

Dr. Robert M. Stwalley III, Chair
School of Agricultural & Biological Engineering

Dr. Allan P. Schinckel
Department of Animal Sciences

Dr. Sadegh Dabiri
School of Agricultural & Biological Engineering

Approved by:
Dr. Nathan S. Mosier

For Sarah

ACKNOWLEDGMENTS

I would like to thank everyone at Purdue University who has supported me and contributed to the success of this project. I am extremely grateful to Dr. Robert Stwalley III for introducing me to the project when I was an undergraduate and for his continued guidance and extensive knowledge throughout my graduate career. I would like to thank Dr. Allan Schinckel and Dr. Sadegh Dabiri for serving on my committee and for providing additional direction on this project. Many thanks to Scott Brand, Eric Kong, Paul Thieme, and Aaron Etienne for always finding time to lend a hand. Thank you to Morgan Burgett, Nadia Flores, and Abby McGregor for their continual commitment to the project and my many other friends for their assistance rebuilding and installing the hog cooling pads at the Animal Science Research & Education Center. Thank you to Brian Ford and the ASREC swine unit staff for their assistance in keeping everything running smoothly. I would also like to acknowledge the School of Agricultural & Biological Engineering, Purdue AgSEED, Purdue Trask Innovation Fund, and the Wabash Heartland Innovation Network for funding this project. Thank you to Jake Piekarski for always being there for me and his many words of support. Finally, special thanks to my wife, Sarah Libring, and my mom, Barb Yakely-Field, for always encouraging and inspiring me.

TABLE OF CONTENTS

LIST OF TABLES

LIST OF FIGURES

ABSTRACT

The Purdue hog cooling pad has previously been demonstrated to adequately mitigate heat stress in lactating sows by conductively transferring heat from the sow to cold water running through the cooling pad. The cooling effectiveness describes how much heat is removed per liter of water flushed through the cooling pad. Past studies indicated that intermittent flow of the cooling water could achieve greater cooling effectiveness than continuous flow systems. An electronic control system was implemented on the current cooling pad design to allow for automated control of a solenoid valve based on a preprogrammed flush condition. The control schemes were categorized into two groups: temporal and temperature threshold. The temporal schemes opened the solenoid for 30 seconds before closing it for 3, 6, or 9 minutes. The temperature threshold control schemes utilized feedback from temperature probes embedded beneath the surface of the cooling pad to open the solenoid for 30 seconds when a surface temperature of at least 28.0, 29.5, or $31.0°C$ was detected. The temperature threshold control schemes achieved greater heat transfer rates (348, 383, 268 W) versus the temporal control schemes (324, 128, 84 W). The cooling effectiveness for all control schemes ranged from 46.6 to 64.7 kJ/L. Intermittent flow control schemes did achieve greater cooling effectiveness than continuous flow systems from previous studies, but they did so at lower heat transfer efficiencies.

1. INTRODUCTION

Heat stress is a major issue affecting the swine industry today. It can cause reduced feed intake, reduced milk production, and can lead to the death of the animal. Current commercial heat stress mitigation methods cannot effectively remove heat from lactating sows and other research solutions lack commercial viability. A thermally conductive cooling pad that could easily be implemented on a large scale was developed at Purdue University (Schinckel & Stwalley, 2015) to efficiently remove excess heat and mitigate heat stress in lactating sows. Now, an electronic control system has been implemented (Field et al., 2019; Field et al., 2020). This allowed for intermittent flow schemes to be evaluated and compared with previously tested continuous flows.

1.1 Background

Lactating sows have been determined to be a lifecycle stage of hogs that is the most susceptible to heat stress (Black, Mullan, Lorschy, & Giles, 1993; Pang, Li, Zheng, Lin, & Liu, 2016). Heat stress in lactating sows has been shown to reduce feed intake, milk production, subsequent fertility, and can ultimately lead to death in extreme situations (Baumgard & Rhoads, 2013; Ross et al., 2015). This problem exists due to the disparity between the thermal neutral zone of lactating sows, and that of piglets, particularly when they are first born (Baumgard & Rhoads, 2013; Black et al., 1993; Pedersen, Malmkvist, Kammersgaard, & Jorgensen, 2013). Over the past few decades, sows have been genetically selected to produce larger litters and have greater milk production (Cabezon, Schinckel, Richert, Peralta, & Gandarillas, 2017b; Cabezon, Schinckel, Smith, et al., 2017; Ross et al., 2015). As a result, the present-day sow produces significantly more heat than the average sow in the past (Maskal et al., 2018a; Renaudeau et al., 2012). Additionally, the mean piglet birth weight has decreased due to increased litter sizes, which increases their susceptibility to hypothermia at temperatures below their thermoneutral zone (Quiniou, Dagorn, Gaudré, 2002). Heat stress is a contributing factor to the seasonal decreases in fertility during hot, summer months (Renaudeau et al., 2012; Ross et al., 2015). With more than fifty percent of 2018 pork production and nearly fifty percent of 2019 pork production taking place in China, Brazil, and Vietnam (USDA: Foreign Agricultural Service, 2019), a significant number of hogs are produced in tropical and subtropical climates, where the detrimental effects of heat stress are apparent for more than a few months each year.

Various efforts have been made to selectively cool sows, without cooling piglets, to help mitigate the effects of heat stress without decreasing the ambient temperature of the farrowing house (Pang, Li, Xin, Yuan, & Wang, 2010; Perin et al., 2016; Silva et al., 2006; van Wagenberg, van der Peet-Schwering, Binnendijk, & Claessen, 2006). One such effort was the development of a cooling pad at Purdue University (Schinckel & Stwalley, 2015). Initial development occurred as part of a senior capstone project (Geis, Zumwalt, & Carter, 2015). Multiple rounds of manufacturing, testing, and modification have been completed with this cooling pad design (Cabezon, Johnson, Schinckel, & Stwalley, 2020; Cabezon, Maskal, et al., 2018; Cabezon, Schinckel, Marchant-Forde, Johnson, & Stwalley, 2017; Cabezon, Schinckel, Smith, et al., 2017; Cabezon, Schinckel, Stwalley, & Stwalley, 2018; Cabezon, Schinckel, & Stwalley, 2017; Cabezon, Field, Winslow, Schinckel, & Stwalley, 2020; Maskal et al., 2018; Parois et al., 2018; Smith et al., 2017), with the aim to create a commercially viable product, that has well-characterized heat transfer properties, while effectively and efficiently removing excess heat from crated, lactating sows in farrowing houses without causing any adverse effects to the sow or piglets. It has been shown that intermittent flows allow for more efficient heat transfer by increasing the amount of heat removed from the sow per liter of water used (Cabezon, Schinckel, et al., 2018; Cabezon, Field, Winslow, et al., 2020). The addition of an electronic control system will allow for automated control of this intermittent flow, allowing more extensive testing of nonconstant flow control schemes and moving the system towards a commercially viable design. It will also allow the amount of cooling to be varied for each sow, accounting for some variation in heat production between sows, as recommended in Cabezon, Schinckel, Richert, Peralta, & Gandarillas (2017a).

1.2 Research Goals

1. Design and implement a microcontroller based electronic control system that will control the coolant flow rate of the cooling pad;
2. Develop a program for a temporal control scheme that will flush the coolant from the pad once per set time;
3. Develop a program for a temperature threshold control scheme that will flush the coolant from the pad based on feedback from temperature sensors embedded inside the cooling pad;
4. Perform calibration of sensors before testing and verification, along with before and after testing to ensure sensor measurements are accurate;
5. Sufficiently test the two control schemes at the Purdue Animal Science Research & Education Center (ASREC) swine facility to determine the average heat transfer and heat transfer efficiency under multiple conditions for each control scheme; and
6. Determine if either control scheme is significantly more efficient than the other and make recommendations for future improvement of the cooling pad control system.

2. LITERATURE REVIEW

2.1 Effects of Heat Stress on Sows

Heat stress causes both short-term and long-term negative effects in sows. In extreme cases, severe heat stress can cause death (Baumgard and Rhoads 2013, Ross, Hale et al. 2015). The short-term effects of heat stress include increased skin temperature, increased internal temperature, and increased respiration rate (Mayorga, Renaudeau et al. 2019). Sows experiencing heat stress will also have reduced feed intakes in order to reduce internal heat production (Quiniou and Noblet 1999, Renaudeau, Collin et al. 2012, Baumgard and Rhoads 2013, Mayorga, Renaudeau et al. 2019). Reduced feed intakes result in reduced milk production (Quiniou and Noblet 1999, Renaudeau, Collin et al. 2012), which affects piglet growth and ultimately causes lighter litter weights at weaning (Quiniou and Noblet 1999). At high ambient temperatures, lactating sows have been shown to spend more time sitting and standing, less time nursing, and making more frequent trips to the feeder and waterer without using them (Murphy, Nichols et al. 1987, Silva, Oliveira et al. 2006, Silva, Oliveira et al. 2009, de Oliveira, Ferreira et al. 2011). Long-term effects of heat stress can cause sows to have increased wean-to-estrus intervals and reduced future litter sizes (Quiniou and Noblet 1999, Pang, Li et al. 2016). This ultimately makes the sow less productive for the remainder of her life, resulting in economic losses.

2.2 Methods of Mitigating Heat Stress

Methods of mitigating heat stress in sows can be categorized into two main groups, based on whether the main goal is to improve the sow's ability to manage excess heat or to remove this excess heat from the sow. Methods that utilize mass transfer through the sow, dietary supplements, or genetic selection are part of the former group, while methods focusing on latent, convective, radiative, or conductive heat transfer are part of the latter group.

2.2.1 Mitigating Heat Stress through Heat Management

Heat management methods allow the sow to be less affected by high ambient temperatures through a variety of different techniques. Utilizing mass transfer through the sow, such as providing chilled drinking water to reduce the sow's temperature internally, was examined by Jeon et al. (2006) and Jeon & Kim (2014). Dietary supplements and variations to improve the sow's ability to manage high ambient temperatures and heat stress have also been studied (Black, Mullan et al. 1993). Genetic selection of sows that appear more heat tolerant has also been suggested (Mayorga, Renaudeau et al. 2019).

Mass Transfer Methods

Cool drinking water acts as a heat sink when consumed, absorbing heat from the animal. By providing colder drinking water, an equal volume of water can remove more energy from the sow by the time an equilibrium temperature is reached, resulting in a lower equilibrium temperature. Chilled drinking water at $10°C$ and $15°C$ were both shown to reduce heat stress in lactating sows, including 40% increased feed intake, 20% increased milk production, and 20% decreased respiration rates compared to sows that were provided with $22°C$ drinking water. This resulted in piglets of sows with access to chilled water having significantly heavier weaning weights due to the increased milk production (Jeon, Yeon et al. 2006). Chilled drinking water at $15°C$ provided in different ways (free access, restricted access, and restricted access with a sound stimulus) versus $22°C$ drinking water showed similar results to this previous study (Jeon and Kim 2014).

While this method has been shown to be effective at removing heat the from the sows, the authors do note that the power required to continuously cool the drinking water was significant (Jeon and Kim 2014). The necessary water tank size would also need to increase with the number of sows on the farm to ensure enough water was available at any given time, which would likely prevent a commercial system based on this technique from being feasible. However, if cool groundwater is available without additional power input, then it could help mitigate heat stress in the sows. Locations with hotter climates will have warmer groundwater though, likely making this process of limited utility. As a result, other cooling systems should also be implemented.

Dietary Supplement Methods

Dietary supplements and variations help mitigate heat stress by increasing the energetic efficiency of the feed, therefore reducing internal heat production of the sow and providing precursor substances to help the sow more effectively remove heat. It has been shown that feeds with increased fat and/or decreased fiber cause the sow to produce less heat (Black, Mullan et al. 1993). Reduction of the percentage of crude protein to net energy in the feed was also shown to reduce the decrease in feed intake at high ambient temperatures (Renaudeau, Quiniou et al. 2001, Silva, Noblet et al. 2009). Crude glycerol, a coproduct from the production of biodiesel, was added to the feed of lactating sows because of its hyperhydrating properties in humans. While it did not help mitigate heat stress in the sows, it was suggested that it may need to be added to the sows' water supply to be effective (Schieck, Kerr et al. 2010). Kumar et al. (2017) found that adding fermentation products from various bacteria did not mitigate the effects of heat stress, but it did help protect the sows' intestines from cytokines and heat shock proteins. One study examined the supplementation of L-citrulline, a nitric oxide precursor. Nitric oxide acts as a vasodilator, facilitating peripheral blood flow during times of heat stress and potentially allowing the sows to more easily reject heat to the environment. The study found that 1% L-citrulline supplementation reduced pre-weaning piglet mortality by 16.1% and significantly reduced sow respiration rates, but it did not reduce sow rectal temperatures (Liu, de Ruyter et al. 2019). Black et al. (1993) noted that while diet changes can benefit sows in hot environments, the benefits of different diets are small relative to the benefits of improving environmental heat transfer from the sow.

Genetic Selection to Mitigate Heat Stress

Renaudeau et al. (2012) suggested that if genetic selection for thermal tolerance of swine was successful, it could be the most cost-effective method to mitigate the effects of heat stress, but that there are significant thermal tolerance variations between animals even of the same breed. Mayorga et al. (2019) noted that while genetic selection could be a solution to mitigate heat stress, it will be a long-term solution, and it will likely have tradeoffs with thermoneutral performance. As a result, genetic selection will take years to potentially become a viable solution for mitigating heat stress and cannot be immediately effective. There is also no way to know in advance if the detriments to thermoneutral performance will be worth the gains in thermal tolerance.

2.2.2 Mitigating Heat Stress through Heat Transfer

There are four modes of heat transfer available to hogs to remove excess heat. These are conduction, convection, radiation, and latent heat transfer through the evaporation of water. Due to swine's inability to sweat, the animal's evaporative cooling mechanisms are limited to panting. Methods that utilize heat transfer from the sow usually focus primarily on one of these four modes of heat transfer (Bjerg et al., 2019).

Convective Cooling Systems

Convective cooling systems for swine utilize moving air to remove heat and reduce heat stress. Cooling fans act to cool the entire farrowing house, which is detrimental to piglets when the air temperature is less than the lower bound of the piglets' thermoneutral zone. When the air temperature is greater than the skin temperature of the sow, the process acts in reverse, heating the sow and increasing heat stress. As a result, cooling fans are only an effective method to reduce heat stress within a narrow environmental temperature band, making them a poor choice for mitigating heat stress in lactating sows. Most other heat transfer systems utilize a combination of convection and another mode of heat transfer, and these will be examined based on their other method of heat transfer.

Evaporative Cooling Systems

Evaporative cooling systems for swine utilize the evaporation of water to remove excess heat from the animal. These systems include snout coolers, drip coolers, misters, and sprinkler systems. The snout cooling system used by Perin et al. (2016) utilized evaporative cooling to reduce the temperature of the air before blowing it at the snout of the sow. This system is an example of one that uses both convection and evaporative cooling. The evaporative snout cooling system reduced sow rectal temperatures, increased sow feed intakes, and increased piglet weaning weights. The individual sow output of the system was $250\ m^3/hr$ through a $95\ mm$ duct. (Perin, Gaggini et al. 2016). While effective at mitigating heat stress, this system had an air velocity of $56.6\ km/h$ ($35.2\ mph$). The power required to run this cooling system was large and impractical for scaling to a commercial system. Additionally, excess cooling air could negatively affect piglets, particularly right after farrowing.

Drip coolers, misters, and sprinkler systems all act by depositing liquid water on the sow. As the water evaporates, it removes heat from the sow. Drip coolers aimed at sows' necks and shoulders have been shown to decrease heat stress in sows and significantly increase weaning weights of piglets when set to a flow rate of three liters per hour (Murphy, Nichols et al. 1987). However, this experiment was only conducted at $28°C$. It is likely that at higher temperatures, the benefits of the drip coolers would be at least partially offset by the additional humidity added to the air as the water from the drippers evaporates. Misters and sprinkler systems are also prone to this problem at higher ambient temperatures. Additionally, these systems create slippery surfaces that can increase the likelihood of injury to sows in the farrowing crates. When these systems fail, and water is sprayed onto walkways, this can also pose an additional risk to personnel at the facility.

Radiative Cooling Systems

Radiative cooling systems for swine use the temperature differential between the animal and a cold sink to draw heat away from the animal electromagnetically, without direct fluid flow or contact with the cool surface. The major benefit of radiative cooling is that it does not strongly depend on the relative humidity of the air. This allows it to be much more effective at heat transfer than previous cooling methods in hot and humid environments. A water-cooled cover installed over the sow crate with internal cooling pipes was developed by Pang et al. (2010) and shown to effectively cool the area where the sow would be without significantly increasing relative humidity. While the authors acknowledge some convective heat transfer occurs, the majority of the heat transfer from the sow is due to thermal radiation. Different tube sizes and spacing, as well as the presence or absence of an aluminum canopy were examined to determine which combination best transferred heat away from the sow (Pang, Li et al. 2010). The system was further tested on sows in gestation crates and shown to have increased heat transfer up to a flow rate of about $4\ L/min$. Additionally, significant differences were found between respiration rates and skin temperatures for sows with and without the water-cooled cover (Pang, Li et al. 2011). This system was recently tested with lactating sows against a sprinkler-based cooling system. At ambient temperatures of less than $30°C$, no significant differences between groups were seen for respiration rates or skin temperatures. However, at temperatures greater than $30°C$ (the maximum ambient temperature reached during the study was $38.5°C$) sows under the water-cooled cover showed significantly decreased respiration rates and skin temperatures, demonstrating the effectiveness of the system under hot and humid conditions (Pang, Li et al. 2016).

Conductive Cooling Systems

Conductive cooling systems for swine remove heat from the animal through direct contact. This has been examined through the use of different floor cooling techniques. A system was developed in the Netherlands that utilized steel pipes underneath a solid portion of the farrowing crate floor beneath the sow's shoulder. The water flow rate in the pipes was constant at $3.3\ L/min$, and the system removed approximately $107\ W$ from each farrowing crate. Approximately 54% of this heat was removed from the sow, with the remaining 46% being removed from the environment (van Wagenberg, van der Peet-Schwering et al. 2006).

A different floor cooling system that utilized a pre-molded concrete floor plate was developed at the Universidade Federal de Viçosa, Brazil in 2003. Empty spaces exist in the plate that water is pumped through to cool the sow. This cooling plate increased sow daily feed intake by 15.5%, increased piglet weaning weight by 21%, and decreased respiratory rates, skin temperatures, and rectal temperatures during high ambient temperatures (Silva, Oliveira et al. 2006). This system was tested in conjunction with amino acid supplementation in the diet, and results again indicated reduced heat stress in lactating sows (Silva, Oliveira et al. 2009). De Oliveira et al. (2011) compared sows with and without this floor cooling system and found sows with the floor cooling made less trips to the drinker without drinking and spent less time standing, indicating a higher level of comfort. The plate measured 1.75 meters long by 0.50 meters wide by 0.075 meters thick, with nine 0.035 meter diameter by 1 meter long areas for water to flow through (Silva, Oliveira et al. 2006). An approximate density for concrete is $2300\ kg/m^3$ (Gere and Goodno 2012). As a result, the approximate mass of the concrete floor cooling system was 59.4 kg.

Purdue University Hog Cooling Pad

The Purdue hog cooling pad was originally prototyped as an Agricultural Systems Management capstone project. The original design utilized six lengths of copper pipe that entered and exited on the left side of the cooling pad and was built on a wooden base (Geis, Zumwalt et al. 2015). The main goal during the cooling pad development was to reduce or eliminate heat stress in the sow using a relatively portable and efficient system that could easily be installed in conventional farrowing crates. The pad design aimed to maximize conductive heat transfer from the sow, while minimizing heat transfer from the environment (Cabezon, Schinckel et al. 2017).

The design of the cooling pad consisted of four layers of material. Most of the cooling pad was made of high-density polyethylene (HPDE). Sections in the HDPE were cut-out for copper pipes, which were then attached to an aluminum clip. This aluminum clip was held in close contact with a top aluminum plate to maximize conductive heat transfer through the top surface of the pad, where the sow would lay. The HDPE acted to insulate the sides and bottom of the cooling pad to reduce the amount of energy spent on cooling the ambient air instead of the sow (Geis, Zumwalt et al. 2015, Cabezon, Schinckel et al. 2017).

Six-Pipe Design

Multiple tests were done on the six-pipe design of the cooling pad to determine its thermal capacity (Cabezon, Schinckel et al. 2017) and heat transfer properties (Cabezon, Schinckel et al. 2018), including its efficiency at removing heat from the sow and its effectiveness while doing so under various conditions. Multiple flow rates from 1 L/min up to 14.1 L/min were studied, and a heat capacity of the initial prototype cooling pad of approximately 19 kJ/K was determined. This allowed the cooling pad to react quickly to changing temperatures of the sow and ambient air, compared to other floor cooling solutions (Cabezon, Schinckel et al. 2017). Further work was done using flow rates from 1.1 liters per minute to 5.3 liters per minute. With $17°C$ cooling water running through the pad at different flow rates, heat rejection ranged from 98 W to 296 W, while effectiveness ranged from 2.84 kJ/L to 5.57 kJ/L. The greatest heat rejection occurred at the greatest flow rate of 5.3 L/min, while the greatest effectiveness occurred at a flow rate of 2.4 L/min (Cabezon, Schinckel et al. 2018).

Table 1 displays the heat rejection rate and cooling effectiveness for various coolant cycles and flow rates from Cabezon et al. (2018). The effective flow rate based on the coolant cycle has been included for each flow rate tested.

Table 1: Heat Transfer Properties of Hog Cooling Pad

Coolant Cycle (on-off, min)	Low Flow Rate ($2.6\ L/min$)			High Flow Rate ($5.0\ L/min$)		
	Effective Flow Rate (L/min)	Heat Rejection (W)	Effectiveness (kJ/L)	Effective Flow Rate (L/min)	Heat Rejection (W)	Effectiveness (kJ/L)
1-1	1.3	135	6.36	2.5	227	4.32
1-2	0.87	147	7.71	1.67	203	5.53
1-3	0.65	127	8.46	1.25	200	6.55
2-2	1.3	150	5.69	2.5	240	4.88
2-3	0.52	136	6.20	1.0	197	4.79
3-3	1.3	240	7.86	2.5	202	4.03

Cabezon et al. (2018) concluded that the cooling pad operated most efficiently with a short "on" period where water was able to flow through the pad, followed by a long "off" period where the water in the pad was allowed to warm sufficiently before being flushed. As the water is not flowing during the "off" periods, this demonstrated the benefits of conductive heat transfer with limited water usage, particularly with the lower of the two flow rates that were tested.

Eight-Pipe Design

A second cooling pad design was built in late 2015 that increased the number of cooling pipes inside the pad from six to eight. Additionally, the inlet and outlet pipes were moved to the front of the cooling pad from the left side after the first prototype was built. This made the flow of water symmetric, with the water from the inlet (presumably the coldest water in the cooling pad) starting in the center and working its way to the left and right sides before exiting the pad. The eight-pipe design was shown to have a smoother temperature distribution across the top of the cooling pad than the six-pipe design. At a continuous flow rate of 2.6 L/min, the eight-pipe design had a 16.7% increased heat rejection rate and a 16.1% increased effectiveness (Cabezon, Winslow et al. 2019). Table 2 reproduces the heat rejection rate and cooling effectiveness for various coolant cycles on both pad designs from Cabezon, Field, Winslow, Schinckel, & Stwalley (2019). The effective flow rate based on the coolant cycle has been included.

Table 2: Heat Transfer Properties Comparison of Hog Cooling Pads

2.6 L/min Flow Rate		**6 Pipe Design**		**8 Pipe Design**	
Coolant Cycle (on-off, min)	**Effective Flow Rate (L/min)**	**Heat Rejection (W)**	**Effectiveness (kJ/L)**	**Heat Rejection (W)**	**Effectiveness (kJ/L)**
1-1	1.3	187	8.3	285	11.3
1-2	0.87	174	11.7	240	16.0
1-3	0.65	148	13.6	222	18.9

The authors concluded that the eight-pipe design was the superior design and studied the ability of the new design to reduce heat stress in lactating sows. Multiple more studies were conducted with continuous flow rates using live animals. For flow rates of $0.25\ L/min$, $0.55\ L/min$, and $0.85\ L/min$, and an ambient temperature of $35°C$, the eight-pipe cooling pad design was shown to significantly reduce sow respiration rates and rectal temperatures after 90 minutes of cooling for medium and high flow rates (Smith, Cabezon et al. 2017), and sow respiration rates, rectal temperatures, and vaginal temperatures for all flow rates (Cabezon, Schinckel et al. 2017). For the same flow rates and ambient temperature, cooled sows had significantly reduced heart rates and spent more time laying down, when compared to uncooled sows (Parois, Cabezon et al. 2018). For flow rates of $0.25\ L/min$ and $0.5\ L/min$, increased ambient temperatures were shown to increase the heat transfer into the cooling pad (Maskal, Cabezon et al. 2018), the higher flow rate was shown to be necessary above $27°C$ and 40-45% relative humidity (Cabezon, Maskal et al. 2018), and respiration rates and rectal temperatures were significantly reduced for cooled sows when compared to uncooled sows.

Intermittent flow rates with longer "off" periods were recently studied in Cabezon, Johnson, Schinckel, & Stwalley (2019). The $2.6\ L/min$ flow rate was retained from the previous intermittent flow study (Cabezon, Winslow et al. 2019), but the cycle times examined were a 30 second pulse once every 2, 3, 6, or 9 minutes, at ambient temperatures of $23°C$, $28°C$, and $33°C$. Table 3Table 3 summarizes the heat rejection rate and cooling effectiveness values for each flow rate and ambient temperature from Cabezon, Johnson, Schinckel, & Stwalley (2019), with the addition of the effective flow rate. The cooling effectiveness was calculated by determining the energy rejected in one cooling cycle and dividing it by the volume of one flush, which was 1.3 liters in this case.

Table 3: Heat Rejection Rates and Cooling Effectiveness for Intermittent Flow Rates on the Purdue Hog Cooling Pad

$2.6\ L/min$		Ambient Barn Temperature					
Flow Rate		$23°C$		$28°C$		$33°C$	
Cycle Time	Effective Flow Rate (L/min)	Heat Rejection (W)	Effectiveness (kJ/L)	Heat Rejection (W)	Effectiveness (kJ/L)	Heat Rejection (W)	Effectiveness (kJ/L)
9 min	**0.14**	132	54.8	132	54.8	133	55.2
6 min	**0.22**	168	46.5	212	58.7	156	43.2
3 min	**0.43**	234	32.4	438	60.6	354	49.0
2 min	**0.65**	X	X	X	X	531	49.0

A two-temperature threshold flush was also tested by Cabezon, Johnson, Schinckel, & Stwalley (2019), where the water would begin to flow when the upper threshold was reached, and continue to flush the cooling pad until the temperature was brought below the lower threshold. This temperature threshold flushing would allow for variation in heat production between sows to be compensated, preventing over and undercooling. The authors concluded that a more functional control system was needed to do more in depth testing of intermittent flows.

3. METHODS

3.1 System Design

The system used for mitigating heat stress consisted of two main parts, the cooling pad that had been used in previous hog cooling pad experiments (Cabezon, Schinckel et al. 2017, Cabezon, Schinckel et al. 2017, Cabezon, Schinckel et al. 2017, Smith, Cabezon et al. 2017, Cabezon, Maskal et al. 2018, Cabezon, Schinckel et al. 2018, Maskal, Cabezon et al. 2018, Maskal, Cabezon et al. 2018, Parois, Cabezon et al. 2018, Cabezon, Johnson et al. 2019, Cabezon, Winslow et al. 2019) and the electronic control system that was designed and retrofitted onto the cooling pads to allow for intermittent flow control schemes to be implemented (Field & Stwalley, 2018; Field et al., 2019).

3.1.1 Cooling Pad Design

The cooling pad itself consists of a high-density polyethylene (HDPE) base, a series of copper pipes, aluminum extrusion, and aluminum diamond plate. The high-density polyethylene base is built from two pieces, each 0.61 meters wide and 0.025 meters thick, nominally two feet wide by one inch thick. The main section is 1.22 meters (4 feet) long, and the head section is 0.61 meters (2 feet) long. The slots for the copper pipes and temperature sensors were milled using a computer numerical controlled (CNC) gantry sheet router. Additionally, the area where the aluminum extrusion sits was recessed, so the top of the extrusion could be flush with the top of the HDPE. The HDPE was reused from previous hog cooling experiments (Cabezon, Schinckel et al. 2017, Cabezon, Schinckel et al. 2017, Cabezon, Schinckel et al. 2017, Smith, Cabezon et al. 2017, Cabezon, Maskal et al. 2018, Cabezon, Schinckel et al. 2018, Maskal, Cabezon et al. 2018, Maskal, Cabezon et al. 2018, Parois, Cabezon et al. 2018, Cabezon, Johnson et al. 2019, Cabezon, Winslow et al. 2019).

The copper pipes from the previous cooling pads were all replaced before these experiments, since they had corroded and begun leaking. Half inch nominal, type L (medium walled) copper pipes were used for all replacements. The design of the pipes can be seen in Figure 1.

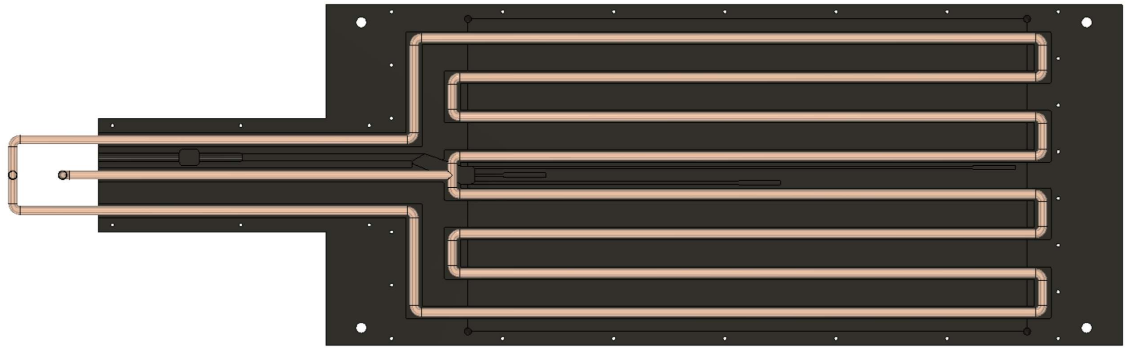

Figure 1: Cooling Pad Pipe Layout for 8-Pipe Second Prototype

Water flowed into the center pipe and then worked its way towards the outside edges of the cooling pad. This allowed the coolest water, and therefore the greatest heat transfer, to occur in the center, where the sow most often has the greatest contact with the cooling pad. All current experiments used an 8-pipe cooling design, instead of the original 6-pipe design seen in Figure 2Figure 2, used for early cooling pad experiments (Cabezon, Schinckel et al. 2017, Cabezon, Schinckel et al. 2018).

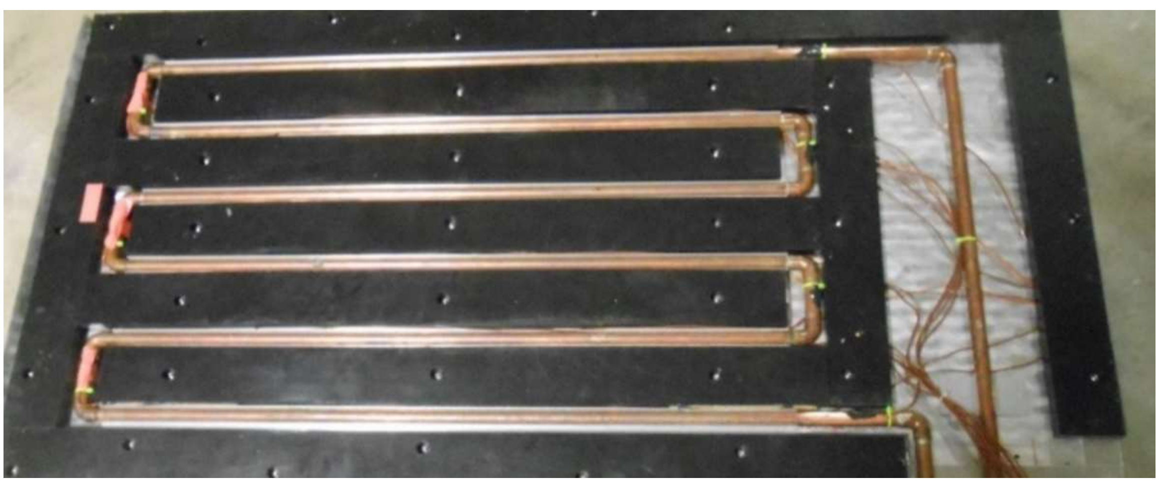

Figure 2: Original 6-Pipe Cooling Pad Design (Cabezon, Schinckel et al. 2017)

To further increase the heat transfer between the sow and the water in the copper pipes, ThinFin C from Radiant Design & Supply (Bozeman, MT) was attached to the top side of the copper pipes. This aluminum extrusion clips tightly to the copper pipe and aids in heat transfer from the upper surface of the cooling pad. As it is only available in one width and two standard lengths, the ThinFin C was cut to width and length to fit on the closely spaced copper pipes. The

ThinFin C can be seen partially installed in the newer 8-pipe design in Figure 3. The temperature sensors inside the cooling pad can also be seen in Figure 3.

Figure 3: ThinFin C Attached to Copper Pipes in the 8-Pipe Design

Except for the inlet and outlet pipes, the pipes and ThinFin C are covered with a piece of 3.18 mm (0.125 inch) thick aluminum diamond plate. This plate protected the sensors and pipes inside the cooling pad, and it also provided a textured surface to help prevent the sow from slipping, if the cooling pad became wet. The space underneath the diamond plate where the inlet and outlet pipes extend was filled with expanding window and door foam sealer to prevent debris from entering through this gap and affecting the heat transfer capabilities of the cooling pad. A cross-section of the cooling pad where the copper pipe and ThinFin C are can be seen in Figure 4.

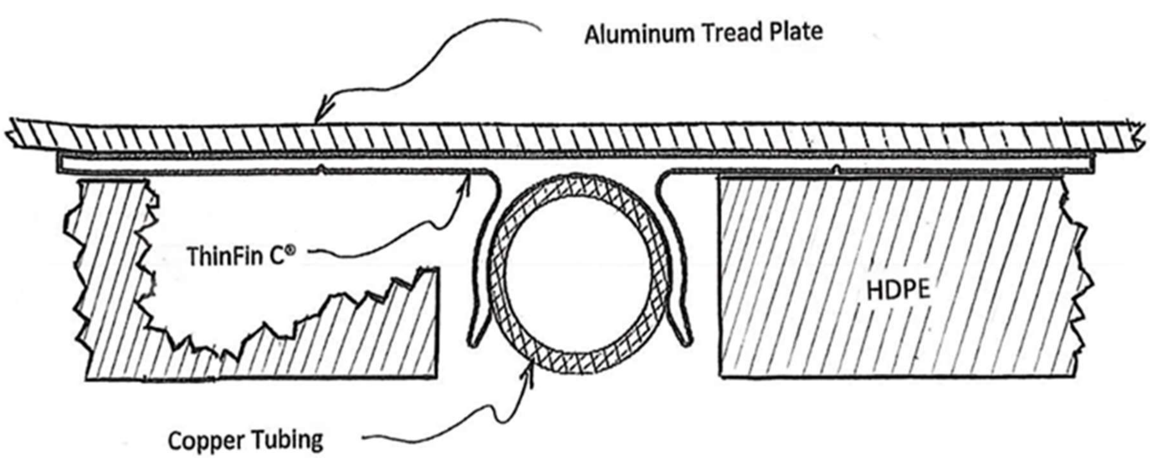

Figure 4: Cross-Section of Hog Cooling Pad (Cabezon, Schinckel et al. 2017)

All cooling pads were connected to a single high pressure plenum with pressure regulating valves between the plenum and each pad. This ensured that the flow rate through the cooling pads would not be affected by the number of pads operating at a given time.

3.1.2 Control System Design

The control system for the hog cooling pad was a microcontroller-based system mounted on the vertical extensions from the inlet and outlet pipes on the cooling pad. Due to the corrosive nature of the air in the farrowing house, all sensitive electronics were sealed inside an IP68 enclosure. This enclosure was a Polycase® ML-46F*1508. External connections were made through watertight pass-through connectors. A PVC pipe was installed between the inlet pipe and one of the outlet pipes on the cooling pad to protect the temperature sensor wires from piglets. A 12V, IP67 rated power supply was attached above the control box to provide power for the flow solenoid. The control system inside the enclosure can be seen in Figure 5.

Figure 5: Control Box & Electronics

Feather® M0 WiFi

The microcontroller used on each cooling pad was an Adafruit® Feather® M0 WiFi, seen in Figure 6. It is an Arduino© style microcontroller that utilizes a 32-bit Atmel ATSAMD21G18 chip with an ARM® Cortex® M0+ processor that runs at 48 MHz. In addition, it has 256 KB of flash memory and 32 KB of SRAM. This is 8 times more flash and 16 times more RAM than the processor on a standard Arduino© Uno R3. The microcontroller was powered by a micro USB cable that supplied 5V via a standard AC power to USB adaptor. It uses 3.3V logic and has a maximum power consumption of about 2 Watts (Adafruit® 2019). This low power consumption helped minimize heat inside the sealed control box and extend the life of the electronics.

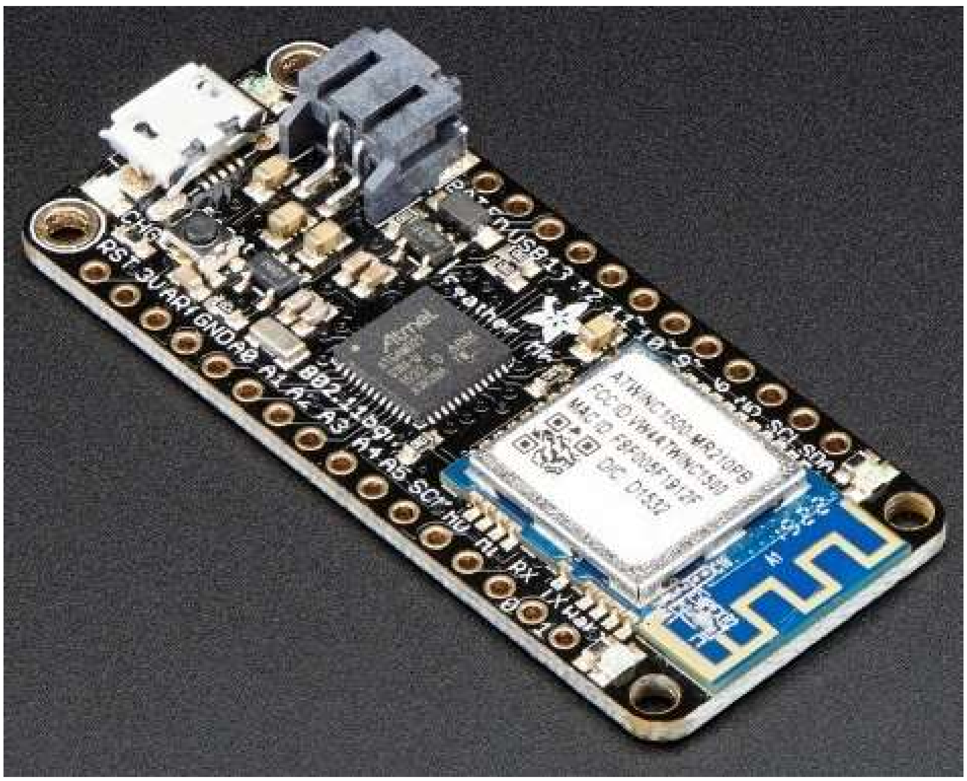

Figure 6: Adafruit® Feather® M0 WiFi (Adafruit® 2019)

Additionally, the Adafruit® Feather® M0 WiFi has an Atmel® ATWINC1500 WiFi module, which is capable of connecting to 802.11b/g/n networks with WEP, WPA, WPA2 encryption. It also has the ability to act as an access point so that a user can connect to it, much like a router, or host a basic webpage (Adafruit® 2019). While ultimately not used during this series of experiments, having this capability available on the microcontroller will allow for wireless data transfer in the future.

FeatherWings®

FeatherWings® are add-on boards that can be stacked with an Adafruit Feather® to add additional capabilities. Four such boards were used in the control system for the hog cooling pads. The four FeatherWings® used were the FeatherWing® Tripler, Terminal Block Breakout, Non-Latching Mini Relay, and Adalogger® RTC+SD wings, all made by Adafruit®.

The FeatherWing® Tripler is the only wing of the four that does not include additional surface mount or through hole components. It is simply a printed circuit board with headers that allows three Feather® components (Feathers® or FeatherWings®) to be connected side by side, instead of stacked vertically. This allowed all of the electronics to fit side-by-side in the control box, which had limited height. It was assembled using normal height headers on the two outer stacks and long pin stacking headers on the middle stack. This allowed a component to be attached to each of the three locations on the top of the Tripler, with one underneath the middle of the Tripler. The FeatherWing® Tripler can be seen in Figure 7.

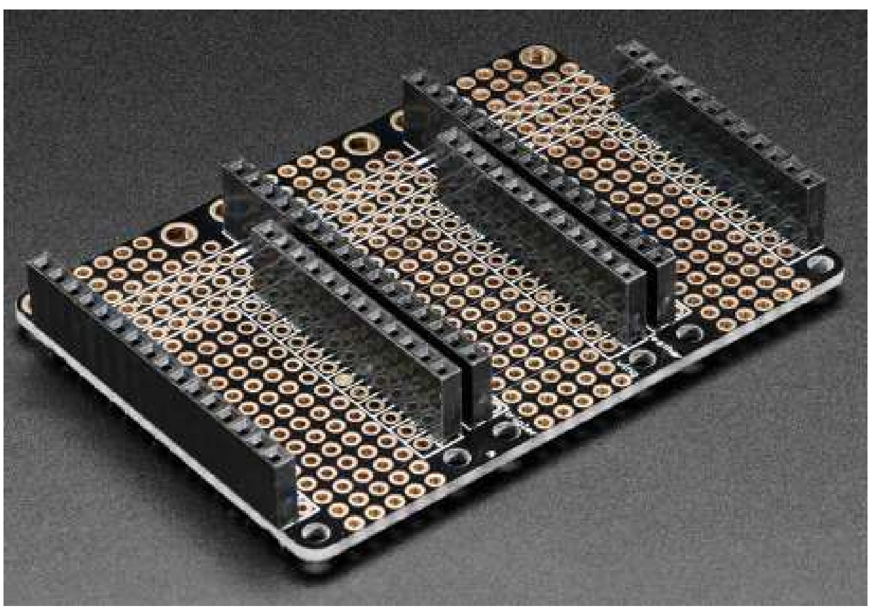

Figure 7: Adafruit® FeatherWing® Tripler (Adafruit® 2019)

The Terminal Block Breakout FeatherWing® was attached to the bottom side of the FeatherWing® Tripler. This was done because the Terminal Block Breakout FeatherWing® is wider than the standard Feather® component footprint, so it would effectively block the use of adjacent stacks, if it were placed on the top of the FeatherWing® Tripler. The Terminal Block Breakout FeatherWing® has two main features: a sliding switch tied to the ENABLE pin and screw terminals that are connected to each of the pins on the Feather® M0 WiFi, allowing stronger connections with wires to be made. The Feather® M0 WiFi itself does not have an on-off switch. Instead, it is on whenever it is plugged-in and receiving power. The switch on the Terminal Block Breakout FeatherWing® acts to enable power to the microcontroller, only when the switch is in the “on” position, allowing the Feather® M0 WiFi to be plugged-in, but off. The power, ground, and signal lines for the temperature sensors and the flow rate sensor were attached directly to the Terminal Block Breakout FeatherWing®. Additionally, this wing is bolted to the ultra-high molecular weight (UHMW) polyethylene electronics baseplate that holds all of the electronics to the inside of the control box. Ultra-high molecular weight polyethylene was selected for its ease of manufacturability, low cost, and its antistatic properties. The Terminal Block Breakout FeatherWing® can be seen in Figure 8.

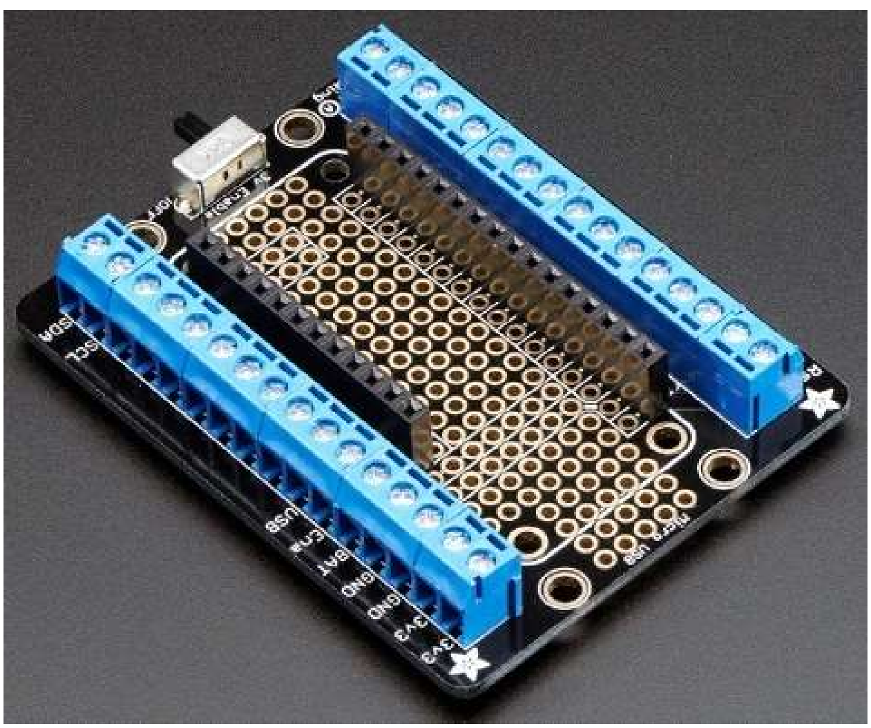

Figure 8: Adafruit® Terminal Block Breakout FeatherWing® (Adafruit® 2019)

On the top side of the FeatherWing® Tripler, were the Feather® M0 WiFi, the Non-Latching Mini Relay FeatherWing®, and the Adalogger® RTC+SD FeatherWing®. The Adalogger® RTC+SD FeatherWing® has two main components, plus the necessary circuitry for them to work. The first is the real time clock (RTC) module. It is an NXP© PCF8523 chip with a 32 KHz crystal and a CR1220 battery (Adafruit® 2019). A setup program is run that loads the current time of the computer into the RTC module. Once this is done, the module holds time, even when power to the Feather® M0 WiFi is off, due to the coin cell battery on the Adalogger® RTC+SD FeatherWing®. The time from the RTC module was used to determine when to output data and to add a timestamp to the outputted data.

The second module on the Adalogger® RTC+SD FeatherWing® was a microSD card reader. A SanDisk® 32 GB microSD card was used on each system. The maximum size of a full timestamp of data is 60 bytes. With data being recorded once every six seconds, assuming the full 32 GB of the microSD card could be written to (actual formatted capacity is less), it would take approximately 109 years of continuous data writing to fill the card. This guaranteed that the capacity of the storage would not be exceeded during the planned experiments. The Adalogger® RTC+SD FeatherWing® can be seen in Figure 9.

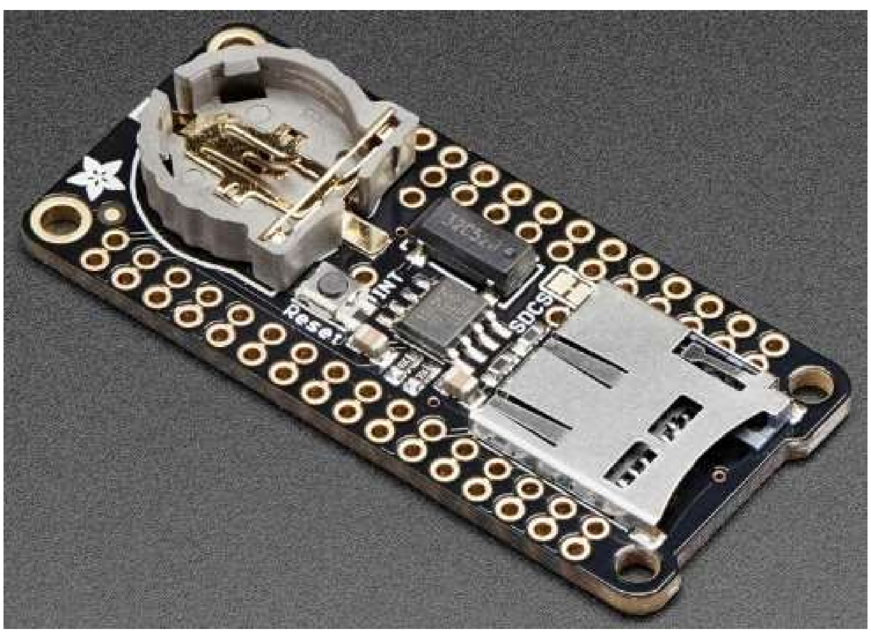

Figure 9: Adafruit® Adalogger® RTC+SD FeatherWing® (Adafruit® 2019)

The final FeatherWing® present on all systems during the experiments was the Non-Latching Mini Relay FeatherWing®. Since the Feather® M0 WiFi ran on 5V/3.3V and was a low current device, it did not have the power necessary to drive the flow solenoid. This FeatherWing® had an electronic relay on it that could be actuated with the power available from the Feather® M0 WiFi, which then controls a 12V power line to actuate the flow solenoid. As it was a non-latching relay, when power was removed, the relay reverted to its passive state. The 12V line was connected to the COM (Common) and NO (Normally Open) pins of the relay, so if the system failed or power was lost, the solenoid would fail closed, preventing overcooling of the sow and exposing her only to conditions equivalent to a sow in a CONTROL group. The Non-Latching Mini Relay FeatherWing® can be seen in Figure 10.

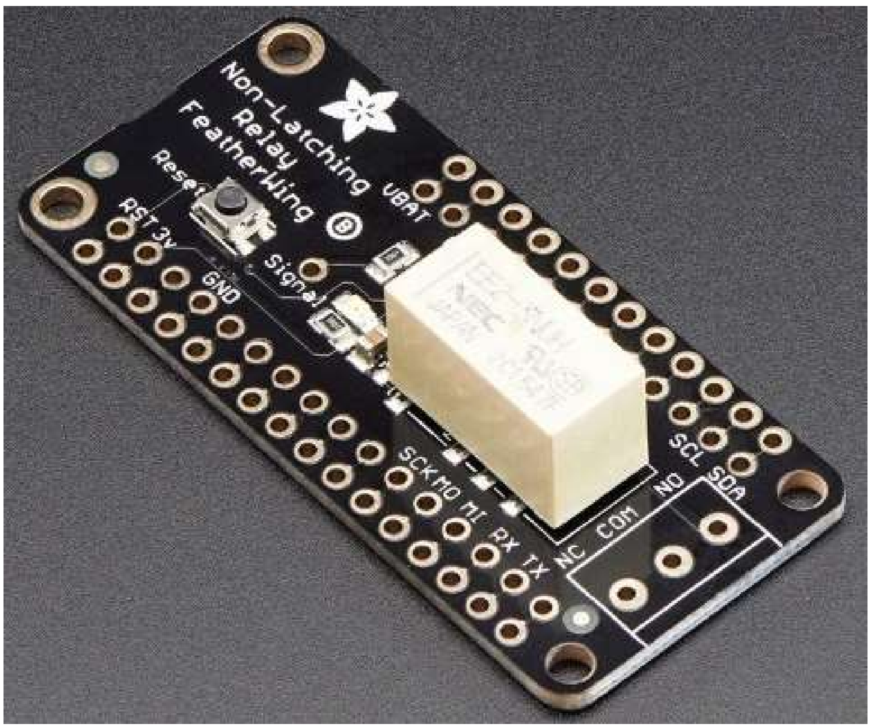

Figure 10: Adafruit® Non-Latching Mini Relay FeatherWing® (Adafruit® 2019)

Temperature Sensors

The temperature sensors used were Maxim Integrated® DS18B20 1-Wire® Digital Thermometers. The sensors used were purchased pre-wired and waterproofed in stainless steel cases. Similar to those used in previous hog cooling pad experiments (Seidel 2017), the only difference with these new sensors was a cylindrical casing with a flat end, rather than a hemispherical end as in previous experiments. The sensors were capable of measuring temperatures from $-55°C$ to $+125$°C with a stated accuracy of $\pm 0.5°C$ over the range of $-10°C$ to $+85°C$ (Maxim Integrated™ 2019). Each sensor also had a unique identification number, allowing multiple sensors to be wired together using the 1-Wire® interface. The pre-wired and waterproofed sensor can be seen in Figure 11.

Figure 11: DFRobot® Pre-Wired & Waterproofed DS18B20 Sensor (Digi-Key Electronics© 2019)

There are six temperature sensors installed on each cooling pad. Three are inside the cooling pad: one each at the front, middle, and rear of the pad, corresponding to the shoulders, belly, and hips of the sow. The inlet and outlet pipes have one sensor each. The temperature difference across these pipes was used to determine the amount of heat removed by the cooling pad. Finally, there is one ambient temperature sensor, placed just outside the crate and at the level of the sow to measure the ambient temperature close to the crate.

Flow Rate Sensor

The flow rate sensor used was DIGITEN® Hall effect flowmeter capable of measuring flows from 0.3 L/min to 10 L/min. This sensor has a small turbine that rotates as water flows through the sensor. One of the turbine blades has a small magnet that passes by the Hall effect sensor once per revolution of the turbine, creating an electrical pulse as it passes by. By knowing the frequency of these pulses and knowing the volume of water that flows through the sensor per one revolution of the turbine, the flow rate can be determined. This flow rate sensor can be seen in Figure 12.

Figure 12: DIGITEN® Flow Rate Sensor (Amazon.com© 2019)

Flow Solenoid

The flow solenoid was actuated based on the different control schemes to start and stop the flow of water through the cooling pad. It was a $12\,VDC$, normally closed, non-latching solenoid that required approximately $4\,W$ to actuate to the open position and allow water to flow through (Adafruit® 2019). It can be seen in Figure 13.

Figure 13: Adafruit® Water Solenoid Valve (Adafruit® 2019)

3.2 Sensor Calibration

Sensor calibration was performed on the temperature sensors and flow rate sensor for each cooling pad. This was to ensure accurate data collection and proper heat transfer between the sow and the cooling pad.

3.2.1 Temperature Sensor Calibration

The temperature sensors were calibrated using a two control points and then determining the necessary offsets. First, the cooling pads were installed in the farrowing house and allowed to equilibrate with the air in the room. The temperature output from each cooling pad was recorded for a minimum of ten minutes at this ambient steady state temperature, T_{amb}. The temperature of the room was confirmed using the thermometer on the wall. Then, due to ease of access, the ambient temperature sensor for each cooling pad was submerged in a bucket of ice water. The temperature of the ice water was recorded using an infrared thermometer for each cooling pad, T_{ice}. The sensor was allowed to sit for a minimum of ten minutes to ensure it had reached equilibrium with the ice water. Using these two measurements, the corrective slope and intercept for each cooling pad was determined using Equation 1, Equation 2, and Equation 3 to convert a measured temperature, T_{meas}, to a real temperature, T_{real}. For a perfect sensor, $m_{corrected}$ should equal one and $b_{corrected}$ should equal zero.

$$m_{corrected} = \frac{T_{amb,real} - T_{ice,real}}{T_{amb,meas} - T_{ice,meas}}$$

Equation 1: Temperature Calibration Corrective Slope

$$b_{corrected} = T_{amb,real} - m_{corrected}T_{amb,meas}$$

Equation 2: Temperature Calibration Corrective Intercept

$$T_{real} = m_{corrected}T_{meas} + b_{corrected}$$

Equation 3: Temperature Calibration Correction

3.2.2 Flow Rate Sensor Calibration

Flow rate sensor calibration was done by manually adjusting the gate valve on the outlet extension pipe and measuring the volume of water exiting the pipe in a set time. The valve would then be adjusted, until the appropriate flow rate was set. The adjustment value in the program was then set, so the flow rate sensor would read the same flow rate as was measured.

3.3 Sensor Verification

Sensor verification was done for both the temperature sensors and flow rate sensor. This was to ensure that the level of accuracy of a sensor did not degrade during the course of the experiments. Verification was done by examining values recorded before and after the experiments to determine if significant changes had occurred.

3.3.1 Temperature Sensor Verification

The verification for the temperature sensors before the experiments used the same data recorded for the ambient temperature calibration. Once the sensors had reached equilibrium with the ambient temperature, the variance for each sensor was determined. A similar set of ambient equilibrium data was recorded after the experiments, and the variance of the sensors was once again calculated. A significant change in variance would indicate that a sensor failed during the course of the experiments.

3.3.2 Flow Rate Sensor Verification

Flow rate sensor verification was performed by measuring the volume of water collected from each cooling pad both before and after the experiments. The flow rate sensor was used to verify proper function of the solenoid, but not to directly measure the rate of water flow through the cooling pad due to the level accuracy of the selected sensor.

3.4 Experimental Design

The experimental design aimed to replicate heat stress conditions in the farrowing house and determine the effectiveness of the cooling pads at mitigating heat stress. Twelve selected sows were selected that were all expected to farrow on approximately the same day. Half of these were first parity sows, while the other half were third parity sows.

3.4.1 Sow Measurements

In addition to the measurements taken with the cooling pad, skin temperature, rectal temperature, and respiration rate were also recorded during the experiments. Skin temperature was measured using an infrared thermometer aimed behind the ear, as seen in Figure 14. Rectal temperature was measured using a digital stick thermometer, as seen in Figure 15. Respiration rate was measured by counting the number of breaths in a set amount of time and then multiplying by the applicable factor to determine breaths per minute.

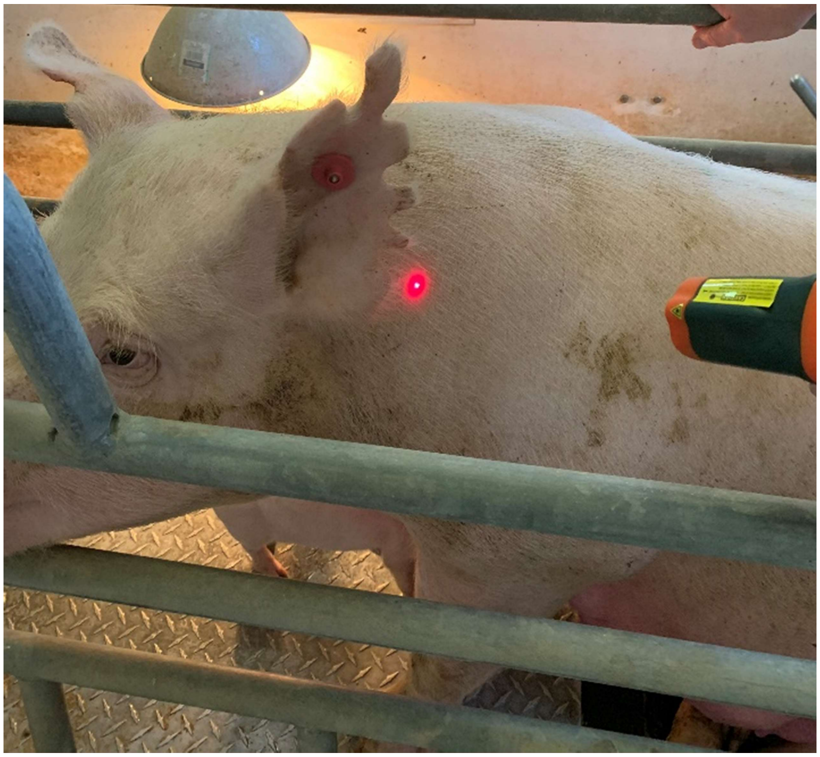

Figure 14: Measuring Sow Skin Temperature behind the Ear

Figure 15: Measuring Sow Rectal Temperature

3.4.2 Protocol Timeline

The protocol to collect the controller testing data is shown in Figure 16 and was used for each experiment conducted. At each time, sow skin temperature, rectal temperature, and respiration rate were measured. Data points 1 and 2 were taken as baseline measurements for the sows before heating or cooling started, so the effects of heat stress and the cooling pad could be compared to each sow individually. The data from these two points were averaged if both were available. The heater was then turned on and set to the desired ambient temperature. Ambient temperatures of $27°C$ and $32°C$ were used for these experiments. Once the room reached the desired temperature, two more data points were collected from each sow, approximately 30 minutes apart (data points 3 and 4). The cooling pads were then turned-on and given 40 minutes to remove any transient cooling effects. Finally, four more data points were collected from each sow, again approximately 30 minutes apart (data points 5, 6, 7, and 8). After the eighth data point was collected for each sow, the room heating was turned off, and the sows were given time to cool-down before the protocol was repeated.

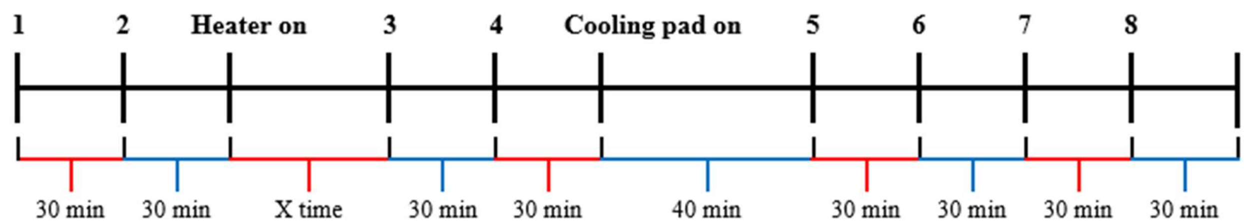

Figure 16: Experiment Protocol for Cooling Pad Controller Testing

3.4.3 Sow Treatment Assignment

Each sow was assigned to each treatment to remove the variation from sow to sow. A total of 16 experimental runs were anticipated. This corresponded to two pad control protocols (TIME and TEMP), two ambient temperatures ($27°C$ and $32°C$), and four treatments (CONTROL, LOW, MEDIUM, and HIGH). The two control types were a temporal control scheme and a temperature threshold control scheme. The four treatments were CONTROL, LOW, MEDIUM, and HIGH and were defined differently for each control scheme.

For both control schemes, the system was set so the solenoid would open for 30 seconds, and the flow rate was set to 4 L/min. This would allow for a 2 liter flush of the cooling water. The copper pipes contain approximately 1.7 liters, so 2 liters was flushed to account for any mixing that might occur. For both control schemes, cooling pads on the CONTROL treatment were set to never flush, but they were operational, so the temperature sensors could record data. The temporal control scheme utilized only the RTC module to make decisions on when to flush the water, with the frequency of flush set by the treatment. The temperature threshold control scheme utilized the three temperature sensors within the cooling pad to determine when the cooling pad should be flushed. However, the time of the last flush was also considered by the microcontroller due to the thermal diffusion delay of a recent flush. This prevented overcooling and provided a more conservative use of resources. Flushing on the temperature threshold control schemes could not occur more than once every two minutes. The threshold temperature was the parameter controlled by the treatment type for the temperature threshold control scheme. The specific parameter for each treatment and control type can be seen in Table 4.

Table 4: Treatment Parameters

	CONTROL	**LOW**	**MEDIUM**	**HIGH**
Temporal Scheme (Flush Frequency/ Effective Flow Rate)	Never 0 L/min	9 minutes OFF 0.21 L/min	6 minutes OFF 0.31 L/min	3 minutes OFF 0.57 L/min
Temperature Threshold Scheme (Threshold Temperature)	None	$28.0°C$	$29.5°C$	$31.0°C$

3.4.4 Cooling Pad Computational Model

A preliminary numerical model was developed using MathWorks MATLAB® to gain insight into the heat transfer throughout the cooling pad and guide future design decisions. The model utilized the finite difference method with two spatial dimensions and explicit forward-difference time-stepping to analyze the transient flow of heat throughout the cooling pad. While limited by small time steps to ensure convergence, the computational demand of an explicit time step was significantly less than that of an implicit time-stepping method. To ensure convergence, the stability criterion shown in Equation 4 was used to determine the timestep size at which the model was critically stable. The thermal diffusivity is α at each node, Δt_{max} is the timestep that causes the system to become critically stable, and Δx_i is the step size in the ith spatial dimension. This predicted timestep value was scaled at 99% to allow for faster computation without risking divergence of the model.

$$\frac{\max(\alpha)\,\Delta t_{max}}{\sum(\Delta x_i)^2} < \frac{1}{2}$$

Equation 4: Explicit FDM Stability Criterion

The symmetry of the cooling pad was used to reduce the computational domain by 50%. Only the section of the cooling pad where the ThinFin C was attached to the copper pipes was modeled to reduce complexity and allow for identical cross-sections throughout the domain. These pieces are connected by short sections of copper pipe that have air between them and the top aluminum diamond plate. This was deemed acceptable since each of these sections has 14 times less length than the ThinFin C sections, and α_{air} is approximately 4.5 times less than α_{Al} for the ThinFin C. Therefore, the heat transfer through these small areas was minimal and could reasonably be neglected.

Additionally, the ThinFin C sections were "unfolded" into a straight line and placed end to end by assuming that there is no heat conducted through the HDPE from one pipe to its neighbor. This was reasonable, since α_{HDPE} was more than 85 times less than α_{air}, and more than 390 times less than α_{Al} and α_{Cu}. This results in a domain that is 4.604 meters (160 inches) long by 0.0286 meters (1.125 inches) tall by 0.0762 meters (3 inches) wide. This domain is symmetric across the width and the computational domain is again halved to only 1.5 inches (0.0381 m).

As heat flows primarily through the top surface of the cooling pad, where the conductive domain is the entire 3.8 cm, to the ½" copper pipe inside the cooling pad where the water is, the area where heat transfer occurs will be primarily within the diagonal formed by the edge of the aluminum plate and the center of the copper pipe. This limited domain is highlighted in Figure 17.

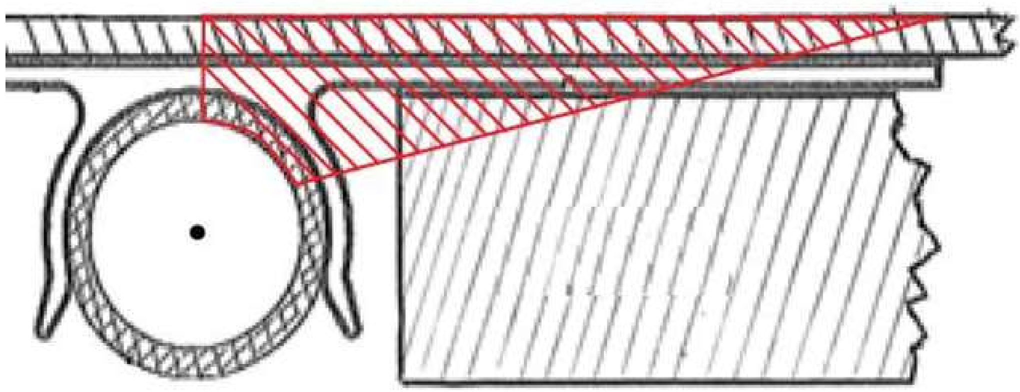

Figure 17: Numerical Model Cross Section Domain

A small angular step $d\theta$ was selected to obtain j angular nodes and k radial nodes were then selected to limit dr_{max}. Each radial line had the same number of nodes and equal node spacing in that line, but dr varied for different θ_j. By maintaining the same number of nodes in each radial line, this grid of nodes allowed the cross-sectional domain to be converted to a rectangular domain. Since the primary direction of heat transfer was assumed to be through these radial lines, an average radius was found using Equation 5, where r_{AVG} is the average radius, θ is the angle of the pipe cross section within the domain, and $r(\phi)$ is a function that describes the top of the cooling pad in polar coordinates. This value was then set to the height of the new rectangle, and the new width was found by maintaining area equal with the original domain.

$$r_{AVG} = \frac{1}{\theta} \int_{\frac{\pi}{2}-\theta}^{\frac{\pi}{2}} r(\phi) d\phi$$

Equation 5: Average Radius of Cross-Section

The transformation of the cross-section domain and the distribution of nodes can be seen in Figure 18. A reduced number of nodes is shown for clarity, rather than the full number of nodes used in the computational model. Properties at each node were determined based on the material at the physical location of each node before the transformation. Instead of unequal dr spacing, this rectangular domain had equally spaced nodes with a distance of dz between them. This value was found by dividing the new height of the domain by the number of radial nodes.

Heat transfer in the transformed domain was mainly in the vertical direction, instead of the radial direction in the original domain.

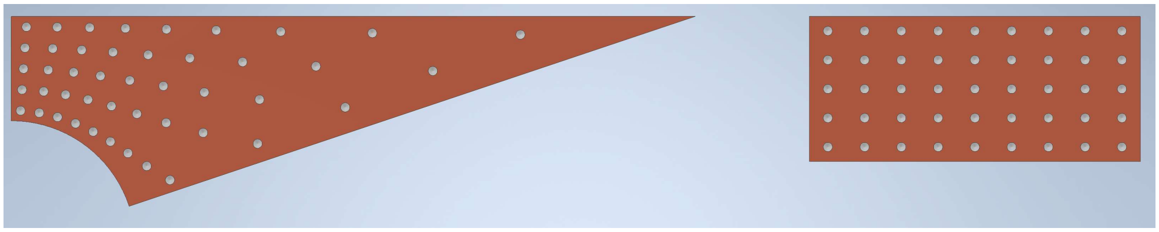

Figure 18: Transformation of Cross-Sectional Nodes

The nodes at the same vertical level in the rectangular domain were then averaged together to create a single node with properties based on the different materials at its nodes. Based on previous assumptions and domain reductions, these properties only varied in height, not with length along the pipe. This resulted in two spatial coordinates: the position of each node along the length of the copper pipe, and the distance between the node and the bottom surface of the domain. For laminar flow in a circular pipe, the critical Reynolds number is generally assumed to be 2300. For the 0.5-inch nominal copper pipe used in the cooling pads, the internal diameter was 1.38 centimeters (0.545 inches). To maintain laminar flow, the maximum velocity could be 0.217 m/s. This corresponds to a maximum volumetric flow rate of approximately 2 L/min. Since the flow is split in the current cooling pad design, the maximum laminar flow rate is approximately 4 L/min. As the distance between nodes along the length was small, it was reasonable to assume a constant surface temperature for pipe surface for each node, and therefore the calculations use a constant Nusselt number of 3.66 to determine the convective heat transfer coefficient for fully developed laminar flow in a circular pipe. The flow is also assumed to be both fully thermally and hydrodynamically developed by the time it reaches the cooling pad. As a result, entrance region effects are neglected in the model.

4. RESULTS

Due to limited lactation time and personnel constraints, only nine of the sixteen anticipated experiments were performed. One experiment was performed at an ambient temperature of $27°C$, and the remaining eight at an ambient temperature of $32°C$. This was determined to be the best use of limited resources, as it allowed a full comparison of control schemes at a level of moderate heat stress and a preliminary analysis of the effects of ambient temperature to still be completed.

4.1 Calibration of Sensors

Sensors were calibrated after installation at the testing facility, shortly before all experiments were conducted. Calibration required approximately one day to complete. The ambient temperature calibration point for each pad was measured in the morning after being at relative steady state during the previous night, and the ice water calibration point was measured during the afternoon. Raw data for calibration is provided in Appendix A.

4.1.1 Temperature Sensor Calibration

The values used for the calibration of the temperature sensors can be seen in Table 5 and Table 6. The calibrated values used the six temperature probes on each cooling pad can be seen in Table 7.

Table 5: Ambient Temperature Sensor Calibration Values

Crate Number	Measured Temperature (°C)	Real Temperature (°C)
1	20.5	21.8
2	21.0	20.5
3	24.0	25.5
4	23.0	23.0
5	22.5	23.0
6	23.5	23.0
7	22.0	21.7
8	25.0	26.2
9	21.5	22.0
10	23.5	23.0
11	23.5	23.0
12	22.0	23.0

Table 6: Ice Water Temperature Sensor Calibration Values

Crate Number	Measured Temperature (°C)	Real Temperature (°C)
1	0	-0.8
2	0	-1.5
3	0	-1.5
4	0.5	-0.4
5	-0.5	0
6	-0.5	-0.1
7	-0.5	-0.1
8	-0.5	-0.5
9	-0.5	-0.6
10	-0.5	-0.6
11	-0.4	0
12	-0.5	0

Table 7: Calibration Coefficients for Temperature Sensors

Crate Number	Slope Coefficient ($m_{corrected}$)	Intercept Coefficient ($b_{corrected}$)
1	1.10	-0.78
2	1.05	-1.50
3	1.13	-1.50
4	1.04	-0.91
5	1.00	0.50
6	0.96	0.37
7	0.97	0.37
8	1.05	0.02
9	1.03	-0.10
10	0.98	-0.12
11	0.96	0.36
12	1.02	0.51

4.1.2 Flow Rate Calibration

The calibration of the flow rate sensors was performed to achieve a flow rate of 4 L/min. The gate valve on each cooling pad was adjusted, until the fluid measured in a graduated cylinder was 2 liters after 30 seconds. The measured flow rate for each cooling pad is shown in Table 8.

Table 8: Flow Rate Calibration Measurements

Crate Number	Measured Flow Rate (L/30s)	Measured Flow Rate (L/min)	Percent Error (%)
1	1.97	3.94	-1.5
2	2.01	4.02	0.5
3	2.00	4.00	0
4	2.04	4.08	2.0
5	1.94	3.88	-3.0
6	2.00	4.00	0
7	1.98	3.96	-1.0
8	1.96	3.92	-2.0
9	1.97	3.94	-1.5
10	1.93	3.86	-3.5
11	1.94	3.88	-3.0
12	2.00	4.00	0

4.2 Verification of Temperature Sensors

The initial variance of each sensor was determined using the same data recorded for the calibration of the temperature sensors. The code was then run again after all experiments were completed to determine the change in variance for each sensor. Sensors with significant increases in variance were removed before all analyses were performed. The variance for each sensor before and after the experiments were performed, in $°C^2$, and can be seen in Table 9. Sensors that could not be read for the post-experiment variance are indicated with an X. The standard deviations of the pre- and post-experiment variances were determined to be PRETEST STD and POSTTEST STD, and the post-experiment variance mean was POSTTEST MEAN. The two conditions for a sensor to be identified as a failed sensor were:

1. Have a post-experiment variance greater than its pre-experiment variance; and
2. Have a post-experiment variance at least two standard deviations above the post-experiment mean.

Sensors that met this failure criteria are highlighted with bold in Table 9.

Table 9: Variance of Temperature Sensors

Crate Number	**Sensor Location**											
	Pad Rear		**Pad Mid**		**Pad Head**		**Inlet**		**Outlet**		**Ambient**	
	Pre	**Post**	**Pre**	**Post**	**Pre**	**Post**	**Pre**	**Post**	**Pre**	**Post**	**Pre**	**Post**
1	**0.08**	**X**	**0.39**	**X**	**0.70**	**X**	0.00	0.04	0.06	0.06	0.00	0.06
2	**0.24**	**X**	**0.07**	**X**	**0.11**	**X**	0.04	0.00	0.00	0.00	0.00	0.00
3	**0.00**	**0.31**	0.05	0.14	0.00	0.06	0.00	0.00	0.00	0.02	0.00	0.03
4	0.00	0.00	0.00	0.06	0.04	0.00	0.00	0.00	0.01	0.06	0.00	0.00
5	0.00	0.00	0.00	0.00	0.00	0.00	0.00	0.00	0.00	0.05	**0.00**	**0.22**
6	0.00	0.00	0.00	0.00	0.00	0.00	0.00	0.00	0.00	0.00	**0.00**	**X**
7	**0.10**	**X**	0.10	0.00	0.01	0.00	0.00	0.00	0.00	0.00	0.00	0.00
8	0.00	0.00	0.04	0.00	0.00	0.00	0.00	0.06	0.00	0.00	0.01	0.00
9	**0.13**	**X**	0.06	0.00	0.00	0.00	0.03	0.00	**0.00**	**X**	0.00	0.04
10	0.00	0.00	0.06	0.00	0.06	0.00	0.00	0.00	0.00	0.06	0.00	0.00
11	0.00	0.00	0.00	0.00	0.00	0.00	0.00	0.06	0.00	0.00	0.00	0.05
12	0.05	0.00	0.00	0.00	0.00	0.00	0.00	0.04	0.00	0.01	0.00	0.00

4.3 Effect of Ambient Temperature on Heat Stress

The heat transfer efficiency and cooling effectiveness at ambient temperatures of $27°C$ and $32°C$ were compared for the single experimental run of temperature threshold control schemes at $27°C$ that was completed. Raw temperature and flow data for these runs is presented in Appendix B. Each sow was only compared to itself given that all sows were not able to receive all treatments at an ambient temperature of $27°C$. The mean values for each treatment group, as well as the increase in heat transfer per degree of ambient temperature increase, can be seen in Table 10.

Table 10: Treatment Averaged Cooling Pad Metrics for Different Ambient Temperatures

Temperature Threshold Treatment Group	Ambient Temperature				Difference Between Ambient Temperatures	
	$27°C$		$32°C$			
	Heat Transfer (W)	Cooling Effectiveness (kJ/L)	Heat Transfer (W)	Cooling Effectiveness (kJ/L)	Heat Transfer (W/°C)	Cooling Effectiveness (kJ/L/°C)
CONTROL	0	0	0	0	0	0
$\mathbf{28.0°C}$	322	33.6	444	35.0	24.5	0.27
$\mathbf{29.5°C}$	X	X	X	X	X	X
$\mathbf{31.0°C}$	195	51.9	308	36.1	22.8	-3.15

4.4 Cooling Pad Metrics

Using all twelve sows, mean values for the average surface temperature of the cooling pad and the average heat transfer efficiency were sampled from the raw data in two ways. First, the data was divided into four, forty minute sections to examine major effects over the time that the cooling pads were turned on. Second, the data for each sow was sampled for each flush cycle, beginning with the 30 second flush. This provided finer resolution data that allowed a curve to be fit to each dependent variable and treatment group. The incremental heat transfer rate, $\Delta\dot{Q}$, was defined according to Equation 6, where $\dot{m}$ is the mass flow rate of water moving through the pipe, c_p is the constant pressure specific heat capacity of the water, and ΔT is the temperature difference between the inlet and outlet pipes of the cooling pad. This value was calculated for each data point before the data was resampled.

$$\Delta\dot{Q} = \dot{m}c_p\Delta T$$

Equation 6: Incremental Heat Transfer Rate

By multiplying these incremental heat transfer rates by the data point sampling frequency, Δt, the incremental energy removed in that time span was determined. These values were then aggregated to determine the total energy removed by the water and divided by the total volume of water used to acquire the cooling effectiveness. Analysis was performed separately on temporal and temperature threshold schemes to simplify comparisons to the control treatment group and allow for greater differences in the model of each control scheme.

The potential effects for 40-minute sampled data were treatment, time, the interaction of treatment and time, sow body weight, parity, sow backfat thickness, and sow loin depth, where time was an integer value from one to four representing which section of the protocol the data were sampled. Effects with P>0.20 were removed and the model was rerun to better elucidate the significance of remaining effects. All analysis was performed in SAS using the PROC MIXED procedure. Figures were generated from the resulting least square means using the Matplotlib package in Python. The only significant interaction between treatment and time was for the average pad temperatures among the temporal schemes, as shown in Figure 19. The average pad temperatures among temperature threshold schemes with no interaction effect can be seen in Figure 20. Additionally, the average heat transfer rates with no interaction effect for temporal and temperature threshold schemes can be seen in Figure 21 and Figure 22, respectively. R2 values for each dependent factor model, both with and without covariates included for models with at least one significant covariate, can be seen in Appendix D: Effects of Covariates.

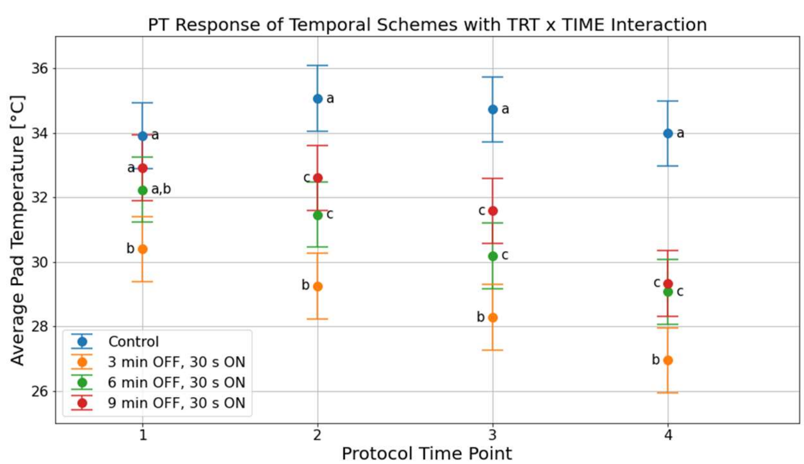

Figure 19: Average Pad Temperatures for Temporal Schemes on 40-Minute Averaged Data

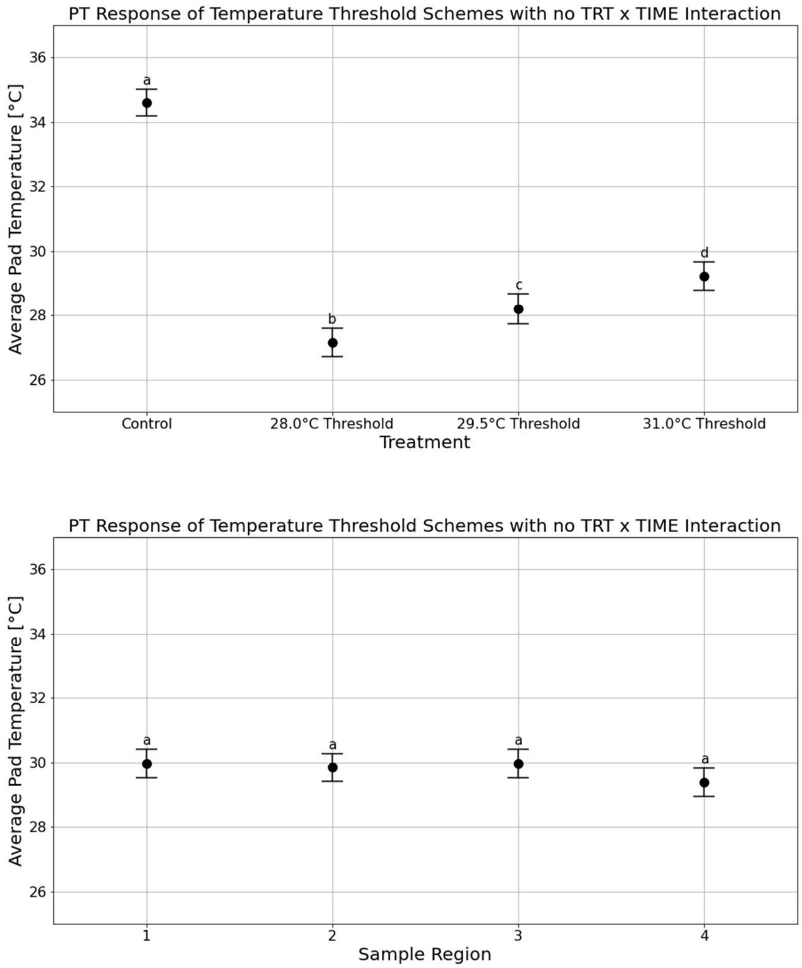

Figure 20: Average Pad Temperatures for Temperature Threshold Schemes (top) and Sample Region (bottom) on 40-Minute Averaged Data

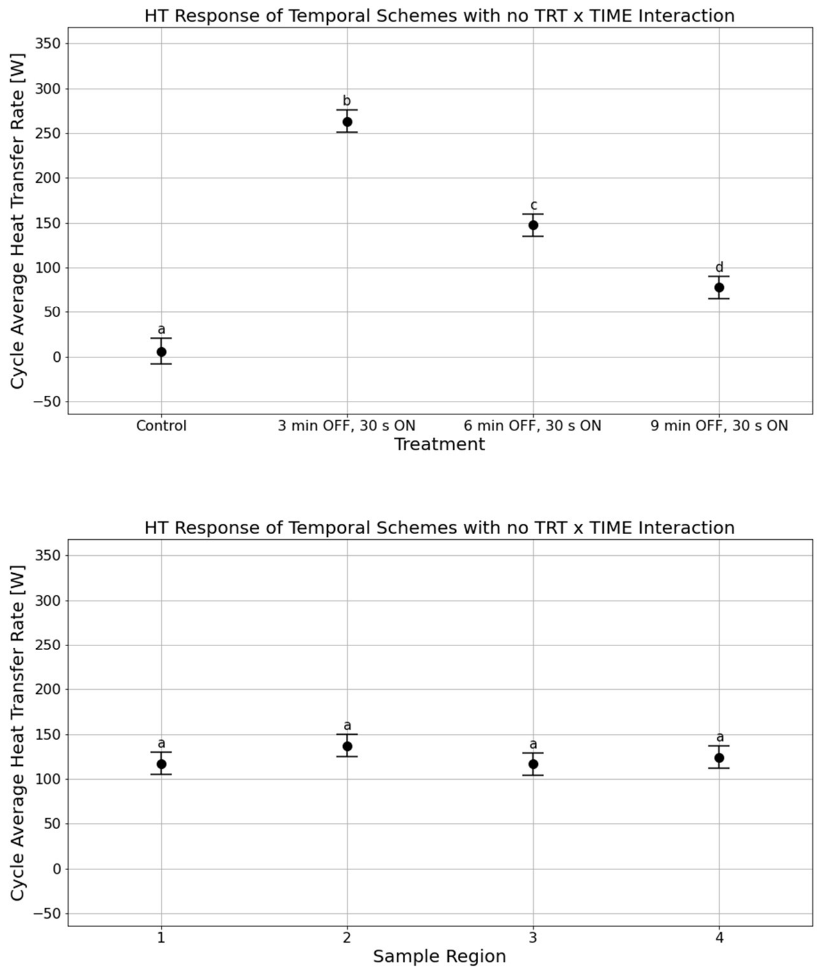

Figure 21: Average Heat Transfer Rates for Temporal Schemes (top) and Sample Region (bottom) on 40-Minute Averaged Data

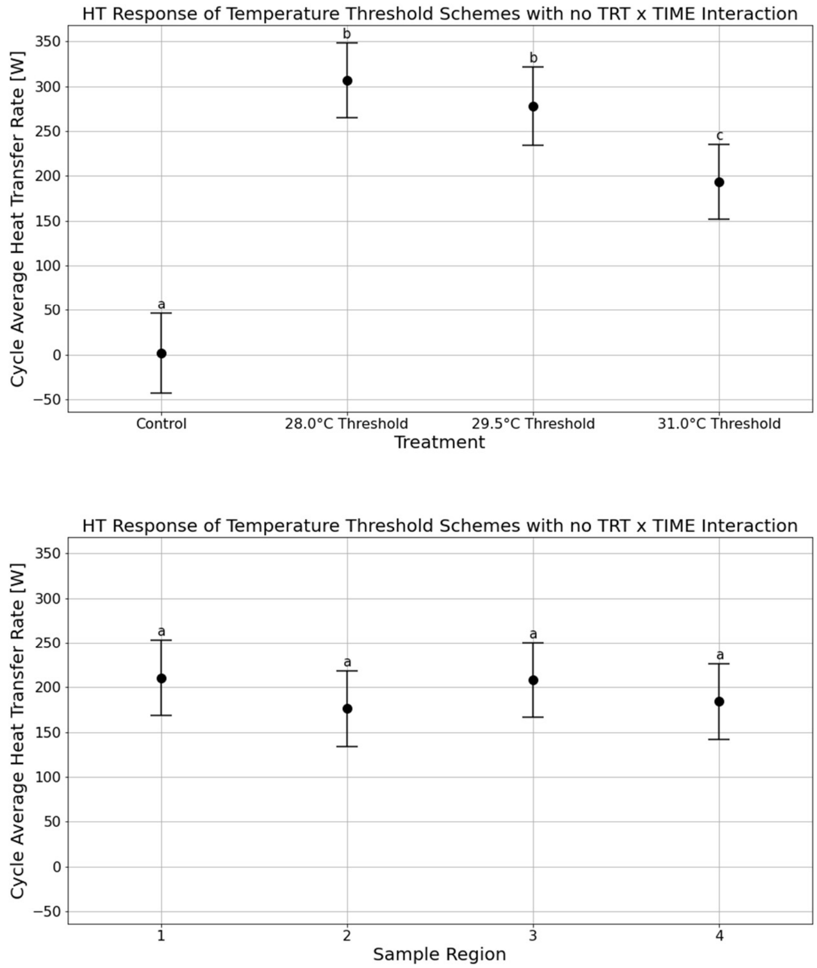

Figure 22: Average Heat Transfer Rates for Temperature Threshold Schemes (top) and Sample Region (bottom) on 40-Minute Averaged Data

For the flush sampled data, the time parameter was the number of seconds between the cooling pad turning on and the start of the flush. The PROC MIXED procedure in SAS was used to determine the significant effects for each dependent variable and subset of the data. Once significant effects were determined, each treatment group was run individually to calculate the coefficients of the fitted curve. The potential effects were treatment, powers of time from one to four, and the interaction of treatment with each power of time. After coefficients for each treatment group were calculated, time was converted from seconds to minutes and figures were generated using the Matplotlib package in Python. The average pad temperatures for the temporal and temperature threshold schemes can be seen in Figure 23 and Figure 24, respectively. The heat transfer rate for the temporal and temperature threshold schemes can similarly be seen in Figure 25 and Figure 26, respectively. The R2 value for each of the fitted curves can be seen in Table 11.

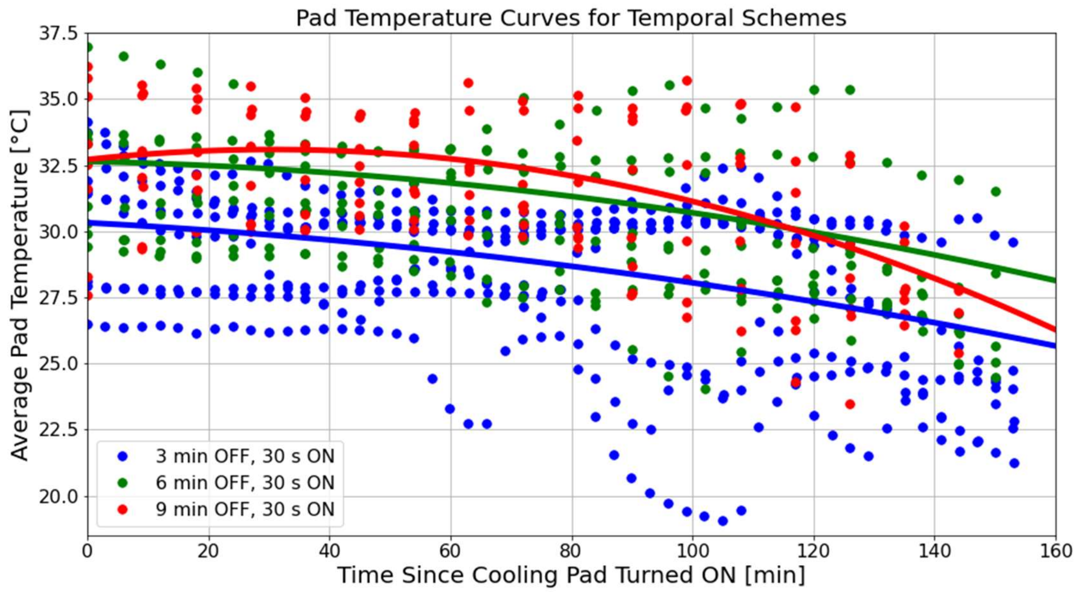

Figure 23: Average Pad Temperatures for Temporal Schemes

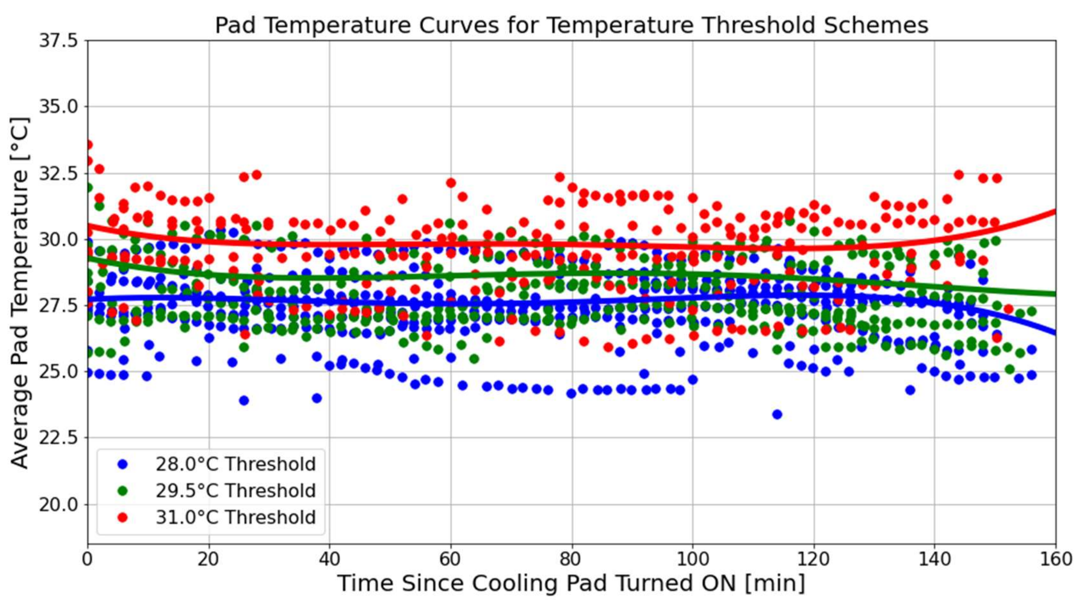

Figure 24: Average Pad Temperatures for Temperature Threshold Schemes

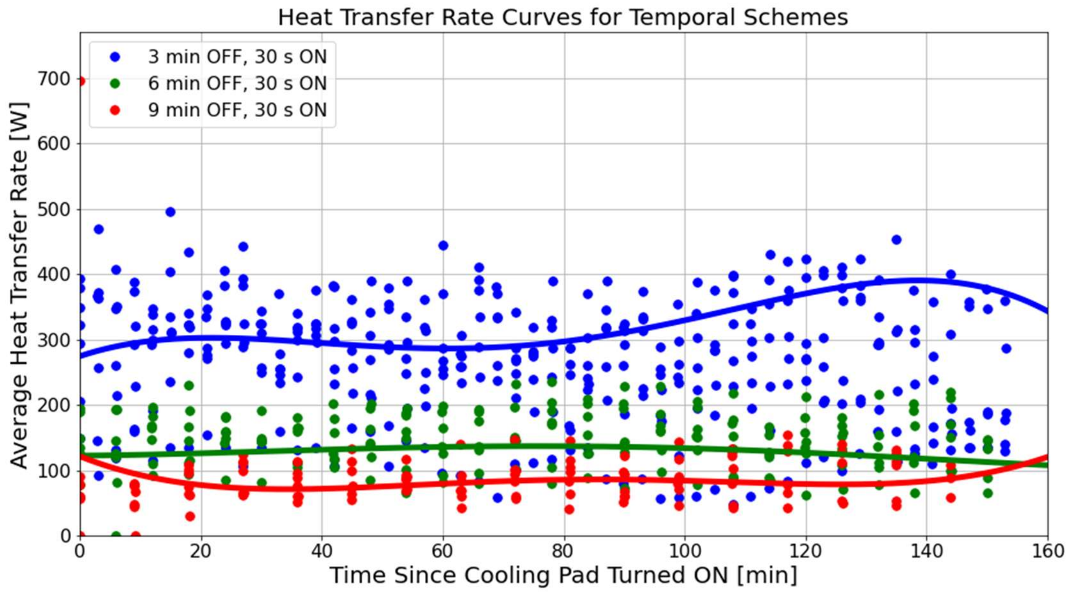

Figure 25: Heat Transfer Rates for Temporal Schemes

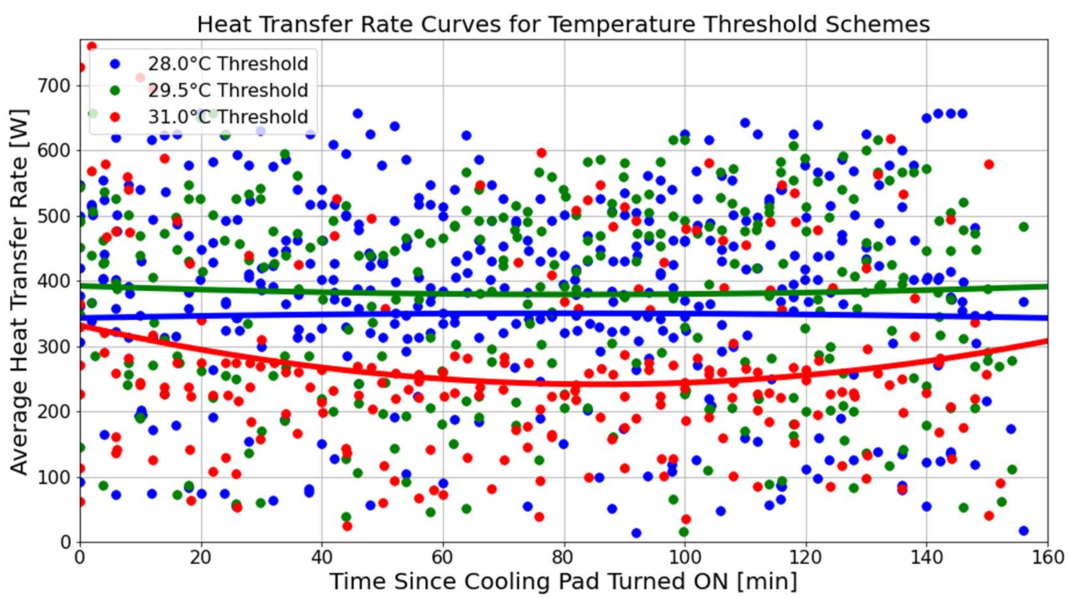

Figure 26: Heat Transfer Rates for Temperature Threshold Schemes

Table 11: R2 Values for Curves Fitted to Flush Sampled Data

Treatment	**Average Pad Temperature R2 Value**	**Heat Transfer Rate R2 Value**
3 MIN	75.51%	60.67%
6 MIN	73.59%	61.93%
9 MIN	74.98%	12.91%
$28.0°C$	88.97%	67.09%
$29.5°C$	77.53%	41.51%
$31.0°C$	91.34%	35.82%

The heat transfer rate curves were sampled at 6 second intervals to match the frequency that the cooling pads recorded data. This resulted in 1601 data points for each treatment group. These values were then used to determine the cooling effectiveness of each control scheme at each time point by calculating an equivalent continuous flow rate based on the total volume flushed during the experiment and the total energy transfer in that time interval. Both the heat transfer rate and cooling effectiveness for each treatment were compared in Python using a one-way ANOVA from the SciPy package. Both the heat transfer rate (F 5, 9600 = 65789, P < 0.0001) and cooling effectiveness (F 5, 9600 = 5109, P < 0.0001) were significant at a 95% confidence level. A Tukey test was then applied to each dataset to determine which pairs of means were significantly different. All treatment pairs were significantly different for heat transfer rate, and all treatment pairs except the 6 MIN – 9 MIN pair (P = 0.3293) were significantly different for cooling effectiveness. The mean and standard error for each treatment group is shown in Table 12. The Tukey adjusted p-values for each pairwise comparison of treatments can be seen in Table 13 and Table 14. Significant differences between treatment groups at $\alpha = 0.05$ are indicated in bold. Treatment groups are summarized in Table 15 using a compact letter display to identify statistically significant differences at the α=0.05 significance level. Figure 27 and Figure 28 graphically compare the mean heat transfer efficiency and cooling effectiveness for each treatment.

Table 12: Cooling Pad Metric Results

Treatment	Heat Transfer Efficiency (W)		Cooling Effectiveness (kJ/L)	
	Mean	Std. Err.	Mean	Std. Err.
3 MIN	324	0.94	60.7	0.18
6 MIN	128	0.20	46.6	0.07
9 MIN	84	0.26	47.0	0.14
$28.0°C$	348	0.05	53.2	0.01
$29.5°C$	383	0.09	63.9	0.02
$31.0°C$	268	0.61	64.7	0.15

Table 13: Heat Transfer Efficiency Tukey-Kramer Adjusted p-Values

	3 MIN	6 MIN	9 MIN	$28.0°C$	$29.5°C$	$31.0°C$
3 MIN		**0.001**	**0.001**	**0.001**	**0.001**	**0.001**
6 MIN			**0.001**	**0.001**	**0.001**	**0.001**
9 MIN				**0.001**	**0.001**	**0.001**
$28.0°C$					**0.001**	**0.001**
$29.5°C$						**0.001**
$31.0°C$						

Table 14: Cooling Effectiveness Tukey-Kramer Adjusted p-Values

	3 MIN	6 MIN	9 MIN	$28.0°C$	$29.5°C$	$31.0°C$
3 MIN		**0.001**	**0.001**	**0.001**	**0.001**	**0.001**
6 MIN			0.3265	**0.001**	**0.001**	**0.001**
9 MIN				**0.001**	**0.001**	**0.001**
$28.0°C$					**0.001**	**0.001**
$29.5°C$						**0.001**
$31.0°C$						

Table 15: Compact Letter Display for $\alpha = 0.05$ Significance Level

	Heat Transfer Efficiency	Cooling Effectiveness
3 MIN	a	a
6 MIN	b	b
9 MIN	c	b
$\mathbf{28.0°C}$	d	c
$\mathbf{29.5°C}$	e	d
$\mathbf{31.0°C}$	f	e

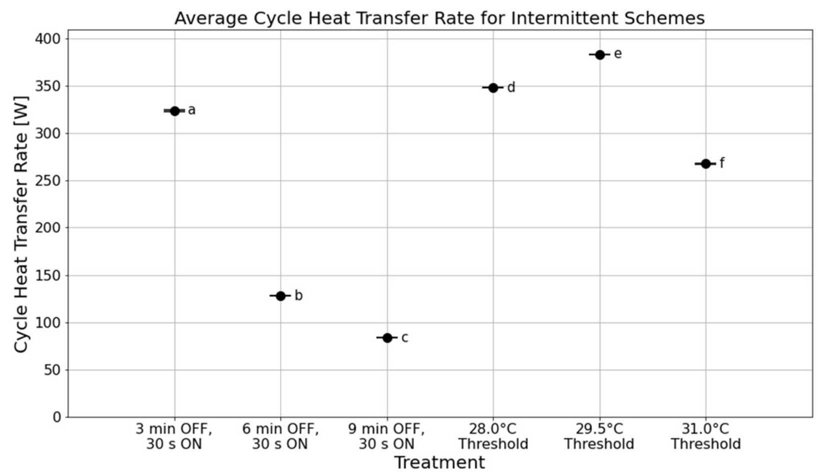

Figure 27: Heat Transfer Efficiency of Each Treatment

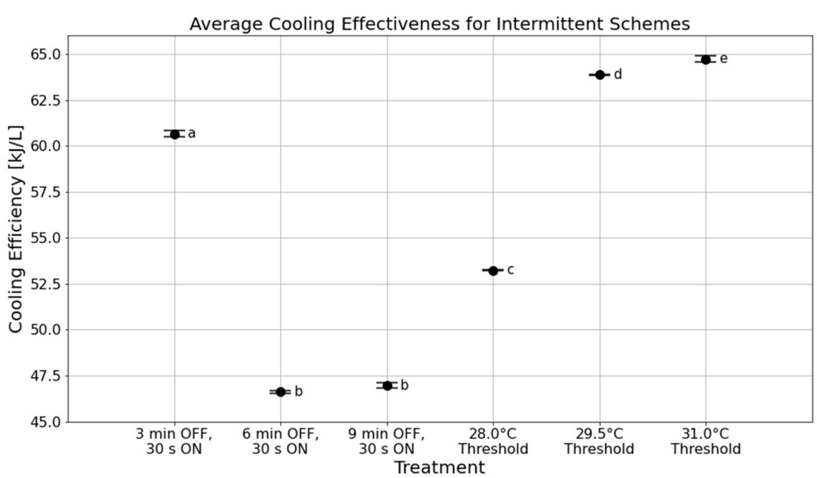

Figure 28: Cooling Effectiveness of Each Treatment

For the temperature threshold control schemes, the flush frequency was variable and depended on how much heat the sow produced. To allow for comparison with temporal control schemes, an average flush frequency was calculated by dividing the total number of flushes by the total time that the cooling pad was operational. The average cycle time for each temperature threshold control scheme can be seen in Table 16.

Table 16: Average Flush Frequencies of Temperature Threshold Control Schemes

Temperature Threshold Control Scheme	Average Cycle Time
$28.0°C$	4 min 36 s OFF, 30 s ON
$29.5°C$	5 min 3 s OFF, 30 s ON
$31.0°C$	7 min 34 s OFF, 30 s ON

4.5 Physiological Metrics

The skin temperature, respiration rate, and rectal temperature of each sow were recorded at each of the eight points identified in the experiment protocol. Raw physiological data for the runs under consideration is shown in Appendix C. Skin temperature, respiration rate, and rectal temperature were each compared among temporal and temperature threshold schemes using the PROC MIXED procedure in SAS. The potential effects considered were treatment, time, the interaction between treatment and time, sow body weight, parity, sow backfat thickness, and sow loin depth, where time was the protocol time point labeled in Figure 16. Effects in the initial model with a P-value greater than 0.20 were removed before continuing, with the same process used for the 40-minute sampled cooling pad data. There was no significant interaction effect on skin temperature for either temporal or temperature threshold schemes, with the resulting least square means shown in Figure 29 and Figure 30, respectively. In both cases, treatment was not significant, and the protocol time point was significant, with the first two time points before the heater was turned on corresponding to lower skin temperatures than the six time points once the room was heated to $32°C$. R2 values for each model can be seen in Appendix D: Effects of Covariates.

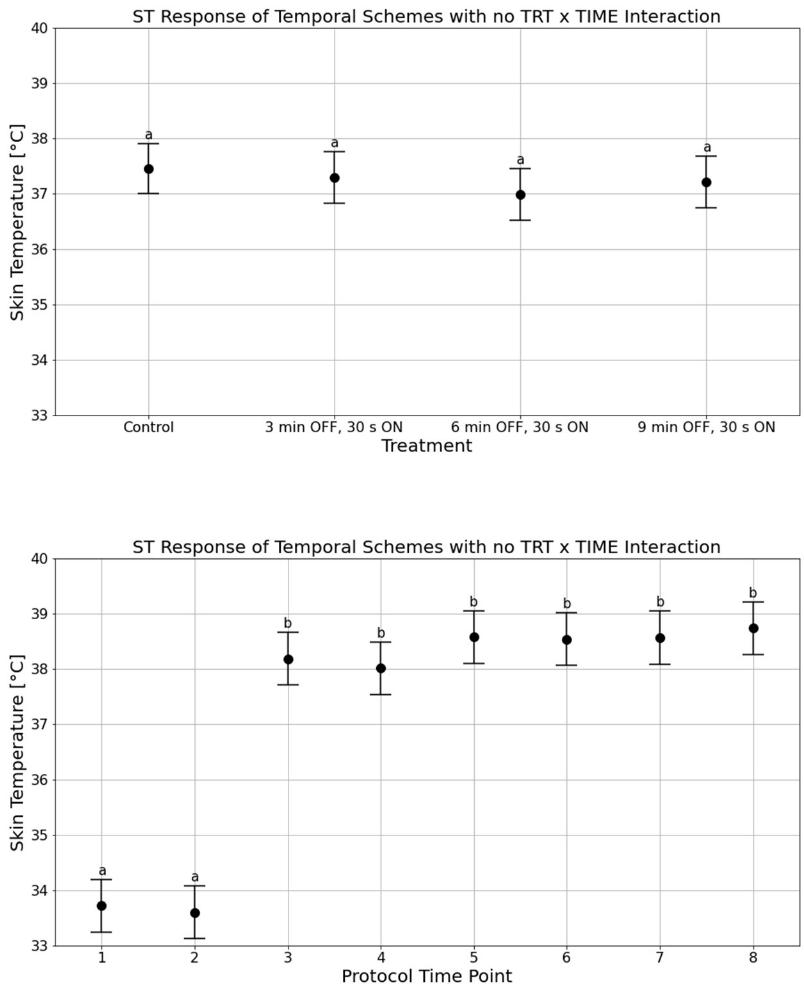

Figure 29: Skin Temperatures for Temporal Schemes (top) and Protocol Time Points (bottom)

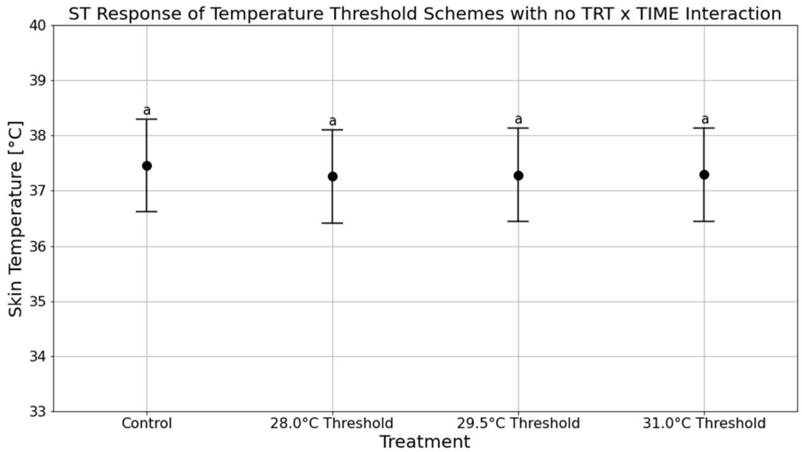

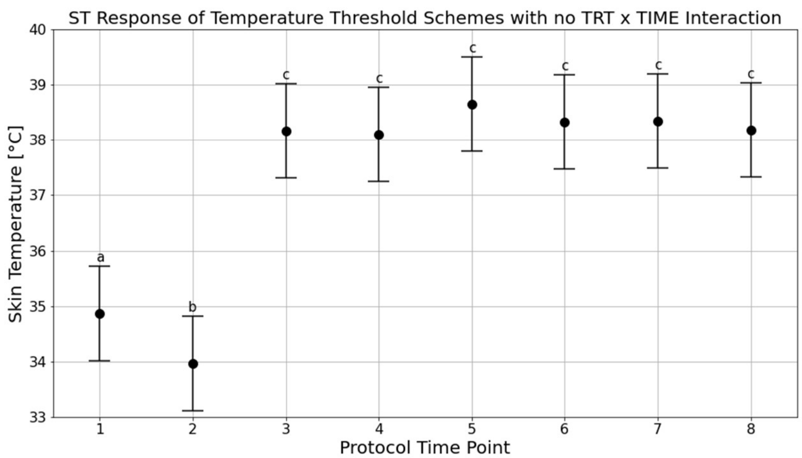

Figure 30: Skin Temperatures for Temperature Threshold Schemes (top) and Protocol Time Points (bottom)

There was a significant interaction between treatment and time for respiration rate for the temperature threshold schemes (P < 0.0001) and a tendency for interaction on the temporal schemes (P = 0.0922). Removal of the interaction from the temporal model resulted in increased AIC and residual variance, indicating a lower quality fit of the data. Therefore, the interaction between treatment and time was retained in the final model. The respiration rates at each protocol time point can be seen in Figure 31 for the temporal schemes, and Figure 32 for the temperature threshold schemes.

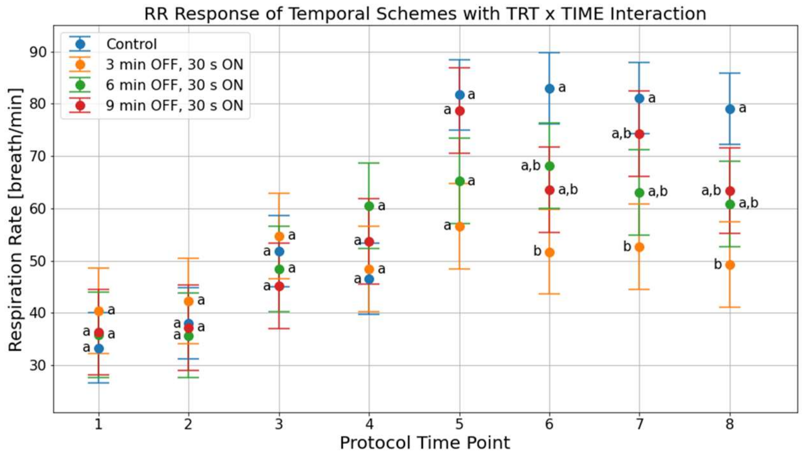

Figure 31: Respiration Rates for Temporal Schemes

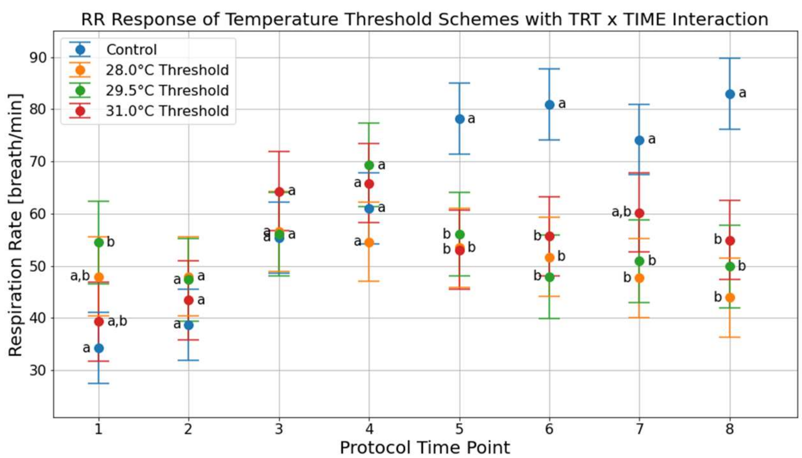

Figure 32: Respiration Rates for Temperature Threshold Schemes

The rectal temperatures also demonstrated a significant interaction effect between treatment and time for the temporal ($P = 0.0004$) and temperature threshold ($P < 0.0001$) schemes. While none of the factors besides treatment, time, and their interaction were significant for the temporal schemes, sow body weight ($P = 0.0379$), parity ($P = 0.0128$), and sow loin depth ($P = 0.0087$) were all significant effects for the temperature threshold control schemes. The rectal temperatures at each protocol time point can be seen in Figure 33 for the temporal schemes, and Figure 34 for the temperature threshold schemes.

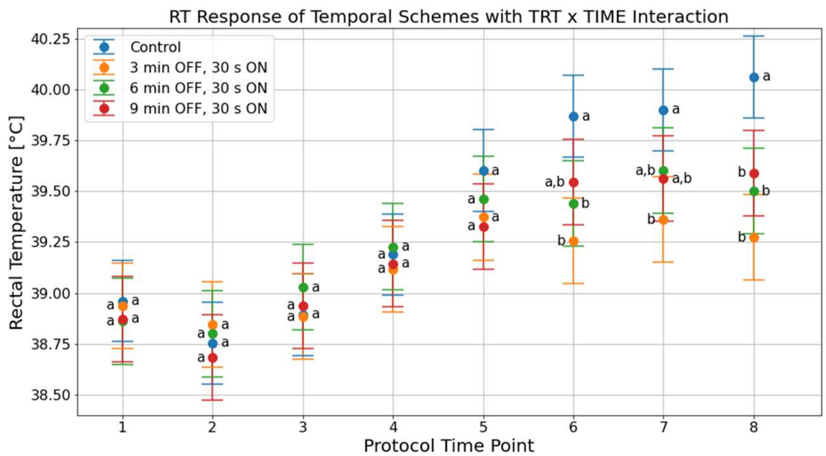

Figure 33: Rectal Temperatures for Temporal Schemes

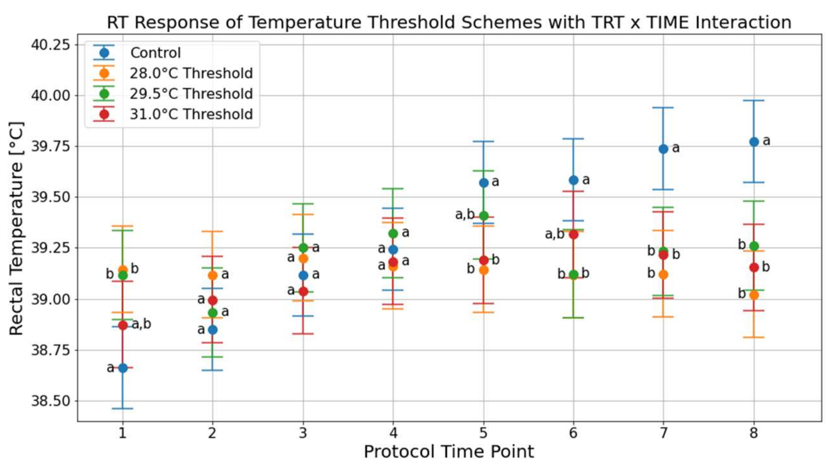

Figure 34: Rectal Temperatures for Temperature Threshold Schemes

4.6 Numerical Heat Transfer Analysis of Cooling Pad

Using the model developed in MATLAB®, parameters were first provided to compare the model outputs with previous cooling pad experiment data. Once verified, the model would be used to examine transient flow behavior at multiple flow rates and sow temperatures to provide guidance on future design modifications.

4.6.1 Verification of Numerical Model

Two sets of previous data were used to verify the accuracy of the model. Table 17 shows the average heat transfer rate and cooling effectiveness obtained by Cabezon et al. (2018) compared with those output by the numerical model for equivalent ambient temperatures and flow rates, along with the percent error in the model.

Table 17: Numerical Model Comparison with Cabezon et al. (2018)

Result Source	Parameters			
	$T_{ambient} = 27°C$		$T_{ambient} = 32°C$	
	$0.25\ L/min$	$0.5\ L/min$	$0.25\ L/min$	$0.5\ L/min$
Cabezon et al. (2018)	116.1 W 27.86 kJ/L	132.1 W 31.70 kJ/L	138.0 W 16.56 kJ/L	181.4 W 21.77 kJ/L
Numerical Model	580.7 W 139.4 kJ/L	580.7 W 69.68 kJ/L	580.7 W 139.4 kJ/L	580.7 W 69.68 kJ/L
Model Percent Error	400.2%	339.6%	320.8%	220.1%

To test the numerical model at higher flow rates, a similar comparison was evaluated using data from Cabezon et al. (2020), as seen in Table 18. This article provides data on both the original 6-pipe cooling pad design and the current 8-pipe design. Verification of the model for both cases will allow future optimization of the number of pipes in the cooling pad.

Table 18: Numerical Model Comparison with Cabezon, Field, Winslow, Schinckel, & Stwalley (2020)

Result Source	Parameters	
	$T_{ambient} = 27°C, 2.6\frac{L}{min}, 18°C\ inlet\ water$	
	$6 - Pipe\ Design$	$8 - Pipe\ Design$
Cabezon et al. (2020)	261.8 W 5.025 kJ/L	305.3 W 5.842 kJ/L
Numerical Model	483.5 W 11.16 kJ/L	580.7 W 13.40 kJ/L
Model Percent Error	84.7%	90.2%

5. DISCUSSION & CONCLUSION

5.1 Comparison of Tested Intermittent Control Schemes

Two major analyses were made utilizing the collected dataset. The first was a partial evaluation of the effect of ambient temperature on the heat transfer efficiency and cooling effectiveness of the Purdue cooling pad system. The second was a detailed examination of different control scheme types and parameters at an ambient temperature of $32°C$.

5.1.1 Preliminary Evaluation of Ambient Temperature

Due to practical limitations within the farrowing barn, only one of the eight anticipated experiments at an ambient temperature of $27°C$ was completed. This prevented a detailed analysis on the effect of ambient temperature. However, a preliminary comparison for each treatment was completed by comparing each sow at $27°C$ to itself at $32°C$. Heat transfer efficiency and cooling effectiveness were calculated for each sow at both ambient temperatures. The difference of each variable between the two ambient temperatures was then divided by the difference in ambient temperatures to examine the change in heat transfer efficiency and cooling effectiveness on a per degree basis. Although the sample sizes were small, and sows were not able to be exposed to all treatments, the heat transfer efficiency and cooling effectiveness showed substantial similarity between the two remaining cooling treatments, as seen in Table 10. Heat transfer efficiency increased on average by $23.65\ W/°C$ and only differed by $1.7\ W/°C$ between the cooling treatments. The cooling effectiveness differed significantly among treatment groups and no clear preliminary trend could be determined. This may suggest a linear relationship between heat transfer efficiency and the ambient temperature of the farrowing barn for temperature threshold control schemes, but all sows should be exposed to all treatments at both ambient temperatures to increase the sample size of each treatment and allow each sow to act as their own control. Additionally, a more thorough study should test the temporal control schemes as well, to examine if the linear relationship applies to all control scheme types. If the preliminary data collected is verified by larger sample sizes, then heat transfer efficiency should be expected to increase at a rate of approximately $23.65\ W/°C$.

5.1.2 Comparison of Control Schemes at 32°C

All eight planned experiments at an ambient temperature of $32°C$ were completed, which allowed every sow to be exposed to every treatment level and type. The $29.5°C$ temperature threshold scheme removed $383\ W$ on average, followed by the $28.0°C$ temperature threshold scheme. The 3 minute OFF temporal scheme also removed greater than 300 W on average. The $31.0°C$ temperature threshold scheme removed greater than 250 W, while the 6 and 9 minute OFF temporal schemes both removed less than $150\ W$. The average OFF cycle time was about 4.5 minutes for the $28.0°C$ temperature threshold scheme, 5 minutes for the $29.5°C$ temperature threshold scheme, and 7.5 minutes for the $31.0°C$ temperature threshold scheme. Interestingly, the 3 minute scheme exhibited a lower average heat transfer efficiency than the $28.0°C$ and $29.5°C$ temperature threshold schemes, even though it had a shorter average cycle time than the temperature threshold schemes.

The cooling effectiveness values for the six cooling treatment groups were significantly different from each other with the exception of the 6 minute OFF and 9 minute OFF temporal schemes, at a significance level of $\alpha = 0.05$. The cooling effectiveness ranged from 46.6 to 60.7 kJ/L among temporal control schemes and 53.2 to 64.7 kJ/L among temperature threshold control schemes.

5.2 Comparison with Previous Studies

The key results for each of the six cooling treatments examined are shown in Table 19 for comparison with past studies. Effective flow rate and cycle time were determined based on the number of flushes during the experiment duration for temperature threshold control schemes.

Table 19: Flow Rates & Cooling Pad Metrics

Treatment	Effective Cycle Time (including 30s flush)	Effective Flow Rate (L/min)	Heat Transfer Efficiency (W)	Cooling Effectiveness (kJ/L)
3 MIN	3.5 min	0.57	324	60.7
6 MIN	6.5 min	0.31	128	46.6
9 MIN	9.5 min	0.21	84	47.0
$\mathbf{28.0°C}$	5.10 min	0.39	348	53.2
$\mathbf{29.5°C}$	5.55 min	0.36	383	63.9
$\mathbf{31.0°C}$	8.07 min	0.25	268	64.7

5.2.1 Comparison with Previous Continuous Flow Studies

Cabezon et al. (2018) utilized the same 8-pipe design of the cooling pad but examined continuous flow rates of 0.25 and $0.5\ L/min$ at an ambient temperature of $32°C$. The $0.25\ L/min$ continuous flow rate was most comparable to the flow rate of the $31.0°C$ temperature threshold scheme, which had 194% the heat transfer efficiency of the continuous flow. Additionally, the intermittent flow control scheme had about 95% more cooling effectiveness than the $0.25\ L/min$ continuous flow. The $28.0°C$ temperature threshold scheme and 3 min OFF temporal scheme had the most similar flow rates to the $0.5\ L/min$ continuous flow, with effective flow rates of 0.39 and $0.57\ L/min$, respectively. They had 92% and 79% greater heat transfer efficiency and 144% and 179% greater cooling effectiveness than the $0.5\ L/min$ continuous flow treatment from Cabezon et al. (2018). This demonstrates that for similar effective flow rates, intermittent flow schemes not only better utilize the cooling capacity of the water by allowing it to warm up more before exiting the cooling pad, they also have greater heat transfer rates, which allows for better mitigation of heat stress in the sow.

Cabezon, Field, Winslow, Schinckel, & Stwalley (2020) performed continuous flow treatments with a continuous flow rate of $2.6\ L/min$ at an ambient temperature of $27°C$. The 8-pipe cooling pad exhibited a heat transfer efficiency of $305.3\ W$ and a cooling effectiveness of $7.05\ kJ/L$. This is a similar heat transfer efficiency to the 3 min OFF temporal scheme, but only about 12% of the cooling effectiveness. Using the preliminary temperature rate increase for heat transfer efficiency calculated previously to estimate the heat transfer of this continuous scheme at $32°C$, the heat transfer efficiency would be approximately 424 W. This demonstrates that continuous flow schemes at similar actual flow rates will remove more heat than intermittent schemes. The cooling effectiveness would be expected to be greater at greater ambient temperatures, but it is improbable that there would be eight times the cooling effectiveness at $5°C$ greater ambient temperature. As a result, the cooling effectiveness of intermittent schemes will still significantly outperform similar continuous flow schemes.

These results reaffirm that intermittent flow control schemes better utilize the cooling water flowing through the cooling pad than continuous flow systems. However, higher levels of heat transfer efficiency can be reached with continuous flow. Continuous flow is primarily convective heat transfer, rather than the intermittent flow control schemes that utilize both conductive and convective heat transfer.

5.2.2 Comparison with Previous Intermittent Flow Studies

The most similar dataset of intermittent flow for comparison to this study was at an ambient temperature of $33°C$ from Cabezon, Johnson, Schinckel, & Stwalley (2019). Due to the difference in flow rates used, two determinations could be made:

1. for a given effective flow rate, what control scheme developed the greatest heat transfer efficiency and cooling effectiveness; and
2. for a given cycle time, which flow rate developed the greatest heat transfer efficiency and cooling effectiveness.

For an effective flow rate of 0.22 L/min, the 6 min cycle time from Cabezon, Johnson, Schinckel, & Stwalley (2019) had approximately 86% more heat transfer efficiency and 9% more cooling effectiveness than the 9 minute temporal control scheme examined in this study. This suggests that for a given effective flow rate, the control scheme with the lower overall flow rate will have better heat transfer efficiency and cooling effectiveness. This is likely due to the exponential decay of temperature difference as the water in the pipes is warmed during the conductive heat transfer portion when the flow is off. More frequent flushing allows for more time transferring heat to the water with a high temperature gradient.

By comparing the 3 minute cycle time from Cabezon, Johnson, Schinckel, & Stwalley (2019) to the 3 min OFF temporal scheme, ($354\,W$ vs $324\,W$) and cooling effectiveness was approximately $11\,kJ/L$ greater for the 3 minute OFF scheme from this study ($49.0\,kJ/L$ vs $60.7\,kJ/L$). This suggests that greater flow rates allow for increased cooling effectiveness. Less frequent flushing allows for a single volume of water to warm up more before being replaced when the cooling pad is flushed.

5.3 Temporal versus Temperature Threshold Control

Overall, the $28.0°C$ and $29.5°C$ temperature threshold schemes tested in this study performed better than all of the temporal control schemes tested. The temporal scheme with the greatest heat transfer efficiency and cooling effectiveness was the 3 min OFF scheme. Heat transfer efficiency decreased with increased cycle time on temporal schemes and increased with decreased threshold temperature on temperature threshold schemes. There was a statistically significant difference ($\alpha = 0.05$) found between each pair of the six control schemes for heat transfer efficiency and each pair except 6 MIN – 9 MIN for cooling effectiveness. The effective flow rates of the temperature threshold control schemes were bounded by the effective flow rates of the 3 minute OFF and 9 minute OFF temporal schemes. The greater heat transfer efficiency of the temperature threshold schemes may be due to the variable cycle time. These schemes allow more frequent flushing during periods of high heat stress and transient response when the cooling pad is initially turned on in a hot environment and then less frequent flushing to maintain the cooling pad surface below the threshold temperature.

Additional studies should be conducted using 4 L/min and the effective cycle times of the temperature threshold control schemes as the cycle times for temporal control schemes to allow for more accurate comparison of the control scheme types. This will allow the increased heat transfer efficiency to be attributed to the difference in effective flow rate, the variable cycle time, or a combination of the two.

5.4 Future Work

The overall cooling pad design is effective at removing heat from the sow while minimizing heat removed from the environment. However, a more effective method should be selected for the manufacture and assembly of the cooling pad to minimize corrosion of electronic components in the farrowing barn. This is particularly necessary if electronic sensors will be used for feedback decisions, such as those in the temperature threshold schemes.

5.4.1 Computational Heat Transfer Model

Due to the disagreement between the current computational model results and those of past studies, further analysis using the model was untenable. The model currently contains a framework that allows for multiple materials, control schemes, and flow rates, but will need further improvement before it can be used to accurately predict the performance of cooling pad designs. A graduate level special project has been planned to work further on this element of the overall investigation into the hog cooling pad.

5.4.2 Internet of Things (IoT) Cooling Pad System

The current cooling pad data retrieval system requires manual collection of each microSD card, which are then individually read and copied to a computer. This also exposes the electronics to the corrosive air in the farrowing environment, shortening the life of the control system. An Internet of Things is currently being developed that will wirelessly collect data from each cooling pad as well as other systems, store the data in a single, central location and provide notifications to farm personnel when certain warning criteria are met. This will not only increase the lifespan of the electronics by minimizing exposure to the air in the farrowing barn, but it will simplify data collection for future studies with larger sample sizes.

5.5 Conclusion

Intermittent flow control schemes were tested using two different control types to increase the cooling effectiveness of the Purdue hog cooling pad system. A preliminary comparison of the control schemes at different ambient temperatures demonstrated greater heat transfer efficiency at greater ambient temperatures. The temperature threshold control schemes outperformed the temporal control schemes used in this study. Past studies utilizing continuous flow cooling exhibited greater heat transfer efficiency, but much lower cooling effectiveness than the intermittent control schemes examined in this study. Previous experiments that used intermittent flow control schemes outperformed comparable control schemes from this study but can be attributed to the lower flow rate used. As a result, the control schemes evaluated here should be reevaluated at lower flow rates for better comparison with past studies. Additionally, optimization of the flush frequency will be necessary to assess the tradeoffs between heat transfer efficiency and cooling effectiveness.

APPENDIX A: RAW CALIBRATION DATA

The data collected for the calibration of the cooling pad data is read out as quickly as possible to increase the number of data points used in computing the mean and variance of each sensor. The first several lines identify each temperature sensor on the cooling pad by its unique ID. The physical position of each ID on the cooling pad was documented when the cooling pads were manufactured. The remainder of the output is the temperature read from each sensor identified when the program started. This loops until the program is terminated. A sample of this raw data is shown in Figure 35.

```
Locating devices...Found 6 devices.
Parasite power is: OFF
Found device 0 with address: 28FF226351170418
Setting resolution to 9
Resolution actually set to: 9
Found device 1 with address: 28FF4A80201704B2
Setting resolution to 9
Resolution actually set to: 9
Found device 2 with address: 28FF79335017048E
Setting resolution to 9
Resolution actually set to: 9
Found device 3 with address: 28FF956A51170495
Setting resolution to 9
Resolution actually set to: 9
Found device 4 with address: 28FF4D74511704D8
Setting resolution to 9
Resolution actually set to: 9
Found device 5 with address: 28FF2F2F501704AD
Setting resolution to 9
Resolution actually set to: 9
Requesting temperatures...DONE
Temperature for device: 0
Temp C: 23.00 Temp F: 73.40
Temperature for device: 1
Temp C: 19.00 Temp F: 66.20
Temperature for device: 2
Temp C: 22.50 Temp F: 72.50
Temperature for device: 3
Temp C: 21.00 Temp F: 69.80
Temperature for device: 4
Temp C: 21.00 Temp F: 69.80
Temperature for device: 5
Temp C: 20.00 Temp F: 68.00
```

Figure 35: Sample Temperature Sensor Calibration Output

APPENDIX B: RAW COOLING PAD DATA

The data collected from the cooling pads during the series of experiments was saved in a text file on each cooling pad until manual retrieval following the study. The temperature of each sensor was read every six seconds. The locations of each sensor ID were provided to the program such that the sensors are read in the same order each time. Values were comma separated and a temperature of 85.00 indicated a failure to read the sensor. The temperature data was output in the order of inlet, outlet, pad rear, pad middle, pad front, ambient. The seventh channel reads 'nan' (not a number) for all times since this sensor was not included in the final design of the system. The UNIX time of the data is output next, allowing correlation with timestamped data recorded outside the cooling pad system, such as that physiological data for each sow in Appendix C. Each data point also included the uncalibrated flowrate from the flowrate sensor and the Boolean state of the solenoid at that time. A sample of the raw cooling pad data can be seen in Figure 36.

```
24.31,24.75,30.50,29.00,26.00,22.69,nan,1570478958,0.00,0
24.25,24.75,30.50,29.00,26.00,22.69,nan,1570478964,0.00,0
85.00,85.00,85.00,85.00,30.00,85.00,nan,1570547538,3.88,1
85.00,85.00,85.00,85.00,30.00,85.00,nan,1570547538,3.88,1
26.50,28.50,33.50,31.00,30.00,26.50,nan,1570547544,4.46,1
26.50,28.50,33.50,31.00,30.00,26.50,nan,1570547550,4.43,1
26.50,28.50,33.50,31.00,30.00,26.50,nan,1570547556,0.49,0
26.50,28.50,33.50,31.00,30.00,26.50,nan,1570547562,0.00,0
26.50,28.50,33.00,31.00,30.00,26.50,nan,1570547568,0.00,0
26.50,28.50,33.00,31.00,30.00,26.50,nan,1570547574,0.00,0
26.00,28.50,33.00,30.50,30.00,26.50,nan,1570547580,0.00,0
26.00,28.50,32.50,30.50,30.00,27.00,nan,1570547586,0.00,0
26.00,28.50,32.50,30.50,30.00,27.00,nan,1570547592,0.00,0
26.00,28.50,32.50,30.50,29.50,27.00,nan,1570547598,0.00,0
26.00,29.00,32.50,30.50,29.50,27.00,nan,1570547604,0.00,0
26.00,29.00,32.50,30.50,29.50,27.00,nan,1570547610,0.00,0
26.00,29.00,32.50,30.50,29.50,27.00,nan,1570547616,0.00,0
26.00,29.00,32.50,30.50,29.50,27.00,nan,1570547622,0.00,0
26.00,29.00,32.50,30.50,29.50,27.00,nan,1570547628,0.00,0
26.00,29.00,32.50,30.00,29.50,27.00,nan,1570547634,0.00,0
25.50,29.00,32.50,30.00,29.50,27.00,nan,1570547640,0.00,1
25.50,29.00,32.50,30.00,29.50,27.00,nan,1570547646,4.31,1
25.50,29.00,32.50,30.00,29.50,27.00,nan,1570547652,4.43,1
25.50,29.00,32.50,30.00,29.50,27.00,nan,1570547658,4.36,1
25.50,29.00,32.50,30.00,29.50,27.00,nan,1570547664,4.33,1
25.00,29.50,32.00,30.00,29.50,27.00,nan,1570547670,4.31,1
25.00,29.50,32.00,30.00,29.50,27.00,nan,1570547676,0.47,0
24.50,29.50,32.00,30.00,29.50,27.00,nan,1570547682,0.00,0
24.50,29.50,31.50,30.00,29.50,27.00,nan,1570547688,0.00,0
```

Figure 36: Raw Cooling Pad Output

APPENDIX C: RAW PHYSIOLOGICAL DATA

The physiological data for each sow was recorded on paper for each study as the data was collected. The control type, date, and ambient room temperature were noted at the top of the sheet. Skin temperature, respiration rate, and rectal temperature were recorded in the appropriate box for each sow. A sample original datasheet can be seen in Figure 37.

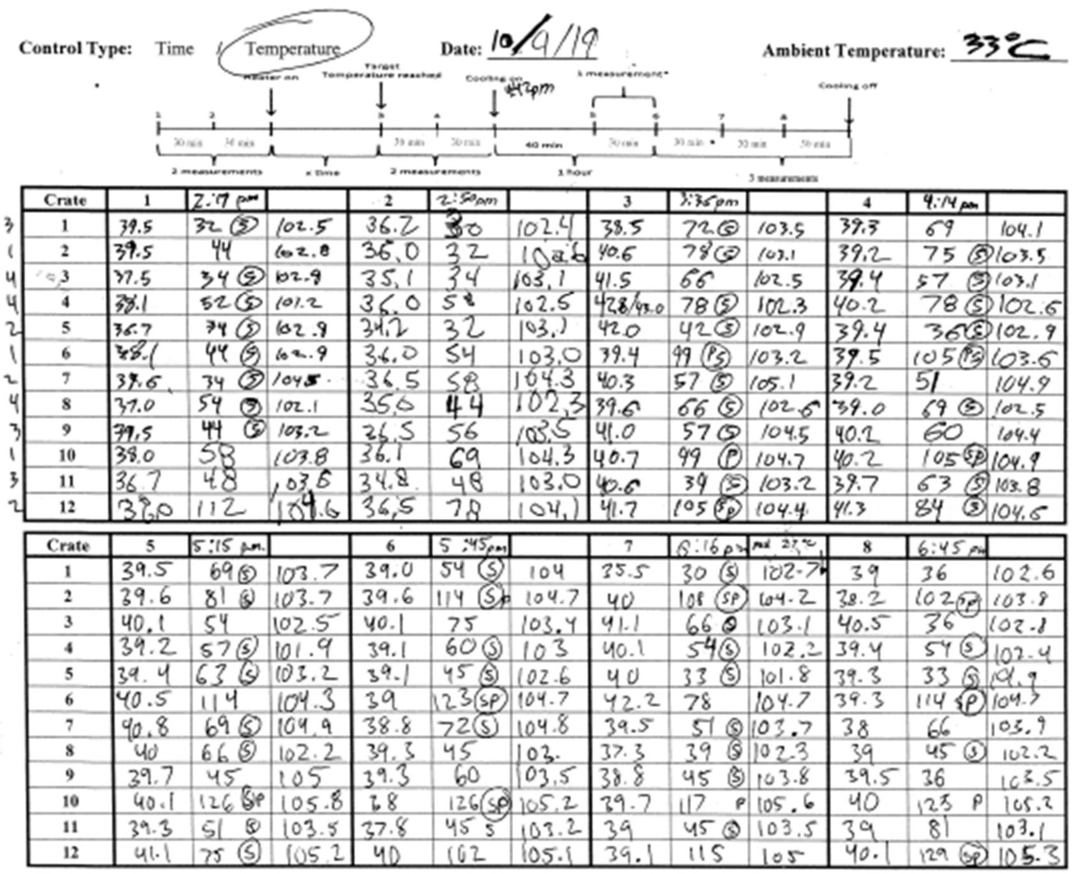

	Crate	1	2:17 pm		2	2:50pm		3	3:36pm		4	4:14 pm	
3	1	39.5	32 S	102.5	36.2	30	102.4	38.5	72 S	103.5	39.3	69	104.1
1	2	39.5	44	102.8	36.0	32	102.6	40.6	78 S	103.1	39.2	75 S	103.5
4	3	37.5	34 S	102.9	35.1	34	103.1	41.5	66	102.5	39.4	57 S	103.1
4	4	38.1	52 S	101.2	36.0	58	102.5	42.8/43.0	78 S	102.3	40.2	78 S	102.6
2	5	36.7	74 S	102.9	34.2	32	103.1	42.0	42 S	102.9	39.4	36 S	102.9
1	6	38.1	44 S	102.9	36.0	54	103.0	39.4	99 PS	103.2	39.5	105 PS	103.6
2	7	37.6	34 S	104.5	36.5	58	104.3	40.3	57 S	105.1	39.2	51	104.9
4	8	37.0	54 S	102.1	35.6	44	102.3	39.6	66 S	102.6	39.0	69 S	102.5
3	9	39.5	44 S	103.2	36.5	56	103.5	41.0	57 S	104.5	40.2	60	104.4
1	10	38.0	58	103.8	36.1	69	104.3	40.7	99 P	104.7	40.2	105 SP	104.9
3	11	36.7	48	103.6	34.8	48	103.0	40.6	39 S	103.2	39.7	63 S	103.8
2	12	38.0	112	104.6	36.5	78	104.1	41.7	105 SP	104.4	41.3	84 S	104.6

Crate	5	5:15 pm.		6	5:45pm		7	6:16 pm	27°C	8	6:45 pm	
1	39.5	69 S	103.7	39.0	54 S	104	35.5	30 S	102.7	39	36	102.6
2	39.6	81 S	103.7	39.6	114 SP	104.7	40	108 SP	104.2	38.2	102 SP	103.8
3	40.1	54	102.5	40.1	75	103.4	41.1	66 S	103.1	40.5	36	102.8
4	39.2	57 S	101.9	39.1	60 S	103	40.1	54 S	102.2	39.4	54 S	102.4
5	39.4	63 S	103.2	39.1	45 S	102.6	40	33 S	101.8	39.3	33 S	101.9
6	40.5	114	104.3	39	123 SP	104.7	42.2	78	104.7	39.3	114 SP	104.7
7	40.8	69 S	104.9	38.8	72 S	104.8	39.5	51 S	103.7	38	66	103.9
8	40	66 S	102.2	39.3	45	103.	37.3	39 S	102.3	39	45 S	102.2
9	39.7	45	105	39.3	60	103.5	38.8	45 S	103.8	39.5	36	103.5
10	40.1	126 SP	105.8	38	126 SP	105.2	39.7	117 P	105.6	40	123 P	105.2
11	39.3	51 S	103.5	37.8	45 S	103.2	39	45 S	103.5	39	81	103.1
12	41.1	75 S	105.2	40	102	105.1	39.1	115	105	40.1	129 SP	105.3

Figure 37: Original Physiological Data Sample

This data was transferred into Microsoft® Excel following the conclusion of all data collection to allow for transfer into different software packages and long-term preservation of the dataset. The entirety of the physiological sow data from the study can be seen in Table 20.

Table 20: Sow Physiological Dataset

Date	Time	Measurement Number	Sow ID	Treatment	Skin Temp	Resp. Rate	Rectal Temp	Ambient Temp	Run
10/8/2019	A	1	1	28.0Thresh	38.4	28	100.7	28.0	1
10/8/2019	A	1	2	28.0Thresh	37.3	27	101.2	28.0	1
10/8/2019	A	1	3	28.0Thresh	36.1	24	100.5	28.0	1
10/8/2019	A	1	4	29.5Thresh	36.8	.	100.4	28.0	1
10/8/2019	A	1	5	29.5Thresh	34.3	.	99.7	28.0	1
10/8/2019	A	1	6	29.5Thresh	36.7	32	100.7	28.0	1
10/8/2019	A	1	7	TempControl	34.4	28	100.4	28.0	1
10/8/2019	A	1	8	TempControl	35.7	38	.	28.0	1
10/8/2019	A	1	9	TempControl	33.0	28	100.4	28.0	1
10/8/2019	A	1	10	31.0Thresh	35	46	101.0	28.0	1
10/8/2019	A	1	11	31.0Thresh	35	36	100.4	28.0	1
10/8/2019	A	1	12	31.0Thresh	36.1	32	.	28.0	1
10/8/2019	A	2	1	28.0Thresh	36.7	32	100.5	28.0	1
10/8/2019	A	2	2	28.0Thresh	35.6	42	101.0	28.0	1
10/8/2019	A	2	3	28.0Thresh	35.3	24	99.9	28.0	1
10/8/2019	A	2	4	29.5Thresh	36.2	33	99.9	28.0	1
10/8/2019	A	2	5	29.5Thresh	33.7	26	99.7	28.0	1
10/8/2019	A	2	6	29.5Thresh	34.6	52	101.1	28.0	1
10/8/2019	A	2	7	TempControl	34.3	17	100.7	28.0	1
10/8/2019	A	2	8	TempControl	35	30	98.8	28.0	1
10/8/2019	A	2	9	TempControl	35.3	22	100.1	28.0	1
10/8/2019	A	2	10	31.0Thresh	35.2	32	100.7	28.0	1
10/8/2019	A	2	11	31.0Thresh	35.5	24	99.7	28.0	1
10/8/2019	A	2	12	31.0Thresh	36.5	.	101.2	28.0	1
10/8/2019	A	3	1	28.0Thresh	39.6	50	99.3	28.0	1
10/8/2019	A	3	2	28.0Thresh	39.5	54	101.9	28.0	1
10/8/2019	A	3	3	28.0Thresh	39.0	60	99.3	28.0	1
10/8/2019	A	3	4	29.5Thresh	39.0	42	99.9	28.0	1
10/8/2019	A	3	5	29.5Thresh	37.8	16	99.3	28.0	1
10/8/2019	A	3	6	29.5Thresh	39.0	46	100.5	28.0	1
10/8/2019	A	3	7	TempControl	36.8	50	101.0	28.0	1
10/8/2019	A	3	8	TempControl	36.5	36	99.9	28.0	1
10/8/2019	A	3	9	TempControl	36.5	36	100.4	28.0	1
10/8/2019	A	3	10	31.0Thresh	37.3	52	101.4	28.0	1
10/8/2019	A	3	11	31.0Thresh	36.5	32	100.7	28.0	1
10/8/2019	A	3	12	31.0Thresh	38.6	44	101.2	28.0	1
10/8/2019	A	4	1	28.0Thresh	38.2	38	100.1	28.0	1
10/8/2019	A	4	2	28.0Thresh	37.0	56	101.9	28.0	1

Table 20 continued

10/8/2019	A	4	3	28.0Thresh	36.7	42	100.4	28.0	1
10/8/2019	A	4	4	29.5Thresh	37.5	60	99.9	28.0	1
10/8/2019	A	4	5	29.5Thresh	36.2	20	100.7	28.0	1
10/8/2019	A	4	6	29.5Thresh	37.5	86	101.2	28.0	1
10/8/2019	A	4	7	TempControl	38.4	29	101.0	28.0	1
10/8/2019	A	4	8	TempControl	38.1	40	99.7	28.0	1
10/8/2019	A	4	9	TempControl	38	32	100.1	28.0	1
10/8/2019	A	4	10	31.0Thresh	38	42	101.6	28.0	1
10/8/2019	A	4	11	31.0Thresh	36.3	36	101.0	28.0	1
10/8/2019	A	4	12	31.0Thresh	38.7	46	101.2	28.0	1
10/8/2019	A	5	1	28.0Thresh	38.1	22	100.5	28.0	1
10/8/2019	A	5	2	28.0Thresh	38.0	34	101.0	28.0	1
10/8/2019	A	5	3	28.0Thresh	39.6	28	101.0	28.0	1
10/8/2019	A	5	4	29.5Thresh	35.5	24	99.4	28.0	1
10/8/2019	A	5	5	29.5Thresh	36.3	22	99.5	28.0	1
10/8/2019	A	5	6	29.5Thresh	38.5	54	101.0	28.0	1
10/8/2019	A	5	7	TempControl	39	30	102.0	28.0	1
10/8/2019	A	5	8	TempControl	38	38	100.7	28.0	1
10/8/2019	A	5	9	TempControl	38.2	30	101.0	28.0	1
10/8/2019	A	5	10	31.0Thresh	37.9	42	100.7	28.0	1
10/8/2019	A	5	11	31.0Thresh	38.1	44	100.4	28.0	1
10/8/2019	A	5	12	31.0Thresh	40	50	102.0	28.0	1
10/8/2019	A	6	1	28.0Thresh	37.5	54	102.0	28.0	1
10/8/2019	A	6	2	28.0Thresh	35.2	35	101.7	28.0	1
10/8/2019	A	6	3	28.0Thresh	37.9	44	102.0	28.0	1
10/8/2019	A	6	4	29.5Thresh	36.8	50	100.5	28.0	1
10/8/2019	A	6	5	29.5Thresh	36.5	36	101.6	28.0	1
10/8/2019	A	6	6	29.5Thresh	36.5	56	101.9	28.0	1
10/8/2019	A	6	7	TempControl	38.2	20	103.5	28.0	1
10/8/2019	A	6	8	TempControl	38	38	101.7	28.0	1
10/8/2019	A	6	9	TempControl	37.5	34	101.5	28.0	1
10/8/2019	A	6	10	31.0Thresh	38	60	103.0	28.0	1
10/8/2019	A	6	11	31.0Thresh	35.7	32	102.2	28.0	1
10/8/2019	A	6	12	31.0Thresh	38.6	64	104.0	28.0	1
10/8/2019	A	7	1	28.0Thresh	36.7	38	101.6	28.0	1
10/8/2019	A	7	2	28.0Thresh	38.0	52	102.7	28.0	1
10/8/2019	A	7	3	28.0Thresh	36.5	36	101.0	28.0	1
10/8/2019	A	7	4	29.5Thresh	35.2	29	101.4	28.0	1
10/8/2019	A	7	5	29.5Thresh	35.0	26	101.9	28.0	1
10/8/2019	A	7	6	29.5Thresh	35.6	60	101.8	28.0	1

Table 20 continued

10/8/2019	A	7	7	TempControl	37.8	46	103.8	28.0	1
10/8/2019	A	7	8	TempControl	37.6	38	102.3	28.0	1
10/8/2019	A	7	9	TempControl	38	36	102.2	28.0	1
10/8/2019	A	7	10	31.0Thresh	37.7	52	102.2	28.0	1
10/8/2019	A	7	11	31.0Thresh	36	32	102.2	28.0	1
10/8/2019	A	7	12	31.0Thresh	40	72	104.0	28.0	1
10/8/2019	A	8	1	28.0Thresh	37.0	30	102.7	28.0	1
10/8/2019	A	8	2	28.0Thresh	38.5	42	103.0	28.0	1
10/8/2019	A	8	3	28.0Thresh	37.0	38	101.4	28.0	1
10/8/2019	A	8	4	29.5Thresh	35.7	52	100.7	28.0	1
10/8/2019	A	8	5	29.5Thresh	35.0	30	101.7	28.0	1
10/8/2019	A	8	6	29.5Thresh	37.0	26	101.6	28.0	1
10/8/2019	A	8	7	TempControl	38.5	39	103.8	28.0	1
10/8/2019	A	8	8	TempControl	38.6	44	102.7	28.0	1
10/8/2019	A	8	9	TempControl	37.8	52	103.1	28.0	1
10/8/2019	A	8	10	31.0Thresh	37.5	56	102.6	28.0	1
10/8/2019	A	8	11	31.0Thresh	37.5	34	102.6	28.0	1
10/8/2019	A	8	12	31.0Thresh	39	49	104.3	28.0	1
10/9/2019	M	1	1	28.0Thresh	32.1	32	100.1	33.0	2
10/9/2019	M	1	2	28.0Thresh	33.6	25	100.5	33.0	2
10/9/2019	M	1	3	28.0Thresh	36.7	24	100.5	33.0	2
10/9/2019	M	1	4	29.5Thresh	31.7	26	100.7	33.0	2
10/9/2019	M	1	5	29.5Thresh	35.0	24	100.1	33.0	2
10/9/2019	M	1	6	29.5Thresh	35.5	28	101.0	33.0	2
10/9/2019	M	1	7	TempControl	34.3	24	101.2	33.0	2
10/9/2019	M	1	8	TempControl	35.6	30	99.6	33.0	2
10/9/2019	M	1	9	TempControl	35.8	28	101.4	33.0	2
10/9/2019	M	1	10	31.0Thresh	35.7	52	102.3	33.0	2
10/9/2019	M	1	11	31.0Thresh	35.1	24	102.5	33.0	2
10/9/2019	M	1	12	31.0Thresh	37.1	28	104.0	33.0	2
10/9/2019	M	2	1	28.0Thresh	34.2	28	100.5	33.0	2
10/9/2019	M	2	2	28.0Thresh	32.0	24	100.1	33.0	2
10/9/2019	M	2	3	28.0Thresh	35.7	32	101.2	33.0	2
10/9/2019	M	2	4	29.5Thresh	34.8	32	100.5	33.0	2
10/9/2019	M	2	5	29.5Thresh	31.6	24	101.1	33.0	2
10/9/2019	M	2	6	29.5Thresh	34.6	32	101.0	33.0	2
10/9/2019	M	2	7	TempControl	34.7	30	101.2	33.0	2
10/9/2019	M	2	8	TempControl	33.7	26	99.5	33.0	2
10/9/2019	M	2	9	TempControl	34.8	26	101.2	33.0	2
10/9/2019	M	2	10	31.0Thresh	34.5	28	102.6	33.0	2

Table 20 continued

10/9/2019	M	2	11	31.0Thresh	34.1	28	102.5	33.0	2
10/9/2019	M	2	12	31.0Thresh	37.1	40	104.3	33.0	2
10/9/2019	M	3	1	28.0Thresh	40.0	48	101.6	33.0	2
10/9/2019	M	3	2	28.0Thresh	39.8	44	102.2	33.0	2
10/9/2019	M	3	3	28.0Thresh	39.8	30	101.9	33.0	2
10/9/2019	M	3	4	29.5Thresh	41.3	41	100.5	33.0	2
10/9/2019	M	3	5	29.5Thresh	38.5	44	101.9	33.0	2
10/9/2019	M	3	6	29.5Thresh	40.5	120	101.8	33.0	2
10/9/2019	M	3	7	TempControl	39.7	36	102.6	33.0	2
10/9/2019	M	3	8	TempControl	38.0	36	100.6	33.0	2
10/9/2019	M	3	9	TempControl	39.4	38	101.7	33.0	2
10/9/2019	M	3	10	31.0Thresh	40.1	98	102.5	33.0	2
10/9/2019	M	3	11	31.0Thresh	40.0	68	102.3	33.0	2
10/9/2019	M	3	12	31.0Thresh	39.8	68	103.4	33.0	2
10/9/2019	M	4	1	28.0Thresh	39.3	76	102.6	33.0	2
10/9/2019	M	4	2	28.0Thresh	39.0	64	103.0	33.0	2
10/9/2019	M	4	3	28.0Thresh	41.0	70	101.7	33.0	2
10/9/2019	M	4	4	29.5Thresh	38.7	124	100.6	33.0	2
10/9/2019	M	4	5	29.5Thresh	38.8	46	101.9	33.0	2
10/9/2019	M	4	6	29.5Thresh	39.7	122	102.5	33.0	2
10/9/2019	M	4	7	TempControl	38.6	52	102.9	33.0	2
10/9/2019	M	4	8	TempControl	39.0	78	101.0	33.0	2
10/9/2019	M	4	9	TempControl	38.5	35	101.9	33.0	2
10/9/2019	M	4	10	31.0Thresh	39.0	96	102.9	33.0	2
10/9/2019	M	4	11	31.0Thresh	38.9	76	102.5	33.0	2
10/9/2019	M	4	12	31.0Thresh	39.7	96	104.2	33.0	2
10/9/2019	M	5	1	28.0Thresh	40.3	36	103.2	33.0	2
10/9/2019	M	5	2	28.0Thresh	39.5	56	101.9	33.0	2
10/9/2019	M	5	3	28.0Thresh	40.1	58	103.2	33.0	2
10/9/2019	M	5	4	29.5Thresh	39.2	48	101.4	33.0	2
10/9/2019	M	5	5	29.5Thresh	40.1	46	102.6	33.0	2
10/9/2019	M	5	6	29.5Thresh	40.0	128	103.9	33.0	2
10/9/2019	M	5	7	TempControl	40.5	56	103.8	33.0	2
10/9/2019	M	5	8	TempControl	39.4	58	101.2	33.0	2
10/9/2019	M	5	9	TempControl	37.6	62	103.1	33.0	2
10/9/2019	M	5	10	31.0Thresh	39.8	57	103.5	33.0	2
10/9/2019	M	5	11	31.0Thresh	38.0	52	102.5	33.0	2
10/9/2019	M	5	12	31.0Thresh	41.0	120	104.7	33.0	2
10/9/2019	M	6	1	28.0Thresh	37.4	32	101.9	33.0	2
10/9/2019	M	6	2	28.0Thresh	38.5	42	102.6	33.0	2

Table 20 continued

10/9/2019	M	6	3	28.0Thresh	39.8	32	102.5	33.0	2
10/9/2019	M	6	4	29.5Thresh	40.0	56	101.2	33.0	2
10/9/2019	M	6	5	29.5Thresh	40.1	38	102.3	33.0	2
10/9/2019	M	6	6	29.5Thresh	39.9	96	103.8	33.0	2
10/9/2019	M	6	7	TempControl	39.5	54	104.2	33.0	2
10/9/2019	M	6	8	TempControl	38.6	60	101.4	33.0	2
10/9/2019	M	6	9	TempControl	39.1	62	103.1	33.0	2
10/9/2019	M	6	10	31.0Thresh	39.2	72	103.5	33.0	2
10/9/2019	M	6	11	31.0Thresh	38.8	64	102.4	33.0	2
10/9/2019	M	6	12	31.0Thresh	40.5	92	104.6	33.0	2
10/9/2019	M	7	1	28.0Thresh	38.3	30	101.9	33.0	2
10/9/2019	M	7	2	28.0Thresh	37.6	36	103.5	33.0	2
10/9/2019	M	7	3	28.0Thresh	38.2	27	102.8	33.0	2
10/9/2019	M	7	4	29.5Thresh	39.0	60	101.2	33.0	2
10/9/2019	M	7	5	29.5Thresh	40.1	32	102.2	33.0	2
10/9/2019	M	7	6	29.5Thresh	40.5	124	104.1	33.0	2
10/9/2019	M	7	7	TempControl	41.1	70	104.4	33.0	2
10/9/2019	M	7	8	TempControl	39.1	58	102.2	33.0	2
10/9/2019	M	7	9	TempControl	39.6	72	103.1	33.0	2
10/9/2019	M	7	10	31.0Thresh	39.0	86	103.4	33.0	2
10/9/2019	M	7	11	31.0Thresh	38.0	62	102.6	33.0	2
10/9/2019	M	7	12	31.0Thresh	39.8	136	104.6	33.0	2
10/9/2019	M	8	1	28.0Thresh	37.7	24	101.4	33.0	2
10/9/2019	M	8	2	28.0Thresh	37.0	36	101.8	33.0	2
10/9/2019	M	8	3	28.0Thresh	39.0	30	102.3	33.0	2
10/9/2019	M	8	4	29.5Thresh	39.0	48	100.9	33.0	2
10/9/2019	M	8	5	29.5Thresh	39.7	32	102.2	33.0	2
10/9/2019	M	8	6	29.5Thresh	39.7	116	102.9	33.0	2
10/9/2019	M	8	7	TempControl	41.2	80	104.4	33.0	2
10/9/2019	M	8	8	TempControl	39.0	74	102.0	33.0	2
10/9/2019	M	8	9	TempControl	40.1	68	103.4	33.0	2
10/9/2019	M	8	10	31.0Thresh	39.0	100	103.9	33.0	2
10/9/2019	M	8	11	31.0Thresh	38.5	54	102.4	33.0	2
10/9/2019	M	8	12	31.0Thresh	40.5	122	105.2	33.0	2
10/9/2019	A	1	1	29.5Thresh	39.5	32	102.5	33.0	3
10/9/2019	A	1	2	TempControl	39.5	44	102.8	33.0	3
10/9/2019	A	1	3	31.0Thresh	37.5	34	102.9	33.0	3
10/9/2019	A	1	4	31.0Thresh	38.1	52	101.2	33.0	3
10/9/2019	A	1	5	28.0Thresh	36.7	34	102.9	33.0	3
10/9/2019	A	1	6	TempControl	38.1	44	102.9	33.0	3

Table 20 continued

10/9/2019	A	1	7	28.0Thresh	39.6	34	104.5	33.0	3
10/9/2019	A	1	8	31.0Thresh	37.0	54	102.1	33.0	3
10/9/2019	A	1	9	29.5Thresh	39.5	44	103.2	33.0	3
10/9/2019	A	1	10	TempControl	38.0	58	103.8	33.0	3
10/9/2019	A	1	11	29.5Thresh	36.7	48	103.6	33.0	3
10/9/2019	A	1	12	28.0Thresh	38.0	112	104.6	33.0	3
10/9/2019	A	2	1	29.5Thresh	36.2	30	102.4	33.0	3
10/9/2019	A	2	2	TempControl	36.0	32	102.6	33.0	3
10/9/2019	A	2	3	31.0Thresh	35.1	34	103.1	33.0	3
10/9/2019	A	2	4	31.0Thresh	36.0	58	102.5	33.0	3
10/9/2019	A	2	5	28.0Thresh	34.2	32	103.1	33.0	3
10/9/2019	A	2	6	TempControl	36.0	54	103.0	33.0	3
10/9/2019	A	2	7	28.0Thresh	36.5	58	104.3	33.0	3
10/9/2019	A	2	8	31.0Thresh	35.0	44	102.3	33.0	3
10/9/2019	A	2	9	29.5Thresh	36.5	56	103.5	33.0	3
10/9/2019	A	2	10	TempControl	36.1	69	104.3	33.0	3
10/9/2019	A	2	11	29.5Thresh	34.8	48	103.0	33.0	3
10/9/2019	A	2	12	28.0Thresh	36.5	78	104.1	33.0	3
10/9/2019	A	3	1	29.5Thresh	38.5	72	103.5	33.0	3
10/9/2019	A	3	2	TempControl	40.6	78	103.1	33.0	3
10/9/2019	A	3	3	31.0Thresh	41.5	66	102.5	33.0	3
10/9/2019	A	3	4	31.0Thresh	42.9	78	102.3	33.0	3
10/9/2019	A	3	5	28.0Thresh	42.0	42	102.9	33.0	3
10/9/2019	A	3	6	TempControl	39.4	99	103.2	33.0	3
10/9/2019	A	3	7	28.0Thresh	40.3	57	105.1	33.0	3
10/9/2019	A	3	8	31.0Thresh	39.6	66	102.6	33.0	3
10/9/2019	A	3	9	29.5Thresh	41.0	57	104.5	33.0	3
10/9/2019	A	3	10	TempControl	40.7	99	104.7	33.0	3
10/9/2019	A	3	11	29.5Thresh	40.6	39	103.2	33.0	3
10/9/2019	A	3	12	28.0Thresh	41.7	105	104.4	33.0	3
10/9/2019	A	4	1	29.5Thresh	39.3	69	104.1	33.0	3
10/9/2019	A	4	2	TempControl	39.2	75	103.5	33.0	3
10/9/2019	A	4	3	31.0Thresh	39.4	57	103.1	33.0	3
10/9/2019	A	4	4	31.0Thresh	40.2	78	102.6	33.0	3
10/9/2019	A	4	5	28.0Thresh	39.4	36	102.9	33.0	3
10/9/2019	A	4	6	TempControl	39.5	105	103.6	33.0	3
10/9/2019	A	4	7	28.0Thresh	39.2	51	104.9	33.0	3
10/9/2019	A	4	8	31.0Thresh	39.0	69	102.5	33.0	3
10/9/2019	A	4	9	29.5Thresh	40.2	60	104.4	33.0	3
10/9/2019	A	4	10	TempControl	40.2	105	104.9	33.0	3

Table 20 continued

10/9/2019	A	4	11	29.5Thresh	39.7	63	103.8	33.0	3
10/9/2019	A	4	12	28.0Thresh	41.3	84	104.6	33.0	3
10/9/2019	A	5	1	29.5Thresh	39.5	69	103.7	33.0	3
10/9/2019	A	5	2	TempControl	39.6	81	103.7	33.0	3
10/9/2019	A	5	3	31.0Thresh	40.1	54	102.5	33.0	3
10/9/2019	A	5	4	31.0Thresh	39.2	57	101.9	33.0	3
10/9/2019	A	5	5	28.0Thresh	39.4	63	103.2	33.0	3
10/9/2019	A	5	6	TempControl	40.5	114	104.3	33.0	3
10/9/2019	A	5	7	28.0Thresh	40.8	69	104.9	33.0	3
10/9/2019	A	5	8	31.0Thresh	40.0	66	102.2	33.0	3
10/9/2019	A	5	9	29.5Thresh	39.7	45	105.0	33.0	3
10/9/2019	A	5	10	TempControl	40.1	126	105.8	33.0	3
10/9/2019	A	5	11	29.5Thresh	39.3	51	103.5	33.0	3
10/9/2019	A	5	12	28.0Thresh	41.1	75	105.2	33.0	3
10/9/2019	A	6	1	29.5Thresh	39.0	54	104.0	33.0	3
10/9/2019	A	6	2	TempControl	39.6	114	104.7	33.0	3
10/9/2019	A	6	3	31.0Thresh	40.1	75	103.4	33.0	3
10/9/2019	A	6	4	31.0Thresh	39.1	60	103.0	33.0	3
10/9/2019	A	6	5	28.0Thresh	39.1	45	102.6	33.0	3
10/9/2019	A	6	6	TempControl	39.0	123	104.7	33.0	3
10/9/2019	A	6	7	28.0Thresh	38.8	72	104.8	33.0	3
10/9/2019	A	6	8	31.0Thresh	39.3	45	103.0	33.0	3
10/9/2019	A	6	9	29.5Thresh	39.3	60	103.5	33.0	3
10/9/2019	A	6	10	TempControl	38.0	126	105.2	33.0	3
10/9/2019	A	6	11	29.5Thresh	37.8	45	103.2	33.0	3
10/9/2019	A	6	12	28.0Thresh	40.0	102	105.1	33.0	3
10/9/2019	A	7	1	29.5Thresh	35.5	30	102.7	33.0	3
10/9/2019	A	7	2	TempControl	40.0	108	104.2	33.0	3
10/9/2019	A	7	3	31.0Thresh	41.1	66	103.1	33.0	3
10/9/2019	A	7	4	31.0Thresh	40.1	54	102.2	33.0	3
10/9/2019	A	7	5	28.0Thresh	40.0	33	101.8	33.0	3
10/9/2019	A	7	6	TempControl	42.2	78	104.7	33.0	3
10/9/2019	A	7	7	28.0Thresh	39.5	51	103.7	33.0	3
10/9/2019	A	7	8	31.0Thresh	37.3	39	102.3	33.0	3
10/9/2019	A	7	9	29.5Thresh	38.8	45	103.8	33.0	3
10/9/2019	A	7	10	TempControl	39.7	117	105.6	33.0	3
10/9/2019	A	7	11	29.5Thresh	39.0	45	103.5	33.0	3
10/9/2019	A	7	12	28.0Thresh	39.1	115	105.0	33.0	3
10/9/2019	A	8	1	29.5Thresh	39.0	36	102.6	33.0	3
10/9/2019	A	8	2	TempControl	38.2	102	103.8	33.0	3

Table 20 continued

10/9/2019	A	8	3	31.0Thresh	40.5	36	102.8	33.0	3
10/9/2019	A	8	4	31.0Thresh	39.4	54	102.4	33.0	3
10/9/2019	A	8	5	28.0Thresh	39.3	33	101.9	33.0	3
10/9/2019	A	8	6	TempControl	39.3	114	104.7	33.0	3
10/9/2019	A	8	7	28.0Thresh	38.0	66	103.9	33.0	3
10/9/2019	A	8	8	31.0Thresh	39.0	45	102.2	33.0	3
10/9/2019	A	8	9	29.5Thresh	39.5	36	103.5	33.0	3
10/9/2019	A	8	10	TempControl	40.0	123	105.2	33.0	3
10/9/2019	A	8	11	29.5Thresh	39.0	81	103.1	33.0	3
10/9/2019	A	8	12	28.0Thresh	40.1	129	105.3	33.0	3
10/10/2019	M	1	1	31.0Thresh	27.4	24	101.9	33.0	4
10/10/2019	M	1	2	29.5Thresh	27.8	20	100.7	33.0	4
10/10/2019	M	1	3	29.5Thresh	28.5	26	101.4	33.0	4
10/10/2019	M	1	4	TempControl	31.5	30	100.1	33.0	4
10/10/2019	M	1	5	31.0Thresh	30.1	22	102.3	33.0	4
10/10/2019	M	1	6	31.0Thresh	33.2	20	100.4	33.0	4
10/10/2019	M	1	7	29.5Thresh	29.4	33	103.1	33.0	4
10/10/2019	M	1	8	28.0Thresh	31.2	42	101.2	33.0	4
10/10/2019	M	1	9	28.0Thresh	31.1	42	102.3	33.0	4
10/10/2019	M	1	10	28.0Thresh	32.7	24	102.5	33.0	4
10/10/2019	M	1	11	TempControl	30.1	36	102.2	33.0	4
10/10/2019	M	1	12	TempControl	32.9	33	101.9	33.0	4
10/10/2019	M	2	1	31.0Thresh	28.2	33	101.2	33.0	4
10/10/2019	M	2	2	29.5Thresh	29.4	36	100.5	33.0	4
10/10/2019	M	2	3	29.5Thresh	31.0	42	101.2	33.0	4
10/10/2019	M	2	4	TempControl	29.4	33	100.2	33.0	4
10/10/2019	M	2	5	31.0Thresh	30.8	48	102.2	33.0	4
10/10/2019	M	2	6	31.0Thresh	33.2	51	100.6	33.0	4
10/10/2019	M	2	7	29.5Thresh	30.2	24	102.5	33.0	4
10/10/2019	M	2	8	28.0Thresh	31.2	33	101.1	33.0	4
10/10/2019	M	2	9	28.0Thresh	30.3	27	102.2	33.0	4
10/10/2019	M	2	10	28.0Thresh	30.2	36	102.5	33.0	4
10/10/2019	M	2	11	TempControl	30.0	42	101.8	33.0	4
10/10/2019	M	2	12	TempControl	32.5	48	102.7	33.0	4
10/10/2019	M	3	1	31.0Thresh	34.0	30	101.0	33.0	4
10/10/2019	M	3	2	29.5Thresh	34.1	39	101.8	33.0	4
10/10/2019	M	3	3	29.5Thresh	35.5	42	102.3	33.0	4
10/10/2019	M	3	4	TempControl	36.0	51	101.3	33.0	4
10/10/2019	M	3	5	31.0Thresh	33.4	39	101.9	33.0	4
10/10/2019	M	3	6	31.0Thresh	34.3	75	100.7	33.0	4

Table 20 continued

10/10/2019	M	3	7	29.5Thresh	35.9	30	103.1	33.0	4
10/10/2019	M	3	8	28.0Thresh	34.9	39	101.2	33.0	4
10/10/2019	M	3	9	28.0Thresh	36.2	42	101.5	33.0	4
10/10/2019	M	3	10	28.0Thresh	34.6	78	101.6	33.0	4
10/10/2019	M	3	11	TempControl	36.8	45	101.9	33.0	4
10/10/2019	M	3	12	TempControl	37.0	54	102.9	33.0	4
10/10/2019	M	4	1	31.0Thresh	34.5	66	101.9	33.0	4
10/10/2019	M	4	2	29.5Thresh	35.8	45	101.7	33.0	4
10/10/2019	M	4	3	29.5Thresh	37.0	51	102.1	33.0	4
10/10/2019	M	4	4	TempControl	37.6	36	101.3	33.0	4
10/10/2019	M	4	5	31.0Thresh	37.1	57	102.0	33.0	4
10/10/2019	M	4	6	31.0Thresh	36.6	126	101.3	33.0	4
10/10/2019	M	4	7	29.5Thresh	36.5	30	103.5	33.0	4
10/10/2019	M	4	8	28.0Thresh	35.8	39	102.1	33.0	4
10/10/2019	M	4	9	28.0Thresh	35.9	36	101.9	33.0	4
10/10/2019	M	4	10	28.0Thresh	36.5	63	101.7	33.0	4
10/10/2019	M	4	11	TempControl	36.6	51	102.3	33.0	4
10/10/2019	M	4	12	TempControl	36.7	60	102.9	33.0	4
10/10/2019	M	5	1	31.0Thresh	37.7	32	102.5	33.0	4
10/10/2019	M	5	2	29.5Thresh	38.1	48	101.9	33.0	4
10/10/2019	M	5	3	29.5Thresh	38.8	63	103.0	33.0	4
10/10/2019	M	5	4	TempControl	40.3	105	102.9	33.0	4
10/10/2019	M	5	5	31.0Thresh	39.3	36	102.2	33.0	4
10/10/2019	M	5	6	31.0Thresh	36.0	110	102.1	33.0	4
10/10/2019	M	5	7	29.5Thresh	37.5	27	102.9	33.0	4
10/10/2019	M	5	8	28.0Thresh	37.2	36	100.8	33.0	4
10/10/2019	M	5	9	28.0Thresh	37.9	33	101.4	33.0	4
10/10/2019	M	5	10	28.0Thresh	37.1	51	102.0	33.0	4
10/10/2019	M	5	11	TempControl	37.4	48	102.9	33.0	4
10/10/2019	M	5	12	TempControl	37.6	102	103.1	33.0	4
10/10/2019	M	6	1	31.0Thresh	37.0	33	102.3	33.0	4
10/10/2019	M	6	2	29.5Thresh	36.9	30	100.5	33.0	4
10/10/2019	M	6	3	29.5Thresh	37.2	63	101.8	33.0	4
10/10/2019	M	6	4	TempControl	37.0	114	101.5	33.0	4
10/10/2019	M	6	5	31.0Thresh	37.7	42	102.1	33.0	4
10/10/2019	M	6	6	31.0Thresh	36.8	96	101.4	33.0	4
10/10/2019	M	6	7	29.5Thresh	38.4	27	102.7	33.0	4
10/10/2019	M	6	8	28.0Thresh	36.5	33	100.7	33.0	4
10/10/2019	M	6	9	28.0Thresh	37.0	48	101.8	33.0	4
10/10/2019	M	6	10	28.0Thresh	36.4	36	101.5	33.0	4

Table 20 continued

10/10/2019	M	6	11	TempControl	35.5	42	102.5	33.0	4
10/10/2019	M	6	12	TempControl	37.7	102	102.3	33.0	4
10/10/2019	M	7	1	31.0Thresh	35.5	30	100.8	33.0	4
10/10/2019	M	7	2	29.5Thresh	35.8	30	100.7	33.0	4
10/10/2019	M	7	3	29.5Thresh	37.7	48	102.0	33.0	4
10/10/2019	M	7	4	TempControl	38.1	72	102.8	33.0	4
10/10/2019	M	7	5	31.0Thresh	36.6	66	102.4	33.0	4
10/10/2019	M	7	6	31.0Thresh	35.2	102	101.2	33.0	4
10/10/2019	M	7	7	29.5Thresh	36.2	27	102.7	33.0	4
10/10/2019	M	7	8	28.0Thresh	36.3	33	101.4	33.0	4
10/10/2019	M	7	9	28.0Thresh	36.4	27	102.0	33.0	4
10/10/2019	M	7	10	28.0Thresh	37.0	72	102.6	33.0	4
10/10/2019	M	7	11	TempControl	35.8	36	102.5	33.0	4
10/10/2019	M	7	12	TempControl	37.9	117	103.6	33.0	4
10/10/2019	M	8	1	31.0Thresh	34.9	33	102.1	33.0	4
10/10/2019	M	8	2	29.5Thresh	36.2	30	101.3	33.0	4
10/10/2019	M	8	3	29.5Thresh	36.6	56	102.4	33.0	4
10/10/2019	M	8	4	TempControl	36.4	126	103.3	33.0	4
10/10/2019	M	8	5	31.0Thresh	36.5	60	101.4	33.0	4
10/10/2019	M	8	6	31.0Thresh	36.1	102	102.1	33.0	4
10/10/2019	M	8	7	29.5Thresh	34.2	27	102.4	33.0	4
10/10/2019	M	8	8	28.0Thresh	34.9	33	100.8	33.0	4
10/10/2019	M	8	9	28.0Thresh	36.3	27	101.6	33.0	4
10/10/2019	M	8	10	28.0Thresh	36.3	54	102.9	33.0	4
10/10/2019	M	8	11	TempControl	35.0	48	103.1	33.0	4
10/10/2019	M	8	12	TempControl	37.8	117	103.6	33.0	4
10/10/2019	A	1	1	TempControl	33.0	36	100.0	33.0	5
10/10/2019	A	1	2	31.0Thresh	30.4	39	101.3	33.0	5
10/10/2019	A	1	3	TempControl	33.3	24	101.9	33.0	5
10/10/2019	A	1	4	28.0Thresh	35.1	90	103.0	33.0	5
10/10/2019	A	1	5	TempControl	35.7	24	101.7	33.0	5
10/10/2019	A	1	6	28.0Thresh	34.0	57	102.1	33.0	5
10/10/2019	A	1	7	31.0Thresh	33.6	28	101.9	33.0	5
10/10/2019	A	1	8	29.5Thresh	34.6	39	101.1	33.0	5
10/10/2019	A	1	9	31.0Thresh	34.8	24	101.8	33.0	5
10/10/2019	A	1	10	29.5Thresh	36.5	96	102.6	33.0	5
10/10/2019	A	1	11	28.0Thresh	35.5	51	102.5	33.0	5
10/10/2019	A	1	12	29.5Thresh	36.2	78	103.9	33.0	5
10/10/2019	A	2	1	TempControl	34.2	30	102.1	33.0	5
10/10/2019	A	2	2	31.0Thresh	34.0	33	101.0	33.0	5

Table 20 continued

10/10/2019	A	2	3	TempControl	35.0	36	102.4	33.0	5
10/10/2019	A	2	4	28.0Thresh	35.3	87	102.6	33.0	5
10/10/2019	A	2	5	TempControl	35.8	39	102.6	33.0	5
10/10/2019	A	2	6	28.0Thresh	35.0	48	102.3	33.0	5
10/10/2019	A	2	7	31.0Thresh	34.0	51	101.4	33.0	5
10/10/2019	A	2	8	29.5Thresh	34.1	42	100.9	33.0	5
10/10/2019	A	2	9	31.0Thresh	34.5	32	102.2	33.0	5
10/10/2019	A	2	10	29.5Thresh	34.7	54	102.3	33.0	5
10/10/2019	A	2	11	28.0Thresh	34.5	36	102.0	33.0	5
10/10/2019	A	2	12	29.5Thresh	36.4	48	103.2	33.0	5
10/10/2019	A	3	1	TempControl	37.0	54	101.7	33.0	5
10/10/2019	A	3	2	31.0Thresh	36.9	48	101.8	33.0	5
10/10/2019	A	3	3	TempControl	37.4	24	102.7	33.0	5
10/10/2019	A	3	4	28.0Thresh	37.9	90	103.4	33.0	5
10/10/2019	A	3	5	TempControl	38.3	51	102.9	33.0	5
10/10/2019	A	3	6	28.0Thresh	38.4	92	102.6	33.0	5
10/10/2019	A	3	7	31.0Thresh	38.0	39	103.1	33.0	5
10/10/2019	A	3	8	29.5Thresh	36.1	36	101.5	33.0	5
10/10/2019	A	3	9	31.0Thresh	33.8	36	102.2	33.0	5
10/10/2019	A	3	10	29.5Thresh	36.2	63	102.8	33.0	5
10/10/2019	A	3	11	28.0Thresh	36.6	32	102.6	33.0	5
10/10/2019	A	3	12	29.5Thresh	37.6	108	103.2	33.0	5
10/10/2019	A	4	1	TempControl	37.1	39	101.8	33.0	5
10/10/2019	A	4	2	31.0Thresh	38.5	66	102.8	33.0	5
10/10/2019	A	4	3	TempControl	37.1	60	103.2	33.0	5
10/10/2019	A	4	4	28.0Thresh	36.7	54	101.5	33.0	5
10/10/2019	A	4	5	TempControl	37.8	36	102.8	33.0	5
10/10/2019	A	4	6	28.0Thresh	37.2	84	102.3	33.0	5
10/10/2019	A	4	7	31.0Thresh	37.6	33	103.3	33.0	5
10/10/2019	A	4	8	29.5Thresh	37.0	63	101.5	33.0	5
10/10/2019	A	4	9	31.0Thresh	37.0	36	102.6	33.0	5
10/10/2019	A	4	10	29.5Thresh	37.0	78	102.8	33.0	5
10/10/2019	A	4	11	28.0Thresh	37.1	45	102.9	33.0	5
10/10/2019	A	4	12	29.5Thresh	37.5	123	103.4	33.0	5
10/10/2019	A	5	1	TempControl	37.4	96	103.3	33.0	5
10/10/2019	A	5	2	31.0Thresh	37.3	60	103.4	33.0	5
10/10/2019	A	5	3	TempControl	38.0	39	102.1	33.0	5
10/10/2019	A	5	4	28.0Thresh	37.1	33	101.1	33.0	5
10/10/2019	A	5	5	TempControl	38.0	51	103.0	33.0	5
10/10/2019	A	5	6	28.0Thresh	37.3	66	102.8	33.0	5

Table 20 continued

10/10/2019	A	5	7	31.0Thresh	38.3	30	103.4	33.0	5
10/10/2019	A	5	8	29.5Thresh	37.3	30	101.5	33.0	5
10/10/2019	A	5	9	31.0Thresh	37.1	48	103.4	33.0	5
10/10/2019	A	5	10	29.5Thresh	37.2	72	103.4	33.0	5
10/10/2019	A	5	11	28.0Thresh	36.4	42	102.8	33.0	5
10/10/2019	A	5	12	29.5Thresh	38.0	87	103.3	33.0	5
10/10/2019	A	6	1	TempControl	37.3	66	103.7	33.0	5
10/10/2019	A	6	2	31.0Thresh	37.7	60	102.7	33.0	5
10/10/2019	A	6	3	TempControl	38.9	63	102.6	33.0	5
10/10/2019	A	6	4	28.0Thresh	38.5	48	102.0	33.0	5
10/10/2019	A	6	5	TempControl	38.9	45	103.5	33.0	5
10/10/2019	A	6	6	28.0Thresh	37.9	39	102.4	33.0	5
10/10/2019	A	6	7	31.0Thresh	38.4	24	102.3	33.0	5
10/10/2019	A	6	8	29.5Thresh	37.6	33	101.4	33.0	5
10/10/2019	A	6	9	31.0Thresh	38.1	39	103.7	33.0	5
10/10/2019	A	6	10	29.5Thresh	37.5	48	103.4	33.0	5
10/10/2019	A	6	11	28.0Thresh	37.8	57	103.1	33.0	5
10/10/2019	A	6	12	29.5Thresh	38.9	42	103.0	33.0	5
10/10/2019	A	7	1	TempControl	37.2	48	103.6	33.0	5
10/10/2019	A	7	2	31.0Thresh	37.0	60	103.2	33.0	5
10/10/2019	A	7	3	TempControl	37.0	66	102.6	33.0	5
10/10/2019	A	7	4	28.0Thresh	36.4	57	101.7	33.0	5
10/10/2019	A	7	5	TempControl	37.8	48	103.5	33.0	5
10/10/2019	A	7	6	28.0Thresh	37.2	72	102.5	33.0	5
10/10/2019	A	7	7	31.0Thresh	38.0	36	103.1	33.0	5
10/10/2019	A	7	8	29.5Thresh	37.8	48	102.0	33.0	5
10/10/2019	A	7	9	31.0Thresh	38.8	48	102.9	33.0	5
10/10/2019	A	7	10	29.5Thresh	38.0	75	103.4	33.0	5
10/10/2019	A	7	11	28.0Thresh	37.5	39	103.1	33.0	5
10/10/2019	A	7	12	29.5Thresh	38.0	51	103.0	33.0	5
10/10/2019	A	8	1	TempControl	38.6	63	103.2	33.0	5
10/10/2019	A	8	2	31.0Thresh	38.2	96	103.2	33.0	5
10/10/2019	A	8	3	TempControl	38.5	57	102.9	33.0	5
10/10/2019	A	8	4	28.0Thresh	37.0	36	101.1	33.0	5
10/10/2019	A	8	5	TempControl	38.0	24	103.9	33.0	5
10/10/2019	A	8	6	28.0Thresh	39.0	96	102.3	33.0	5
10/10/2019	A	8	7	31.0Thresh	38.7	24	102.9	33.0	5
10/10/2019	A	8	8	29.5Thresh	38.6	21	102.2	33.0	5
10/10/2019	A	8	9	31.0Thresh	39.2	42	103.1	33.0	5
10/10/2019	A	8	10	29.5Thresh	38.2	78	103.7	33.0	5

Table 20 continued

10/10/2019	A	8	11	28.0Thresh	36.9	30	103.1	33.0	5
10/10/2019	A	8	12	29.5Thresh	38.6	33	103.4	33.0	5
10/11/2019	M	1	1	3MIN	32.2	27	102.3	33.0	6
10/11/2019	M	1	2	3MIN	30.9	60	101.5	33.0	6
10/11/2019	M	1	3	3MIN	33.0	39	101.3	33.0	6
10/11/2019	M	1	4	6MIN	31.3	33	101.3	33.0	6
10/11/2019	M	1	5	6MIN	32.9	36	101.9	33.0	6
10/11/2019	M	1	6	6MIN	33.8	90	100.8	33.0	6
10/11/2019	M	1	7	TimeControl	34.3	30	102.1	33.0	6
10/11/2019	M	1	8	TimeControl	33.3	42	101.4	33.0	6
10/11/2019	M	1	9	TimeControl	34.4	24	102.1	33.0	6
10/11/2019	M	1	10	9MIN	35.5	27	102.4	33.0	6
10/11/2019	M	1	11	9MIN	33.9	45	101.6	33.0	6
10/11/2019	M	1	12	9MIN	34.6	30	103.7	33.0	6
10/11/2019	M	2	1	3MIN	33.4	33	101.2	33.0	6
10/11/2019	M	2	2	3MIN	35.4	36	101.1	33.0	6
10/11/2019	M	2	3	3MIN	34.0	21	101.4	33.0	6
10/11/2019	M	2	4	6MIN	34.3	57	100.5	33.0	6
10/11/2019	M	2	5	6MIN	35.2	27	101.6	33.0	6
10/11/2019	M	2	6	6MIN	33.8	96	101.3	33.0	6
10/11/2019	M	2	7	TimeControl	33.9	27	101.7	33.0	6
10/11/2019	M	2	8	TimeControl	33.4	33	100.7	33.0	6
10/11/2019	M	2	9	TimeControl	33.0	48	100.9	33.0	6
10/11/2019	M	2	10	9MIN	33.3	45	101.1	33.0	6
10/11/2019	M	2	11	9MIN	33.0	39	102.1	33.0	6
10/11/2019	M	2	12	9MIN	35.0	45	103.5	33.0	6
10/11/2019	M	3	1	3MIN	35.5	48	101.2	33.0	6
10/11/2019	M	3	2	3MIN	36.2	39	101.5	33.0	6
10/11/2019	M	3	3	3MIN	38.2	45	100.3	33.0	6
10/11/2019	M	3	4	6MIN	37.1	72	100.4	33.0	6
10/11/2019	M	3	5	6MIN	37.2	33	102.2	33.0	6
10/11/2019	M	3	6	6MIN	37.9	78	101.2	33.0	6
10/11/2019	M	3	7	TimeControl	37.7	48	101.9	33.0	6
10/11/2019	M	3	8	TimeControl	37.3	54	100.7	33.0	6
10/11/2019	M	3	9	TimeControl	36.5	33	101.2	33.0	6
10/11/2019	M	3	10	9MIN	37.1	93	101.5	33.0	6
10/11/2019	M	3	11	9MIN	36.1	63	102.2	33.0	6
10/11/2019	M	3	12	9MIN	37.8	102	103.0	33.0	6
10/11/2019	M	4	1	3MIN	37.0	36	102.5	33.0	6
10/11/2019	M	4	2	3MIN	36.2	45	102.4	33.0	6

Table 20 continued

10/11/2019	M	4	3	3MIN	37.7	36	102.5	33.0	6
10/11/2019	M	4	4	6MIN	37.4	105	101.4	33.0	6
10/11/2019	M	4	5	6MIN	37.9	81	101.3	33.0	6
10/11/2019	M	4	6	6MIN	37.4	144	100.7	33.0	6
10/11/2019	M	4	7	TimeControl	36.5	30	102.1	33.0	6
10/11/2019	M	4	8	TimeControl	36.5	42	101.8	33.0	6
10/11/2019	M	4	9	TimeControl	37.0	0	101.8	33.0	6
10/11/2019	M	4	10	9MIN	36.3	114	102.8	33.0	6
10/11/2019	M	4	11	9MIN	35.9	27	102.2	33.0	6
10/11/2019	M	4	12	9MIN	36.2	51	103.3	33.0	6
10/11/2019	M	5	1	3MIN	36.0	24	101.5	33.0	6
10/11/2019	M	5	2	3MIN	34.7	78	103.0	33.0	6
10/11/2019	M	5	3	3MIN	35.3	51	102.7	33.0	6
10/11/2019	M	5	4	6MIN	33.7	62	101.4	33.0	6
10/11/2019	M	5	5	6MIN	36.0	75	102.9	33.0	6
10/11/2019	M	5	6	6MIN	37.1	78	103.1	33.0	6
10/11/2019	M	5	7	TimeControl	37.2	72	103.0	33.0	6
10/11/2019	M	5	8	TimeControl	35.8	78	102.3	33.0	6
10/11/2019	M	5	9	TimeControl	37.0	66	102.1	33.0	6
10/11/2019	M	5	10	9MIN	35.8	132	103.2	33.0	6
10/11/2019	M	5	11	9MIN	36.0	63	102.3	33.0	6
10/11/2019	M	5	12	9MIN	36.2	108	103.8	33.0	6
10/11/2019	M	6	1	3MIN	35.3	36	101.5	33.0	6
10/11/2019	M	6	2	3MIN	37.3	63	103.1	33.0	6
10/11/2019	M	6	3	3MIN	37.9	42	102.6	33.0	6
10/11/2019	M	6	4	6MIN	36.7	51	101.2	33.0	6
10/11/2019	M	6	5	6MIN	37.8	72	102.9	33.0	6
10/11/2019	M	6	6	6MIN	36.5	66	103.5	33.0	6
10/11/2019	M	6	7	TimeControl	37.9	75	103.6	33.0	6
10/11/2019	M	6	8	TimeControl	37.4	57	102.8	33.0	6
10/11/2019	M	6	9	TimeControl	37.7	51	103.0	33.0	6
10/11/2019	M	6	10	9MIN	36.4	66	104.0	33.0	6
10/11/2019	M	6	11	9MIN	36.5	42	102.8	33.0	6
10/11/2019	M	6	12	9MIN	38.3	51	103.4	33.0	6
10/11/2019	M	7	1	3MIN	35.2	36	101.8	33.0	6
10/11/2019	M	7	2	3MIN	36.9	105	102.8	33.0	6
10/11/2019	M	7	3	3MIN	37.3	88	102.4	33.0	6
10/11/2019	M	7	4	6MIN	36.1	54	101.1	33.0	6
10/11/2019	M	7	5	6MIN	37.2	66	103.1	33.0	6
10/11/2019	M	7	6	6MIN	37.4	81	103.9	33.0	6

Table 20 continued

10/11/2019	M	7	7	TimeControl	38.8	48	104.1	33.0	6
10/11/2019	M	7	8	TimeControl	37.5	36	102.9	33.0	6
10/11/2019	M	7	9	TimeControl	37.2	90	103.0	33.0	6
10/11/2019	M	7	10	9MIN	37.6	124	103.8	33.0	6
10/11/2019	M	7	11	9MIN	37.1	54	103.1	33.0	6
10/11/2019	M	7	12	9MIN	38.5	96	103.7	33.0	6
10/11/2019	M	8	1	3MIN	36.0	24	101.6	33.0	6
10/11/2019	M	8	2	3MIN	37.9	105	103.2	33.0	6
10/11/2019	M	8	3	3MIN	38.2	33	102.0	33.0	6
10/11/2019	M	8	4	6MIN	36.7	21	101.0	33.0	6
10/11/2019	M	8	5	6MIN	38.1	69	102.9	33.0	6
10/11/2019	M	8	6	6MIN	38.1	84	104.4	33.0	6
10/11/2019	M	8	7	TimeControl	39.2	75	104.7	33.0	6
10/11/2019	M	8	8	TimeControl	38.3	102	103.0	33.0	6
10/11/2019	M	8	9	TimeControl	38.7	78	103.2	33.0	6
10/11/2019	M	8	10	9MIN	38.8	81	103.8	33.0	6
10/11/2019	M	8	11	9MIN	37.1	57	103.2	33.0	6
10/11/2019	M	8	12	9MIN	38.3	75	103.3	33.0	6
10/11/2019	A	1	1	6MIN	31.5	33	101.0	33.0	7
10/11/2019	A	1	2	TimeControl	31.7	48	101.3	33.0	7
10/11/2019	A	1	3	9MIN	33.0	36	101.2	33.0	7
10/11/2019	A	1	4	9MIN	31.0	24	101.4	33.0	7
10/11/2019	A	1	5	3MIN	31.2	15	102.4	33.0	7
10/11/2019	A	1	6	TimeControl	36.0	21	101.7	33.0	7
10/11/2019	A	1	7	3MIN	35.5	30	102.9	33.0	7
10/11/2019	A	1	8	9MIN	34.0	33	101.3	33.0	7
10/11/2019	A	1	9	6MIN	29.2	27	101.8	33.0	7
10/11/2019	A	1	10	TimeControl	35.0	48	102.1	33.0	7
10/11/2019	A	1	11	6MIN	32.0	30	102.7	33.0	7
10/11/2019	A	1	12	3MIN	32.6	30	102.6	33.0	7
10/11/2019	A	2	1	6MIN	33.0	27	101.8	33.0	7
10/11/2019	A	2	2	TimeControl	34.0	36	101.7	33.0	7
10/11/2019	A	2	3	9MIN	34.4	51	100.0	33.0	7
10/11/2019	A	2	4	9MIN	30.6	24	101.4	33.0	7
10/11/2019	A	2	5	3MIN	32.8	27	101.9	33.0	7
10/11/2019	A	2	6	TimeControl	35.3	36	102.4	33.0	7
10/11/2019	A	2	7	3MIN	35.0	30	102.6	33.0	7
10/11/2019	A	2	8	9MIN	34.5	36	101.4	33.0	7
10/11/2019	A	2	9	6MIN	34.0	36	101.8	33.0	7
10/11/2019	A	2	10	TimeControl	35.1	60	102.2	33.0	7

Table 20 continued

10/11/2019	A	2	11	6MIN	32.3	36	102.9	33.0	7
10/11/2019	A	2	12	3MIN	33.0	33	102.9	33.0	7
10/11/2019	A	3	1	6MIN	37.7	24	101.1	33.0	7
10/11/2019	A	3	2	TimeControl	38.0	39	101.2	33.0	7
10/11/2019	A	3	3	9MIN	38.2	24	102.3	33.0	7
10/11/2019	A	3	4	9MIN	35.1	30	101.4	33.0	7
10/11/2019	A	3	5	3MIN	37.6	75	101.8	33.0	7
10/11/2019	A	3	6	TimeControl	38.6	138	101.9	33.0	7
10/11/2019	A	3	7	3MIN	39.2	45	102.5	33.0	7
10/11/2019	A	3	8	9MIN	38.9	39	101.8	33.0	7
10/11/2019	A	3	9	6MIN	39.0	30	101.9	33.0	7
10/11/2019	A	3	10	TimeControl	38.7	45	102.9	33.0	7
10/11/2019	A	3	11	6MIN	39.1	30	102.5	33.0	7
10/11/2019	A	3	12	3MIN	38.8	27	103.0	33.0	7
10/11/2019	A	4	1	6MIN	37.2	18	102.1	33.0	7
10/11/2019	A	4	2	TimeControl	37.1	33	102.8	33.0	7
10/11/2019	A	4	3	9MIN	37.7	36	102.6	33.0	7
10/11/2019	A	4	4	9MIN	37.4	39	101.6	33.0	7
10/11/2019	A	4	5	3MIN	36.9	42	102.1	33.0	7
10/11/2019	A	4	6	TimeControl	38.0	39	102.9	33.0	7
10/11/2019	A	4	7	3MIN	38.7	39	103.1	33.0	7
10/11/2019	A	4	8	9MIN	38.0	57	102.1	33.0	7
10/11/2019	A	4	9	6MIN	38.3	45	102.6	33.0	7
10/11/2019	A	4	10	TimeControl	38.2	66	103.7	33.0	7
10/11/2019	A	4	11	6MIN	38.0	39	102.7	33.0	7
10/11/2019	A	4	12	3MIN	39.2	30	103.0	33.0	7
10/11/2019	A	5	1	6MIN	37.8	32	102.8	33.0	7
10/11/2019	A	5	2	TimeControl	38.7	84	103.5	33.0	7
10/11/2019	A	5	3	9MIN	39.7	28	103.0	33.0	7
10/11/2019	A	5	4	9MIN	39.4	124	102.0	33.0	7
10/11/2019	A	5	5	3MIN	39.3	36	102.6	33.0	7
10/11/2019	A	5	6	TimeControl	40.1	84	103.9	33.0	7
10/11/2019	A	5	7	3MIN	40.4	54	103.6	33.0	7
10/11/2019	A	5	8	9MIN	39.2	72	102.4	33.0	7
10/11/2019	A	5	9	6MIN	39.8	30	103.0	33.0	7
10/11/2019	A	5	10	TimeControl	39.1	111	104.5	33.0	7
10/11/2019	A	5	11	6MIN	38.6	57	103.4	33.0	7
10/11/2019	A	5	12	3MIN	38.9	36	103.6	33.0	7
10/11/2019	A	6	1	6MIN	38.3	33	102.6	33.0	7
10/11/2019	A	6	2	TimeControl	38.3	132	103.5	33.0	7

Table 20 continued

10/11/2019	A	6	3	9MIN	38.7	69	103.6	33.0	7
10/11/2019	A	6	4	9MIN	38.5	84	102.0	33.0	7
10/11/2019	A	6	5	3MIN	38.5	66	101.7	33.0	7
10/11/2019	A	6	6	TimeControl	39.7	72	104.4	33.0	7
10/11/2019	A	6	7	3MIN	40.2	36	103.8	33.0	7
10/11/2019	A	6	8	9MIN	39.1	66	102.6	33.0	7
10/11/2019	A	6	9	6MIN	38.8	54	103.2	33.0	7
10/11/2019	A	6	10	TimeControl	38.6	90	105.3	33.0	7
10/11/2019	A	6	11	6MIN	37.8	54	103.5	33.0	7
10/11/2019	A	6	12	3MIN	38.2	51	103.5	33.0	7
10/11/2019	A	7	1	6MIN	38.2	27	102.6	33.0	7
10/11/2019	A	7	2	TimeControl	39.0	108	104.0	33.0	7
10/11/2019	A	7	3	9MIN	39.3	88	103.1	33.0	7
10/11/2019	A	7	4	9MIN	38.7	63	102.2	33.0	7
10/11/2019	A	7	5	3MIN	38.6	39	102.7	33.0	7
10/11/2019	A	7	6	TimeControl	40.4	108	104.8	33.0	7
10/11/2019	A	7	7	3MIN	39.1	51	104.0	33.0	7
10/11/2019	A	7	8	9MIN	38.8	99	102.9	33.0	7
10/11/2019	A	7	9	6MIN	38.7	51	103.5	33.0	7
10/11/2019	A	7	10	TimeControl	39.4	147	105.3	33.0	7
10/11/2019	A	7	11	6MIN	37.2	42	103.6	33.0	7
10/11/2019	A	7	12	3MIN	38.1	36	103.0	33.0	7
10/11/2019	A	8	1	6MIN	37.9	33	102.9	33.0	7
10/11/2019	A	8	2	TimeControl	38.7	69	104.7	33.0	7
10/11/2019	A	8	3	9MIN	38.9	54	102.9	33.0	7
10/11/2019	A	8	4	9MIN	38.0	36	102.0	33.0	7
10/11/2019	A	8	5	3MIN	39.0	69	102.5	33.0	7
10/11/2019	A	8	6	TimeControl	39.3	96	105.7	33.0	7
10/11/2019	A	8	7	3MIN	39.5	54	104.0	33.0	7
10/11/2019	A	8	8	9MIN	39.0	60	103.0	33.0	7
10/11/2019	A	8	9	6MIN	38.7	39	103.6	33.0	7
10/11/2019	A	8	10	TimeControl	39.0	83	104.8	33.0	7
10/11/2019	A	8	11	6MIN	38.5	57	104.1	33.0	7
10/11/2019	A	8	12	3MIN	38.5	45	103.6	33.0	7
10/12/2019	M	1	1	9MIN	32.0	30	102.4	33.0	8
10/12/2019	M	1	2	6MIN	29.2	36	100.4	33.0	8
10/12/2019	M	1	3	6MIN	30.3	28	101.3	33.0	8
10/12/2019	M	1	4	TimeControl	30.1	27	100.7	33.0	8
10/12/2019	M	1	5	9MIN	35.1	31	102.1	33.0	8
10/12/2019	M	1	6	9MIN	34.3	36	101.3	33.0	8

Table 20 continued

10/12/2019	M	1	7	6MIN	33.4	21	101.6	33.0	8
10/12/2019	M	1	8	3MIN	34.0	42	100.2	33.0	8
10/12/2019	M	1	9	3MIN	34.5	33	101.6	33.0	8
10/12/2019	M	1	10	3MIN	34.0	69	101.1	33.0	8
10/12/2019	M	1	11	TimeControl	32.7	45	102.6	33.0	8
10/12/2019	M	1	12	TimeControl	34.5	39	103.1	33.0	8
10/12/2019	M	2	1	9MIN	29.1	33	101.3	33.0	8
10/12/2019	M	2	2	6MIN	31.1	36	101.4	33.0	8
10/12/2019	M	2	3	6MIN	30.4	36	101.1	33.0	8
10/12/2019	M	2	4	TimeControl	30.9	42	100.3	33.0	8
10/12/2019	M	2	5	9MIN	33.8	39	102.2	33.0	8
10/12/2019	M	2	6	9MIN	33.7	39	100.3	33.0	8
10/12/2019	M	2	7	6MIN	30.8	21	101.4	33.0	8
10/12/2019	M	2	8	3MIN	33.7	33	100.2	33.0	8
10/12/2019	M	2	9	3MIN	33.2	36	101.3	33.0	8
10/12/2019	M	2	10	3MIN	35.4	78	102.1	33.0	8
10/12/2019	M	2	11	TimeControl	34.8	36	101.1	33.0	8
10/12/2019	M	2	12	TimeControl	35.3	60	102.3	33.0	8
10/12/2019	M	3	1	9MIN	35.6	24	103.1	33.0	8
10/12/2019	M	3	2	6MIN	36.3	21	101.0	33.0	8
10/12/2019	M	3	3	6MIN	38.1	21	102.5	33.0	8
10/12/2019	M	3	4	TimeControl	38.7	48	100.7	33.0	8
10/12/2019	M	3	5	9MIN	38.0	33	102.5	33.0	8
10/12/2019	M	3	6	9MIN	38.8	78	101.0	33.0	8
10/12/2019	M	3	7	6MIN	37.2	45	102.1	33.0	8
10/12/2019	M	3	8	3MIN	37.6	39	101.4	33.0	8
10/12/2019	M	3	9	3MIN	37.3	45	102.2	33.0	8
10/12/2019	M	3	10	3MIN	36.9	63	101.6	33.0	8
10/12/2019	M	3	11	TimeControl	38.2	69	101.9	33.0	8
10/12/2019	M	3	12	TimeControl	38.5	48	103.1	33.0	8
10/12/2019	M	4	1	9MIN	37.8	18	102.8	33.0	8
10/12/2019	M	4	2	6MIN	38.1	30	101.6	33.0	8
10/12/2019	M	4	3	6MIN	38.0	24	102.5	33.0	8
10/12/2019	M	4	4	TimeControl	38.5	63	101.2	33.0	8
10/12/2019	M	4	5	9MIN	38.6	54	102.4	33.0	8
10/12/2019	M	4	6	9MIN	38.6	126	101.2	33.0	8
10/12/2019	M	4	7	6MIN	37.3	21	102.0	33.0	8
10/12/2019	M	4	8	3MIN	38.3	33	100.9	33.0	8
10/12/2019	M	4	9	3MIN	37.1	24	101.3	33.0	8
10/12/2019	M	4	10	3MIN	37.4	69	101.6	33.0	8

Table 20 continued

10/12/2019	M	4	11	TimeControl	38.2	78	102.1	33.0	8
10/12/2019	M	4	12	TimeControl	39.0	66	103.7	33.0	8
10/12/2019	M	5	1	9MIN	38.0	36	102.8	33.0	8
10/12/2019	M	5	2	6MIN	38.3	30	102.4	33.0	8
10/12/2019	M	5	3	6MIN	39.6	60	102.2	33.0	8
10/12/2019	M	5	4	TimeControl	39.2	75	102.2	33.0	8
10/12/2019	M	5	5	9MIN	40.9	84	102.7	33.0	8
10/12/2019	M	5	6	9MIN	39.3	132	102.5	33.0	8
10/12/2019	M	5	7	6MIN	40.6	48	103.2	33.0	8
10/12/2019	M	5	8	3MIN	38.3	48	101.7	33.0	8
10/12/2019	M	5	9	3MIN	38.7	24	101.8	33.0	8
10/12/2019	M	5	10	3MIN	38.5	45	102.1	33.0	8
10/12/2019	M	5	11	TimeControl	38.7	72	103.1	33.0	8
10/12/2019	M	5	12	TimeControl	38.0	111	104.4	33.0	8
10/12/2019	M	6	1	9MIN	36.6	57	102.9	33.0	8
10/12/2019	M	6	2	6MIN	37.5	36	102.7	33.0	8
10/12/2019	M	6	3	6MIN	38.0	88	102.8	33.0	8
10/12/2019	M	6	4	TimeControl	38.7	90	102.4	33.0	8
10/12/2019	M	6	5	9MIN	38.4	63	103.3	33.0	8
10/12/2019	M	6	6	9MIN	37.9	144	102.8	33.0	8
10/12/2019	M	6	7	6MIN	39.2	51	103.4	33.0	8
10/12/2019	M	6	8	3MIN	38.1	57	102.6	33.0	8
10/12/2019	M	6	9	3MIN	38.4	36	101.8	33.0	8
10/12/2019	M	6	10	3MIN	37.5	39	101.9	33.0	8
10/12/2019	M	6	11	TimeControl	38.4	84	103.9	33.0	8
10/12/2019	M	6	12	TimeControl	38.7	102	104.2	33.0	8
10/12/2019	M	7	1	9MIN	36.6	51	102.9	33.0	8
10/12/2019	M	7	2	6MIN	37.0	48	102.9	33.0	8
10/12/2019	M	7	3	6MIN	39.2	42	103.0	33.0	8
10/12/2019	M	7	4	TimeControl	38.9	42	102.1	33.0	8
10/12/2019	M	7	5	9MIN	39.1	66	103.6	33.0	8
10/12/2019	M	7	6	9MIN	39.0	99	103.1	33.0	8
10/12/2019	M	7	7	6MIN	38.5	54	103.6	33.0	8
10/12/2019	M	7	8	3MIN	38.9	66	102.7	33.0	8
10/12/2019	M	7	9	3MIN	38.9	36	102.2	33.0	8
10/12/2019	M	7	10	3MIN	37.2	48	102.7	33.0	8
10/12/2019	M	7	11	TimeControl	37.6	54	104.2	33.0	8
10/12/2019	M	7	12	TimeControl	39.0	120	104.5	33.0	8
10/12/2019	M	8	1	9MIN	38.9	36	103.2	33.0	8
10/12/2019	M	8	2	6MIN	40.0	63	103.1	33.0	8

Table 20 continued

10/12/2019	M	8	3	6MIN	40.4	45	102.8	33.0	8
10/12/2019	M	8	4	TimeControl	39.8	32	102.8	33.0	8
10/12/2019	M	8	5	9MIN	38.7	128	103.8	33.0	8
10/12/2019	M	8	6	9MIN	39.5	150	103.1	33.0	8
10/12/2019	M	8	7	6MIN	40.0	88	103.6	33.0	8
10/12/2019	M	8	8	3MIN	39.8	69	102.5	33.0	8
10/12/2019	M	8	9	3MIN	39.2	28	102.0	33.0	8
10/12/2019	M	8	10	3MIN	38.1	66	103.1	33.0	8
10/12/2019	M	8	11	TimeControl	39.2	93	103.7	33.0	8
10/12/2019	M	8	12	TimeControl	39.7	111	104.9	33.0	8
10/12/2019	A	1	1	TimeControl	32.7	28	102.2	33.0	9
10/12/2019	A	1	2	9MIN	35.0	24	103.0	33.0	9
10/12/2019	A	1	3	TimeControl	36.0	30	102.1	33.0	9
10/12/2019	A	1	4	3MIN	36.8	33	102.4	33.0	9
10/12/2019	A	1	5	TimeControl	36.2	18	104.1	33.0	9
10/12/2019	A	1	6	3MIN	35.7	63	103.1	33.0	9
10/12/2019	A	1	7	9MIN	36.3	51	103.3	33.0	9
10/12/2019	A	1	8	6MIN	36.3	33	102.4	33.0	9
10/12/2019	A	1	9	9MIN	34.8	28	102.7	33.0	9
10/12/2019	A	1	10	6MIN	35.1	66	102.4	33.0	9
10/12/2019	A	1	11	3MIN	35.0	72	104.2	33.0	9
10/12/2019	A	1	12	6MIN	36.8	39	103.1	33.0	9
10/12/2019	A	2	1	TimeControl	29.5	42	101.2	33.0	9
10/12/2019	A	2	2	9MIN	34.0	27	102.7	33.0	9
10/12/2019	A	2	3	TimeControl	32.4	18	102.9	33.0	9
10/12/2019	A	2	4	3MIN	34.5	54	101.8	33.0	9
10/12/2019	A	2	5	TimeControl	34.3	18	103.7	33.0	9
10/12/2019	A	2	6	3MIN	34.9	66	103.0	33.0	9
10/12/2019	A	2	7	9MIN	35.0	24	102.8	33.0	9
10/12/2019	A	2	8	6MIN	34.1	24	102.5	33.0	9
10/12/2019	A	2	9	9MIN	33.8	24	102.3	33.0	9
10/12/2019	A	2	10	6MIN	32.1	30	102.6	33.0	9
10/12/2019	A	2	11	3MIN	35.9	57	103.2	33.0	9
10/12/2019	A	2	12	6MIN	36.2	45	103.0	33.0	9
10/12/2019	A	3	1	TimeControl	39.0	24	102.3	33.0	9
10/12/2019	A	3	2	9MIN	39.5	108	102.6	33.0	9
10/12/2019	A	3	3	TimeControl	40.0	36	102.8	33.0	9
10/12/2019	A	3	4	3MIN	40.6	75	102.7	33.0	9
10/12/2019	A	3	5	TimeControl	40.6	39	103.5	33.0	9
10/12/2019	A	3	6	3MIN	40.2	138	102.9	33.0	9

Table 20 continued

10/12/2019	A	3	7	9MIN	39.1	45	103.0	33.0	9
10/12/2019	A	3	8	6MIN	39.3	48	102.7	33.0	9
10/12/2019	A	3	9	9MIN	38.6	18	102.3	33.0	9
10/12/2019	A	3	10	6MIN	37.8	57	102.9	33.0	9
10/12/2019	A	3	11	3MIN	39.2	60	103.6	33.0	9
10/12/2019	A	3	12	6MIN	39.5	102	104.2	33.0	9
10/12/2019	A	4	1	TimeControl	38.0	45	102.2	33.0	9
10/12/2019	A	4	2	9MIN	39.6	75	103.9	33.0	9
10/12/2019	A	4	3	TimeControl	39.4	27	103.0	33.0	9
10/12/2019	A	4	4	3MIN	39.9	93	103.5	33.0	9
10/12/2019	A	4	5	TimeControl	39.9	69	103.2	33.0	9
10/12/2019	A	4	6	3MIN	39.4	105	103.3	33.0	9
10/12/2019	A	4	7	9MIN	40.1	54	103.7	33.0	9
10/12/2019	A	4	8	6MIN	39.3	60	103.0	33.0	9
10/12/2019	A	4	9	9MIN	39.2	33	102.5	33.0	9
10/12/2019	A	4	10	6MIN	37.3	36	103.3	33.0	9
10/12/2019	A	4	11	3MIN	39.1	51	104.0	33.0	9
10/12/2019	A	4	12	6MIN	39.9	99	105.4	33.0	9
10/12/2019	A	5	1	TimeControl	41.2	78	103.1	33.0	9
10/12/2019	A	5	2	9MIN	41.1	56	103.9	33.0	9
10/12/2019	A	5	3	TimeControl	40.7	81	102.9	33.0	9
10/12/2019	A	5	4	3MIN	40.4	111	104.2	33.0	9
10/12/2019	A	5	5	TimeControl	40.0	68	104.4	33.0	9
10/12/2019	A	5	6	3MIN	39.4	54	104.1	33.0	9
10/12/2019	A	5	7	9MIN	40.7	63	104.3	33.0	9
10/12/2019	A	5	8	6MIN	39.9	60	102.8	33.0	9
10/12/2019	A	5	9	9MIN	39.1	48	102.7	33.0	9
10/12/2019	A	5	10	6MIN	38.0	78	104.3	33.0	9
10/12/2019	A	5	11	3MIN	38.7	93	104.2	33.0	9
10/12/2019	A	5	12	6MIN	.	105	105.5	33.0	9
10/12/2019	A	6	1	TimeControl	41.0	81	103.5	33.0	9
10/12/2019	A	6	2	9MIN	41.1	57	104.2	33.0	9
10/12/2019	A	6	3	TimeControl	40.2	60	104.0	33.0	9
10/12/2019	A	6	4	3MIN	39.3	81	103.7	33.0	9
10/12/2019	A	6	5	TimeControl	40.1	102	104.5	33.0	9
10/12/2019	A	6	6	3MIN	39.0	135	104.8	33.0	9
10/12/2019	A	6	7	9MIN	40.2	48	104.5	33.0	9
10/12/2019	A	6	8	6MIN	39.6	69	103.5	33.0	9
10/12/2019	A	6	9	9MIN	38.8	54	102.9	33.0	9
10/12/2019	A	6	10	6MIN	39.1	36	104.4	33.0	9

Table 20 continued

10/12/2019	A	6	11	3MIN	39.3	60	104.1	33.0	9
10/12/2019	A	6	12	6MIN	40.2	126	103.7	33.0	9
10/12/2019	A	7	1	TimeControl	39.2	42	103.0	33.0	9
10/12/2019	A	7	2	9MIN	38.1	63	103.3	33.0	9
10/12/2019	A	7	3	TimeControl	40.0	66	103.3	33.0	9
10/12/2019	A	7	4	3MIN	39.8	63	103.6	33.0	9
10/12/2019	A	7	5	TimeControl	40.4	111	104.6	33.0	9
10/12/2019	A	7	6	3MIN	40.8	111	104.4	33.0	9
10/12/2019	A	7	7	9MIN	40.3	36	104.3	33.0	9
10/12/2019	A	7	8	6MIN	39.4	78	103.2	33.0	9
10/12/2019	A	7	9	9MIN	39.3	48	102.9	33.0	9
10/12/2019	A	7	10	6MIN	39.0	99	104.6	33.0	9
10/12/2019	A	7	11	3MIN	39.1	57	104.0	33.0	9
10/12/2019	A	7	12	6MIN	39.1	78	105.4	33.0	9
10/12/2019	A	8	1	TimeControl	38.6	42	103.0	33.0	9
10/12/2019	A	8	2	9MIN	38.2	69	103.4	33.0	9
10/12/2019	A	8	3	TimeControl	39.7	57	104.1	33.0	9
10/12/2019	A	8	4	3MIN	39.3	30	102.6	33.0	9
10/12/2019	A	8	5	TimeControl	39.5	111	104.7	33.0	9
10/12/2019	A	8	6	3MIN	39.4	135	105.9	33.0	9
10/12/2019	A	8	7	9MIN	39.5	42	104.4	33.0	9
10/12/2019	A	8	8	6MIN	39.2	36	102.4	33.0	9
10/12/2019	A	8	9	9MIN	39.3	33	103.2	33.0	9
10/12/2019	A	8	10	6MIN	38.6	129	104.5	33.0	9
10/12/2019	A	8	11	3MIN	37.5	66	103.5	33.0	9
10/12/2019	A	8	12	6MIN	39.3	96	104.8	33.0	9

APPENDIX D: EFFECTS OF COVARIATES

To examine the level of level of variance accounted for by covariates included in each SAS PROC MIXED model, those models with significant covariates were also run without the covariates to better understand the amount of variance between sows they accounted for. The five dependent variables examined were skin temperature (ST), respiration rate (RR), rectal temperature (RT), average pad temperature (PT), and cycle heat transfer rate (HT). The covariates considered in each model were parity (PAR), sow body weight (BW), sow back fat thickness (BF), and sow loin depth (LD). The models with and without the covariates can be seen in Table 21.

Table 21: Effects of Included Covariates on Overall Models

Dep. Var.	Control Schemes	Include Covariates	REP Variance	SOW Variance	Residual Variance	Covariates	R^2	Accounted SOW Var.
ST	Temporal	NO	0.7052	0.1789	1.2377	-	79.9%	-
		YES	-	-	-	-	-	
	Temp. Threshold	NO	2.8205	0.08615	1.3549	-	78.8%	95.88%
		YES	2.7449	0.003549	1.3602	BF	78.7%	
RR	Temporal	NO	2.4012	104.92	441.60	-	39.8%	-
		YES	-	-	-	-	-	
	Temp. Threshold	NO	42.1026	180.39	246.02	-	58.6%	-
		YES	-	-	-	-	-	
RT	Temporal	NO	0.3113	0.3601	0.2697	-	76.9%	-
		YES	-	-	-	-	-	
	Temp. Threshold	NO	0.3928	0.3016	0.3187	-	70.9%	83.13%
		YES	0.3996	0.05088	0.3184	BW, PAR, LD	70.9%	
PT	Temporal	NO	1.7038	3.0018	2.0817	-	82.4%	-
		YES	-	-	-	-	-	
	Temp. Threshold	NO	0.2697	1.6578	1.3378	-	89.8%	54.66%
		YES	0.2812	0.7517	1.3368	PAR	89.8%	
HT	Temporal	NO	258.16	686.30	1604.64	-	85.4%	75.16%
		YES	272.37	170.48	1604.47	BW, BF	85.4%	
	Temp. Threshold	NO	3254.37	4806.92	7668.18	-	72.1%	-
		YES	-	-	-	-	-	

REFERENCES

Adafruit®. (2019a). Adafruit Feather M0 WiFi - ATSAMD21 + ATWINC1500. Retrieved from https://www.adafruit.com/product/3010

Adafruit®. (2019b). Adafruit Non-Latching Mini Relay FeatherWing. Retrieved from https://www.adafruit.com/product/2895

Adafruit®. (2019c). Adalogger FeatherWing - RTC + SD Add-on For All Feather Boards. Retrieved from https://www.adafruit.com/product/2922

Adafruit®. (2019d). Assembled Terminal Block Breakout FeatherWing for all Feathers. Retrieved from https://www.adafruit.com/product/2926

Adafruit®. (2019e). FeatherWing Tripler Mini Kit - Prototyping Add-on For Feathers. Retrieved from https://www.adafruit.com/product/3417

Adafruit®. (2019f). Plastic Water Solenoid Valve - 12V - 1/2" Nominal. Retrieved from https://www.adafruit.com/product/997

Amazon.com®. (2019). DIGITEN® G3/8" Water Flow Sensor, Hall Effect Sensor Switch Flow Meter Flowmeter Counter 0.3-10L/min - Arduino, Raspberry Pi, and Reverse Osmosis Filter Compatible. Retrieved from https://www.amazon.com/DIGITEN-Sensor-Flowmeter-Counter-0-3-10L/dp/B07QNMZ35C/ref=sr_1_15?keywords=flow+meter+arduino&qid=1572969333&sr=8-15

Baumgard, L. H., & Rhoads, R. P. (2013). Effects of Heat Stress on Postabsorptive Metabolism and Energetics. Annual Review of Animal Biosciences, Vol 1, 1, 311-337. doi:10.1146/annurev-animal-031412-103644

Bjerg, B., Brandt, P., Sorensen, K., Pedersen, P., & Zhang, G. (2019). Review of Methods to Mitigate Heat Stress among Sows. 2019 ASABE Annual International Meeting, St. Joseph, MI. doi:10.13031/aim.201900741

Black, J. L., Mullan, B. P., Lorschy, M. L., & Giles, L. R. (1993). Lactation in the Sow During Heat-Stress. Livestock Production Science, 35(1-2), 153-170. doi:10.1016/0301-6226(93)90188-n

Cabezon, F. A., Johnson, J. S., Schinckel, A. P., & Stwalley, R. M. (2020). Effect of Barn Temperatures on Sow Cooling Panel Performance and Sow Physiological Conditions. Purdue University. Manuscript in preparation.

Cabezon, F. A., Maskal, J., Schinckel, A. P., Marchant-Forde, J. N., Johnson, J. S., & Stwalley, R. M. (2018). Evaluation of Floor Cooling on Lactating Sows Under Mild and Moderate Heat Stress. Journal of Animal Science, 96, 7-7.

Cabezon, F. A., Schinckel, A. P., Marchant-Forde, J. N., Johnson, J. S., & Stwalley, R. M. (2017). Effect of floor cooling on late lactation sows under acute heat stress. Livestock Science, 206, 113-120. doi:10.1016/j.livsci.2017.10.017

Cabezon, F. A., Schinckel, A. P., Richert, B. T., Peralta, W. A., & Gandarillas, M. (2017a). Development and application of a model of heat production for lactating sows. Journal of Animal Science, 95, 30-30. doi:10.2527/asasmw.2017.064

Cabezon, F. A., Schinckel, A. P., Richert, B. T., Peralta, W. A., & Gandarillas, M. (2017b). Technical Note: application of models to estimate daily heat production of lactating sows. Professional Animal Scientist, 33(3), 357-362.

Cabezon, F. A., Schinckel, A. P., Smith, A. J., Marchant-Forde, J. N., Johnson, J. S., & Stwalley, R. M. (2017). Initial evaluation of floor cooling on lactating sows under acute heat stress. Professional Animal Scientist, 33(2), 254-260. doi:10.15232/pas.2016-01584

Cabezon, F. A., Schinckel, A. P., Stwalley, C. S., & Stwalley, R. M. (2018). Heat Transfer Properties of Hog Cooling Pad. Transactions of the Asabe, 61(5), 1693-1703. doi:10.13031/trans.12351

Cabezon, F. A., Schinckel, A. P., & Stwalley, R. M. (2017). Thermal Capacity of Hog-Cooling Pad. Applied Engineering in Agriculture, 33(6), 891-899. doi:10.13031/aea.12333

Cabezon, F. A., Field, T. C., Winslow, E., Schinckel, A. P., & Stwalley, R. M. (2020). Heat Transfer Performance Effects of Coil Density on Hog Cooling Panel. Manuscript submitted for publication.

de Oliveira, G. M., Ferreira, A. S., Oliveira, R. F. M., Silva, B. A. N., de Figueiredo, E. M., & Santos, M. (2011). Behaviour and performance of lactating sows housed in different types of farrowing rooms during summer. Livestock Science, 141(2-3), 194-201. doi:10.1016/j.livsci.2011.06.001

Digi-Key Electronics®. (2019). DFR0198. Retrieved from https://www.digikey.com/product-detail/en/dfrobot/DFR0198/1738-1311-ND/7597054

Field, T. C., Schinckel, A. P., & Stwalley, R. M. (2020). Impact of Variation in Electronic Control Scheme Parameters for Hog Cooling Pads. 2020 ASABE Annual International Meeting, St. Joseph, MI. https://elibrary.asabe.org/abstract.asp?aid=51456

Field, T. C., Burgett, M. I., Schinckel, A. P., & Stwalley, R. M. (2019). Electronic Control for Hog Cooling Pads. 2019 ASABE Annual International Meeting, St. Joseph, MI. http://elibrary.asabe.org/abstract.asp?aid=50600&t=5

Field, T. C. & Stwalley, R. M. (2018). Development of a Hog Cooling Panel. ASABE Annual International Meeting, St. Joseph, MI. https://elibrary.asabe.org/abstract.asp?aid=49500

Geis, E., Zumwalt, D., & Carter, J. (2015). Sow Cooling Pad. Agricultural & Biological Engineering. Purdue University.

Gere, J. M., & Goodno, B. J. (2012). Mechanics of Materials: Cengage Learning.

Jeon, J. H., & Kim, D. H. (2014). Methods to supply chilled drinking water for lactating sows during high ambient temperatures. Italian Journal of Animal Science, 13(4). doi:10.4081/ijas.2014.3431

Jeon, J. H., Yeon, S. C., Choi, Y. H., Min, W., Kim, S., Kim, P. J., & Chang, H. H. (2006). Effects of chilled drinking water on the performance of lactating sows and their litters during high ambient temperatures under farm conditions. Livestock Science, 105(1-3), 86-93. doi:10.1016/j.livsci.2006.04.035

Kumar, S., Bass, B. E., Bandrick, M., Loving, C. L., Brockmeier, S. L., Looft, T., . . . Allen, H. K. (2017). Fermentation products as feed additives mitigate some ill-effects of heat stress in pigs. Journal of Animal Science, 95(1), 279-290. doi:10.2527/jas2016.0662

Liu, F., de Ruyter, E. M., Athorn, R. Z., Brewster, C. J., Henman, D. J., Morrison, R. S., . . . Dunshea, F. R. (2019). Effects of L-citrulline supplementation on heat stress physiology, lactation performance and subsequent reproductive performance of sows in summer. Journal of Animal Physiology and Animal Nutrition, 103(1), 251-257. doi:10.1111/jpn.13028

Maskal, J., Cabezon, F. A., Schinckel, A. P., Marchant-Forde, J. N., Johnson, J. S., & Stwalley, R. M. (2018a). Evaluation of floor cooling on lactating sows under mild and moderate heat stress. Professional Animal Scientist, 34(1), 84-94. doi:10.15232/pas.2017-01661

Maxim Integrated®. (2019). DS18B20 Programmable Resolution 1-Wire Digital Thermometer. Retrieved from https://datasheets.maximintegrated.com/en/ds/DS18B20.pdf

Mayorga, E. J., Renaudeau, D., Ramirez, B. C., Ross, J. W., & Baumgard, L. H. (2019). Heat stress adaptations in pigs. Animal Frontiers, 9(1), 54-61. doi:10.1093/af/vfy035

Murphy, J. P., Nichols, D. A., & Robbins, F. V. (1987). Drip cooling of lactating sows. Applied Engineering in Agriculture, 3(2), 200-202.

Pang, Z. Z., Li, B. M., Xin, H. W., Xi, L., Cao, W., Wang, C. Y., & Li, W. (2011). Field evaluation of a water-cooled cover for cooling sows in hot and humid climates. Biosystems Engineering, 110(4), 413-420. doi:10.1016/j.biosystemseng.2011.08.012

Pang, Z. Z., Li, B. M., Xin, H. W., Yuan, X. Y., & Wang, C. Y. (2010). Characterisation of an experimental water-cooled cover for sows. Biosystems Engineering, 105(4), 439-447. doi:10.1016/j.biosystemseng.2010.01.002

Pang, Z. Z., Li, B. M., Zheng, W. C., Lin, B. Z., & Liu, Z. H. (2016). Effects of water-cooled cover on physiological and production parameters of farrowing sows under hot and humid climates. International Journal of Agricultural and Biological Engineering, 9(4), 178-184. doi:10.3965/j.ijabe.20160904.1858

Parois, S. P., Cabezon, F. A., Schinckel, A. P., Johnson, J. S., Stwalley, R. M., & Marchant-Forde, J. N. (2018). Effect of Floor Cooling on Behavior and Heart Rate of Late Lactation Sows Under Acute Heat Stress. Frontiers in Veterinary Science, 5. doi:10.3389/fvets.2018.00223

Pedersen, L. J., Malmkvist, J., Kammersgaard, T., & Jorgensen, E. (2013). Avoiding hypothermia in neonatal pigs: Effect of duration of floor heating at different room temperatures. Journal of Animal Science, 91(1), 425-432. doi:10.2527/jas.2011-4534

Perin, J., Gaggini, T. S., Manica, S., Magnabosco, D., Bernardi, M. L., Wentz, I., & Bortolozzo, F. P. (2016). Evaporative snout cooling system on the performance of lactating sows and their litters in a subtropical region. Ciencia Rural, 46(2), 342-347. doi:10.1590/0103-8478cr20141693

Quiniou, N., Dagorn, J., & Gaudré, D. (2002). Variation of Piglets' Birth Weight and Consequences on Subsequent Performance. Livestock Production Science, 78, 63-70.

Quiniou, N., & Noblet, J. (1999). Influence of high ambient temperatures on performance of multiparous lactating sows. Journal of Animal Science, 77(8), 2124-2134.

Renaudeau, D., Collin, A., Yahav, S., de Basilio, V., Gourdine, J. L., & Collier, R. J. (2012). Adaptation to hot climate and strategies to alleviate heat stress in livestock production. Animal, 6(5), 707-728. doi:10.1017/s1751731111002448

Renaudeau, D., Quiniou, N., & Noblet, J. (2001). Effects of exposure to high ambient temperature and dietary protein level on performance of multiparous lactating sows. Journal of Animal Science, 79(5), 1240-1249.

Ross, J. W., Hale, B. J., Gabler, N. K., Rhoads, R. P., Keating, A. F., & Baumgard, L. H. (2015). Physiological consequences of heat stress in pigs. Animal Production Science, 55(11-12), 1381-1390. doi:10.1071/an15267

Schieck, S. J., Kerr, B. J., Baidoo, S. K., Shurson, G. C., & Johnston, L. J. (2010). Use of crude glycerol, a biodiesel coproduct, in diets for lactating sows. Journal of Animal Science, 88(8), 2648-2656. doi:10.2527/jas.2009-2609

Schinckel, A. P. & Stwalley, R. M. (2015). Systems and Methods to Cool an Animal. U.S. Patent Application No. 20190045739A1. Washington, DC: U.S. Patent and Trademark Office.

Seidel, D. S. (2017). Investigation Into the Effects of Temperature Probe Orientation on the Purdue Swine Cooling Pad.

Seidel, D. S., Field, T. C., Schinckel, A. P., Stwalley, C. S., & Stwalley, R. M. (2020). Effects of Temperature Probe Orientation on the Purdue Hog Cooling Pad Data Acquisition. Computers and Electronics in Agriculture, August 2020, Vol.175.

Silva, B. A. N., Noblet, J., Donzele, J. L., Oliveira, R. F. M., Primot, Y., Gourdine, J. L., & Renaudeau, D. (2009). Effects of dietary protein level and amino acid supplementation on performance of mixed-parity lactating sows in a tropical humid climate. Journal of Animal Science, 87(12), 4003-4012. doi:10.2527/jas.2008-1176

Silva, B. A. N., Oliveira, R. F. M., Donzele, J. L., Fernandes, H. C., Abreu, M. L. T., Noblet, J., & Nunes, C. G. V. (2006). Effect of floor cooling on performance of lactating sows during summer. Livestock Science, 105(1-3), 176-184. doi:10.1016/j.livsci.2006.06.007

Silva, B. A. N., Oliveira, R. F. M., Donzele, J. L., Fernandes, H. C., Lima, A. L., Renaudeau, D., & Noblet, J. (2009). Effect of floor cooling and dietary amino acids content on performance and behaviour of lactating primiparous sows during summer. Livestock Science, 120(1-2), 25-34. doi:10.1016/j.livsci.2008.04.015

Smith, A. J., Cabezon, F. A., Schinckel, A. P., Marchant-Forde, J. N., Johnson, J. S., & Stwalley, R. M. (2017). Initial evaluation of floor cooling on lactating sows under acute heat stress. Journal of Animal Science, 95, 183-184. doi:10.2527/asasmw.2017.379

USDA: Foreign Agricultural Service. (2019). Livestock and Poultry: World Markets and Trade. Retrieved from https://downloads.usda.library.cornell.edu/usda-esmis/files/73666448x/g445ct12h/ff365k146/Livestock_poultry.pdf

van Wagenberg, A. V., van der Peet-Schwering, C. M. C., Binnendijk, G. P., & Claessen, P. J. P. W. (2006). Effect of floor cooling on farrowing sow and litter performance: Field experiment under Dutch conditions. Transactions of the Asabe, 49(5), 1521-1527.